AD-A031 746 DAVID W TAYLOR NAVAL SHIP RESEARCH AND DEVELOPMENT CE--ETC F/G 20/4
A NEW EXPERIMENTAL FACILITY FOR THE PERFORMANCE EVALUATION OF S--ETC(U)
DEC 75 S E CALLANEN
UNCLASSIFIED SPD-671-01 NL

1 OF 2
AD
A031746

FG (12)

SPD-671-01

A NEW EXPERIMENTAL FACILITY FOR THE PERFORMANCE EVALUATION OF STRUT-POD WATERJET INLETS AT CAVITATION SCALED CRAFT SPEEDS IN EXCESS OF 100 KNOTS

ADA031746

DAVID W. TAYLOR NAVAL SHIP RESEARCH AND DEVELOPMENT CENTER

Bethesda, Md. 20084

A NEW EXPERIMENTAL FACILITY FOR THE PERFORMANCE EVALUATION OF STRUT-POD WATERJET INLETS AT CAVITATION SCALED CRAFT SPEEDS IN EXCESS OF 100 KNOTS

by

Stephen E. Callanen

APPROVED FOR PUBLIC RELEASE: DISTRIBUTION UNLIMITED

SHIP PERFORMANCE DEPARTMENT REPORT

D D C
RECEIVED
NOV 9 1976
D

December 1975

SPD-671-01

MAJOR DTNSRDC ORGANIZATIONAL COMPONENTS

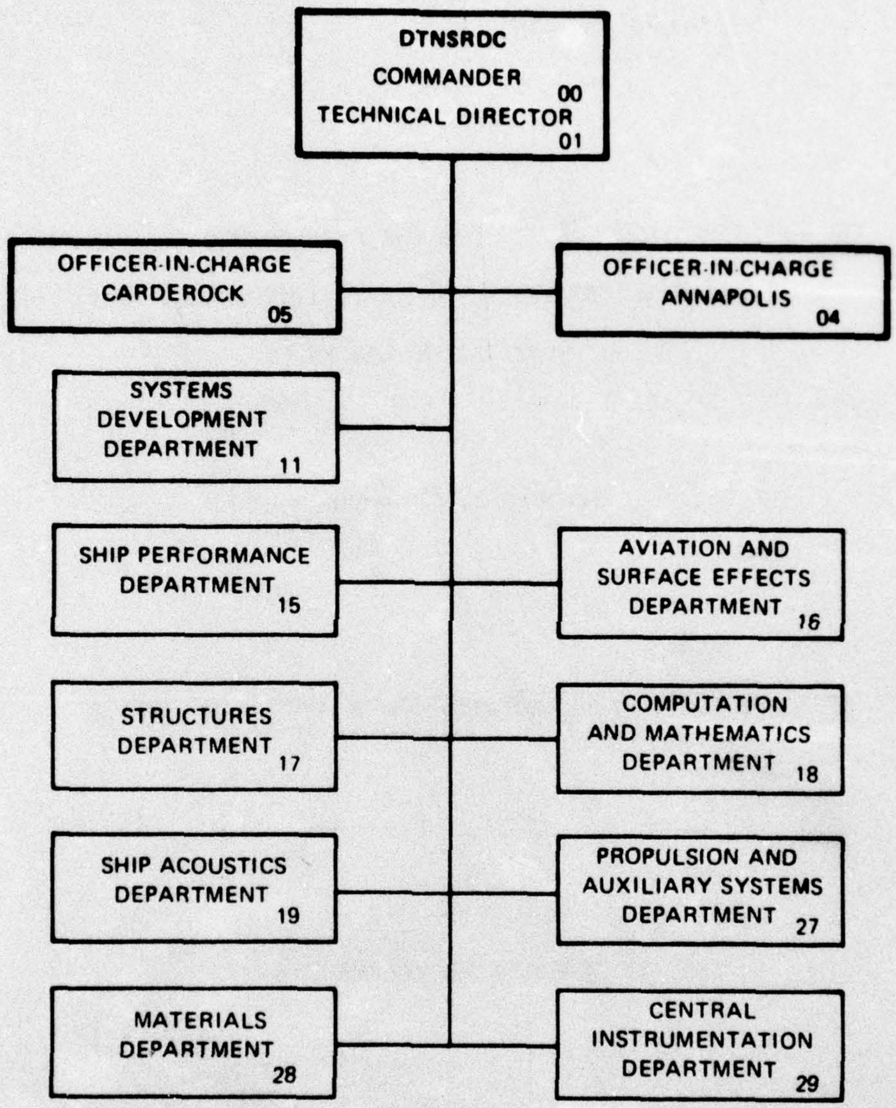

UNCLASSIFIED

SECURITY CLASSIFICATION OF THIS PAGE (When Data Entered)

REPORT DOCUMENTATION PAGE

READ INSTRUCTIONS BEFORE COMPLETING FORM

(14) 1. REPORT NUMBER: SPD-671-01	2. GOVT ACCESSION NO.
3. RECIPIENT'S CATALOG NUMBER	
(6) 4. TITLE (and Subtitle): A NEW EXPERIMENTAL FACILITY FOR THE PERFORMANCE EVALUATION OF STRUT-POD WATERJET INLETS AT CAVITATION SCALED CRAFT SPEEDS IN EXCESS OF 100 KNOTS.	5. TYPE OF REPORT & PERIOD COVERED: (9) Final rept.,
	6. PERFORMING ORG. REPORT NUMBER
(10) 7. AUTHOR(s): Stephen E. Callanen	8. CONTRACT OR GRANT NUMBER(s)
9. PERFORMING ORGANIZATION NAME AND ADDRESS: David W. Taylor Naval Ship R&D Center, Bethesda, Maryland 20084	10. PROGRAM ELEMENT, PROJECT, TASK AREA & WORK UNIT NUMBERS: Task Area 83246, SF 43 432; Task No. 17713, 17231; Work Units 1-1532-301-02, 1-2721-147-06
11. CONTROLLING OFFICE NAME AND ADDRESS: Naval Sea Systems Command, Washington, D.C. 20350	(11) 12. REPORT DATE: Dec[redacted]75
	13. NUMBER OF PAGES: 120
14. MONITORING AGENCY NAME & ADDRESS (if different from Controlling Office): (12) 131p.	15. SECURITY CLASS. (of this report): UNCLASSIFIED
	15a. DECLASSIFICATION/DOWNGRADING SCHEDULE

16. DISTRIBUTION STATEMENT (of this Report)

APPROVED FOR PUBLIC RELEASE: DISTRIBUTION UNLIMITED

17. DISTRIBUTION STATEMENT (of the abstract entered in Block 20, if different from Report)

18. SUPPLEMENTARY NOTES

19. KEY WORDS (Continue on reverse side if necessary and identify by block number)

dynamometer, six-component dynamometer, ram inlets, cavitation performance, sub and supercavitating pods and struts, six-component force balance, waterjet inlets

20. ABSTRACT (Continue on reverse side if necessary and identify by block number)

A new DTNSRDC waterjet inlet experimental facility capable of simulating cavitating conditions which exist on the waterjet inlets of high-speed dynamic-lift type craft is thoroughly described. Included is a detailed discussion of the design and calibration of a new six-component force and moment dynamometer. The primary purpose of this report is to serve as a reference manual for future users of the waterjet inlet testing facility by providing background information, and by demonstrating the measurement capabilities of the system.

TABLE OF CONTENTS

	page
ABSTRACT	1
INTRODUCTION	1
TEST APPARATUS	5
36-INCH VARIABLE PRESSURE WATER TUNNEL	5
Mini-Computer Data Acquisition System	5
EXTERNAL FLOW LOOP ASSEMBLY	7
Piping Circuit	7
Variable Speed Pump	10
Static Pressure Sensor Above Test Section	12
Flow-Rate Measurement	14
SIX-COMPONENT FORCE BALANCE DYNAMOMETER	23
Flexible Coupling	23
Flexures	25
Force-Measuring Block-Gage Elements	27
Calibration Matrices	27
Equations for Computing Resultant Forces and Moments Applied to the Dynamometer	30
Loading Capacities	31
Calculation of Individual Block-Gage Loadings	32
Yaw Adjustment	38
Pitch Adjustment	38

ACCESSION for
NTIS White Section ☑
DDC Buff Section ☐
UNANNOUNCED ☐
JUSTIFICATION
BY
DISTRIBUTION/AVAILABILITY CODES
Dist. AVAIL. and/or SPECIAL
A

DDC
RECEIVED
NOV 9 1976
D

Transition Sections.............................. 39

Mounting of Dynamometer in Tunnel................ 39

Electrical and Pressure Feed-Throughs............ 40

DYNAMOMETER CALIBRATION................................... 41

HARDWARE.. 41

PROCEDURE... 44

TEST PROCEDURE.. 48

SUMMARY OF WATERJET TEST FACILITY CAPABILITY.............. 53

RECOMMENDATIONS FOR FUTURE IMPROVEMENTS................... 55

ACKNOWLEDGMENTS... 60

REFERENCES.. 60a

APPENDIX A - Description of Models Tested................. 61

APPENDIX B - Worthington Corporation - Rating Curves for Horizontal Split Case Double Suction Centrifugal Pump Type 8 LR-13 "A"............ 66

APPENDIX C - Pressure Transducer Calibration (Hardware and Procedure)............................... 67

APPENDIX D - Listing of DTNSRDC Manufacturing Drawings for Waterjet Inlet Testing Facility.................................. 70

APPENDIX E - Listing of Computer Program for Determining Calibration Loading Conditions and Resultant Forces Acting on Block-Gages........ 72

APPENDIX F - Output of Computer Program for Determining Calibration Loading Conditions and Resultant Forces Acting on Block-Gages.... 73

APPENDIX G - Listing of Computer Program for Determining Inverse Calibration Matrix of Interaction Effects by Method of Least Squares........... 75

APPENDIX H - Output of Computer Program for Determining Calibration Matrix of Interaction Effects by Method of Least Squares..... 78

APPENDIX I - Listing of Computer Program for Least Squares Calibration of Pressure Transducers Using CEC Electromanometer System.. 81

APPENDIX J - Output of Computer Program Used for Least Squares Calibration of Pressure Transducers Using CEC Electromanometer System.. 82

LIST OF TABLES

	Page
Table 1 - Summary of Flow Meter Data	17
Table 2 - Inverse Matrix Calibration Coefficients for Waterjet Dynamometer	28
Table 3 - Summary of Model Data	63

LIST OF FIGURES

Figure 1 - Schematic Drawing of DTNSRDC 36-inch Variable Pressure Water Tunnel

Figure 2 - Mini-Computer Data Acquisition System

Figure 3 - Block Diagram of Data Acquisition System

Figure 4 - Schematic Cross Section of Waterjet Test Loop Piping Circuit

Figure 5 - Piping on Discharge Side of Pump

Figure 6 - Control Unit for Variable Speed Pump Drive System

Figure 7 - Piping at Top of Tunnel Test Section

Figure 8 - Schematic Drawing of Supercavitating Model Mounted Beneath 6-Component Dynamometer in DTNSRDC 36-inch Variable Pressure Water Tunnel

Figure 9 - Six-Component Dynamometer with Transition Section For Supercavitating Model Installed

Figure 10 - Ronningen-Petter Ful-Stream Pressure Sensor Shown in Cross Section

Figure 11 - Bailey Meter Company Orifice Plate Flow Tube Assembly

Figure 12 - Bailey Meter Company Multiplate Flow Straightener

Figure 13 - ITT Barton Portable Flow Indicator with Differential Pressure Transducer Attached

Figure 14 - Annubar Flow Measuring Element

Figure 15 - Comparison of Flow Rates Measured with Orifice Plate and Annubar Sensor

Figure 16 - Measured Drag Coefficients for Subcavitating Model as a Function of Inlet Velocity Ratio

Figure 17 - Measured Drag Coefficients For Supercavitating Model as a Function of Inlet Velocity Ratio

Figure 18 - Six-Component Dynamometer - Looking Forward

Figure 19 - Ormond and DTNSRDC Isolation Flexures at Aft End of 6-Component Dynamometer

Figure 20 - DTNSRDC Force Measuring Block-Gage Cube

Figure 21 - Dynamometer Schematic Side View Elevation

Figure 22 - Dynamometer Schematic End View Looking Aft

Figure 23 - Dynamometer Schematic Plan View

Figure 24 - Six-Component Dynamometer Showing Yaw Plate Alignment Holes

Figure 25 - Four Views of Transition Section Used with Subcavitating Model

Figure 26 - Four Views of Transition Section Used with Supercavitating Model

Figure 27 - Six-Component Dynamometer Mounted in Calibration Stand

Figure 28 - Top View of Calibration Stand Showing Top of Dynamometer Calibration Bar

Figure 29 - Dynamometer Undergoing Final Calibration Checks Inside Tunnel Test Section

Figure 30 - Photographs Showing Development of External Lip Cavitation as the Inlet Velocity Ratio is Decreased at a Constant Free Stream Velocity of 31 ft/sec ($\sigma = 0.25$)

Figure 31 - Supercavitating Model Mounted Beneath 6-Component Dynamometer in DTNSRDC 36-Inch Variable Pressure Water Tunnel

Figure 32 - Drawing of Supercavitating Model

Figure 33 - Internal View of Supercavitating Model Showing Splitter Vanes in Elbow and Strut

Figure 34 - Subcavitating Model Mounted Beneath 6-Component Dynamometer in DTNSRDC 36-Inch Variable Pressure Water Tunnel

Figure 35 - Drawing of Subcavitating Model

Figure 36 - Total Pressure Taps at Top of Supercavitating Strut

Figure 37 - CEC Electromanometer System Used for Calibrating Pressure Transducers

ABSTRACT

A new DTNSRDC waterjet inlet experimental facility capable of simulating cavitating conditions which exist on the waterjet inlets of high-speed dynamic-lift type craft is thoroughly described. Included is a detailed discussion of the design and calibration of a new six-component force and moment dynamometer. The primary purpose of this report is to serve as a reference manual for future users of the waterjet inlet testing facility by providing background information, and by demonstrating the measurement capabilities of the system.

INTRODUCTION

The purpose of this report is to describe a new David W. Taylor Naval Ship Research and Development Center (DTNSRDC) facility designed to permit the total performance characterization of strut-pod waterjet inlets at cavitation scaled conditions corresponding to prototype craft speeds in excess of 100-knots.

The development of this waterjet inlet testing facility represents one phase of a major waterjet inlet development effort. The overall program objective includes plans for the design and evaluation of flush and semi-flush inlets, such as those being considered for use on surface effect vehicles and high speed planing craft, as well as the strut-pod inlets currently being used on hydrofoils.

The waterjet inlet has long been identified as one of the most critical components in waterjet propulsion systems and one of the most complex to design. The design of an inlet for application on a high-speed dynamic-lift type vehicle involves many trade offs or compromises to satisfy the requirement for no adverse internal or external cavitation at both low-speed takeoff (hump) and high-speed cruise conditions. The additive drag of the inlet should be minimized and the flow stream should be diffused to produce acceptable pressure and velocity conditions at the inlet flange of the pump. The flow stream must also be turned through several bends in the ducting circuit without causing cavitation or unacceptable hydrodynamic losses. The degree of difficulty of the inlet design problem increases considerably as the cruise speed requirements go up and the spread between takeoff speed and cruise speed widens.

In spite of the problem of optimizing the design of waterjet inlet-ducting systems and the fact that the efficiency of waterjet systems will never match the efficiency of well designed marine propellers, waterjet systems continue to remain strong propulsor candidates for certain types of craft and certain mission requirements. Two of the most important inherent advantages of waterjet systems are lower radiated noise and higher reliability (fewer moving parts) than can be achieved with supercavitating propellers driven through long transmission shafts with heavily loaded angle-drives and sophisticated lube-oil systems. The PGH-2 (Tucumcari) demonstrated that waterjet systems can have high reliability.

Minimal experimental effort has been expended to validate the strut-pod-ducting design methods employed on the Tucumcari, PHM, and SES 100 A, and in general, published experimental data on the drag characteristics of strut-pod waterjet inlets is limited. Undoubtedly, one of the primary reasons for the dearth of experimental data on these inlet types has been the lack of suitable facilities for the investigation of such devices. Most tests have been conducted with towing carriages or small water channels which were not designed to accommodate the evaluation of waterjet inlets. Adding to the dilemma of where to best evaluate waterjet inlets, is the fact that the physical constraints imposed by each type of inlet render it practically impossible to design a single, multipurpose facility capable of testing all types of waterjet inlets.

The facility described in this report utilizes the open-jet test section of the DTNSRDC 36-inch variable pressure water tunnel and is best suited for the evaluation of strut-pod type inlets. However, flush-inlet testing could also be achieved with the same basic flow-loop arrangement and hardware by substituting the closed-jet section in the tunnel and mounting flush-type inlets in the hatch cover.

The new DTNSRDC strut-pod inlet test facility possesses a unique combination of capabilities heretofore unavailable to the Navy. It is the first facility of its size for evaluating ram-inlets that permits simulation of cavitating conditions at craft speeds in excess of 100 knots, while measuring all six force and moment components acting on the inlet-strut assembly. In addition, the inlet forces and moments are measured free of interaction effects from pumps and nozzles. The yaw angle is easily adjustable in one degree increments through plus or minus ten degrees and the pitch angle can be varied with shims. Pressure taps can be located in the model to measure pressure distributions at the inlet and at the top of the strut. Hydrodynamic loss coefficients for the inlet-strut duct system can then be computed. Minimum IVR limits can be determined by visual observation of cavity growth on the external surfaces of the inlet. Maximum IVR limits can be detected by inlet choking. Model vibration frequencies can be measured, and lift/drag ratios for various strut-pod-foil configurations can be determined. All test data can be rapidly collected and analyzed with existing programs on a mini-computer.

In order to thoroughly evaluate the performance capabilities and limitations of the new waterjet inlet experimental facility, two previously tested strut-pod models (Appendix A) were examined over a wide range of cavitation numbers, advance speeds, and inlet velocity ratios. A small sampling of data collected during these preliminary experiments is presented in this report. A detailed description of the results from these inlet experiments will be provided in a follow-on report.

TEST APPARATUS

The waterjet inlet experimental facility consists of three major parts: 1) the DTNSRDC open-jet 36-inch variable pressure water tunnel with its computerized data acquisition system, 2) the external flow loop assembly with its variable speed pump, and 3) the six-component force-balance dynamometer located inside the tunnel test section. Each of these major system components will be discussed in the following sections.

36-INCH VARIABLE PRESSURE WATER TUNNEL

A schematic of the water tunnel is shown in Figure 1. The test section has a variable pressure range from 2 to 60 PSI absolute and a maximum flow rate of 50 knots (84.5 ft/sec). A complete description of the tunnel and its capabilities is contained in References 1 and 2.

Mini-Computer Data Acquisition System

The mini-computer data acquisition system pictured in Figure 2 is a rather recent addition to the tunnel facility and provides a greatly expanded data analysis capability. The computer eliminates the problems and inaccuracies encountered with analog tape recording systems by directly reading each data channel in digital form from the output of the analog-to-digital converter. When the memory bank of the computer is filled, the test data contained within the computer is written in digital form on magnetic tape and thereby preserved for future analysis.

The computer's ability to perform immediate preliminary analysis of the raw test data was an invaluable aid in examining the measured force, moment, and flow-rate values at the conclusion of each set of data collection runs. From these measured values, it was possible to make timely judgements concerning the selection of appropriate tunnel velocity and pressure conditions for subsequent test runs.

The mini-computer system is composed of the following hardware items depicted in Figures 2 and 3: 1) an "Interdata"* computer with 24K memory, 2) an "Analogic"** Series AN-5200 analog to digital converter, 3) a "Tri-Data"*** Model 1024 "Cartri File" cartridge type tape recorder, 4) a "Teletype"**** model 33 automatic send-receive (ASR) terminal, and 5) a "Printec"***** Model 100 printer.

The mini-computer's machine language data collect program was set up to record average values from twelve data channels over a five second data collection interval. During each five second

---

*Interdata Inc., Oceanport, New Jersey

**Analogic Corporation, Wakefield, Massachusetts

***Tri-Data Corporation, Mountain View, California

****Teletype Corporation, Skokie, Illinois

*****Printer Technology Inc., Woburn, Massachusetts collection interval the twelve data channels were sampled sequentially 2,048 times. This means that a 12-channel data collection cycle was completed every 0.0024 seconds and that the time interval between individual data collect points was 0.0002 seconds. Because of the rapid speed at which the computer sequentially collected data, it was assumed for practical purposes that the steady state tunnel conditions, as characterized by the 12-data channels, were recorded and averaged simultaneously over the same time base.

The analog to digital converter has a 13 bit (including sign) A to D capability, a conversion speed of 2 micro-seconds per bit, a frequency response of 38 kilo-hertz per channel, and it can handle signal amplitudes between ± 5 volts.

EXTERNAL FLOW LOOP ASSEMBLY

The external flow loop is pictured in Figure 4 with the water tunnel shown in cross section. The purpose of the flow loop is to control the flow rate through the waterjet inlet, and hence the inlet velocity ratio. With this variable speed pump system, the flow rate is infinitely variable between the blocked no-flow condition and the maximum flow condition, which is determined by inlet choking.

Piping Circuit

A six-inch I.D. aluminum pipe extends from the top of the test section down to the diffuser section located near the pump. This diffuser section serves as a transition piece between the 6-inch I.D. vertical aluminum pipe and the 10-inch I.D. elbow which connects to the suction side of the pump. Obviously a larger diameter pipe could be used between the test section and the pump to reduce pressure losses if necessary. However, the six-inch I.D. pipe worked quite satisfactorily with the flow rates and pump suction heads encountered in our test program.

As a precaution against electrolytic corrosion between the aluminum pipe and the stainless clad tunnel, cathodic protection was provided between the aluminum-steel interface flanges with special phenolic insulating gaskets, sleeves, and washers.* In addition, type 3003 aluminum alloy pipe was used because of its superior corrosion resistance properties.

The water tunnel test section is soft mounted on springs and therefore it was necessary to place a flexible rubber coupling in the aluminum pipe leading from the test section. All piping above the flexible coupling is anchored to, and moves with, the test section. Below the flexible joint, the aluminum pipe is anchored to the building structure.

A strainer is located on the discharge side of the pump as a precaution to protect the sharp edged flow measuring orifice plate

---

*Manufactured by Central Plastics Co., Shawnee, Oklahoma and PSI Products Inc., Burbank, California from debris which might find its way into the piping circuit. The greatest opportunity for foreign material to enter the flow loop presents itself during assembly and disassembly of the piping in the proximity of the tunnel test section.

Two valves are installed in the flow loop at the point where the water is discharged back into the lower horizontal branch of the tunnel (Figure 4). A gate valve is located directly over the tunnel hatch cover to provide for positive shut-off when the flow loop is not in use. A butterfly valve is located upstream from the gate valve to provide a simple throttling capability, and to provide a quick and easy means of establishing a blocked flow condition when tests are in progress.

An unsuccessful attempt was made to provide a capability for visually observing cavitation inception within the flow loop by installing a transparent plexiglass spool piece above the tunnel test section at the lowest pressure point in the piping circuit. Unfortunately, the plexiglass section became highly stressed and cracked as it was being bolted into position and, therefore, had to be replaced with an aluminum spool piece.

Variable Speed Pump

The pump is a standard commercial Worthington* double-suction single-stage centrifugal type 8LR-13"A" with a 12-inch diameter impeller, an 8-inch diameter discharge, and a nominal capacity between 2000 and 2500 GPM at a rated speed of 1750 RPM (Figure 5 and References 3,4 and 5). This type pump is well suited for waterjet inlet choking tests because it can operate with relatively low net positive suction heads. The maximum flow rate through the loop was only about 810 GPM for the models tested and, therefore, the pump capacity was not a factor in limiting the maximum obtainable inlet velocity ratio (i.e., flow rate through the model inlet).

The head-capacity curves for this pump at four different impeller speeds are included in Appendix B for future reference. No attempt was made during the test program to characterize pump performance corresponding to flow conditions in the tunnel test section. Pump speed and flow rate data were recorded during the tests, but the suction and discharge pressures at the pump were not. An in depth understanding of pump head-capacity relationships was simply unnecessary for the evaluation of the waterjet inlets which were tested.

The pump is driven with a General Electric "Speed Variator" (Model 6V75F 3178) D-C SCR variable speed drive system which consists of: 1) a 75 horse-power, 1750 RPM, 550 volt, 110 amp, stabilized shunt wound D-C motor, 2) an SCR power conversion unit

*Worthington Pump International, East Orange, New Jersey which converts three phase A-C power into adjustable voltage D-C power for driving the motor armature, the drive regulator, and other required control devices, and 3) an operator's control unit including the speed setting potentiometer and start-stop buttons. The power conversion unit is supplied from a 480 volt, 3-phase, 60 Hertz source. The operator's control unit (Figure 6) was modified at DTNSRDC (drawing B-922-1) to provide finer speed control and remote monitoring of motor voltage and current. The motor controller is located at the tunnel control console during tests and is operated by the tunnel operator.

The variable speed drive system is designed to provide continuous operation at rated torque over a speed range of 60-100 percent, smooth adjustable acceleration from zero to any preset speed, and essentially zero speed regulation (no change in speed with change in load) at any selected speed within the controlled speed range. Additional electrical features of the drive system include:

a) adjustable protective current limit within the range of 80%-150%

b) adjustable maximum speed

c) undervoltage protection by use of a motor disconnect contactor

d) static instantaneous overcurrent (IOC) trip for protection of motor, load, and power unit

e) motor thermal overload protection by motor thermostat

f) A-C line-phase sequence indication

g) loss of phase protection

h) A-C and D-C line-voltage surge protection

i) A-C current limiting line fuses

For detailed information on the variable speed drive system refer to the General Electric instruction manual listed as Reference 6.

Motor speed was monitored with a "Dynapar"* Model 80H-600 Rotopulser mounted on the end of the motor shaft opposite the pump. The photo-electric Rotopulser produces 600 pulses per revolution and is similar to the units currently used at the tunnel for measuring the RPM of the main impeller shaft and the right-angle drive dynamometer. Existing tunnel facility signal conditioning systems were used with the new Rotopulser. A detail of the pump, motor, and Rotopulser assembly is shown on DTNSRDC Drawing E-3056-22.

Static Pressure Sensor Above Test Section

At the top of the tunnel test section a special patented "Ronningen-Petter" pressure transmitting device** was inserted into

*Dynapar Corporation, Gurnee, Illinois

**Dover Corporation, Ronningen-Petter Division, Portage, Michigan the piping circuit between the hatch cover and 90 degree elbow (Figure 7). The purpose of this pressure transmitting spool piece was to provide an average static pressure measurement above the dynamometer for determining the internal pressure forces exerted vertically at the top of the transition section. The transition section is located inside the tunnel between the top of the strut and the dynamometer's flexible coupling as shown in Figures 8 and 9. For further discussion of the transition section see the section of this report entitled Transition Sections.

A schematic cross section of the Ronningen-Petter Ful-Stream pressure transmitter is shown in Figure 10. The flow loop static pressure is sensed by the flexible cylinder and transmitted via the captive sensing liquid to the externally mounted pressure transducer shown in Figure 7. Also shown in Figure 7 is the valve used to protect the pressure transducer from over-pressure during tunnel filling operations.

With 2 and 4 PSIA tunnel test section pressures and high flow rates through the loop, it was not possible to accurately determine the extremely low pressures which existed at the Ronningen-Petter device. These low pressures could not be accurately measured because of difficulty encountered in trying to reference the output of the absolute pressure transducer to the atmospheric pressure value used as a reference for the tunnel test section.

Nevertheless, the data obtained from the absolute pressure transducer qualitatively match the pressure data obtained from static manometer taps located inside the tunnel and immediately below the Ronningen-Petter device. Cavitation inception within the flow loop was immediately evidenced by extremely low pressure readings from the Ronningen-Petter sensor.

Flow-Rate Measurement

The flow rate through the loop was measured with two devices: 1) Bailey Meter Company thin-plate square-edged concentric orifice flow tube assembly with flow straightener, and 2) a patented "Annubar" flow measuring element.*

The orifice plate located in the vertical leg on the discharge side of the pump was considered the primary flow metering device. An orifice-type meter was selected over more sophisticated devices, such as venturi, sonic, or magnetic flowmeters, because of its high accuracy (high predictability of discharge coefficient), ease of installation and/or replacement, inherent simplicity, and relatively low cost.

Orifice plate calibration factors (discharge coefficients)

---

* Dieterich Standard Corporation, Ellison Instrument Division, Boulder, Colorado

have been so well established and standardized by the American Society of Mechanical Engineers and the International Standards Association that orifice-type flow meters are used extensively for important measurements without calibration.* The accuracy tolerance assigned to the discharge coefficients used to compute flow rates with square-edged concentric orifices having flange taps is $\pm$0.55 percent of the coefficient value.** This accuracy figure applies to the 8-inch I.D. pipe size used in the waterjet flow loop and to orifice plates with orifice-to-pipe diameter ratios (d/D) between 0.20 and 0.70. The fact that the orifice type flow meter could be confidently used without a primary calibration was an important consideration in its selection. Without proper facilities, it is not an easy task to calibrate a flow tube assembly designed to measure up to 2,000 GPM and, therefore, considerable savings were realized by choosing a primary flow metering element which did not require calibration.

The disadvantages normally associated with orifice plates have no bearing on this particular application. The relatively high unrecoverable pressure loss caused by orifice plates is of no consequence since adequate pump head exists and operational efficiency is not a consideration. The square root calculation,

---

* Reference 7, p. 43

** Reference 7, p. 188

required to compute flow rate from the differential pressure measured across the orifice, is automatically accomplished with the computerized data acquisition system.

The accuracy of head-type flow meters falls off below 20 or 30 percent of full rated flow and, therefore, several orifice plates were purchased - each sized for a different flow rate, but with the same differential pressure at full flow. Orifice plates with 500, 1,000, 1,500, and 2,000 GPM capacities are available to accommodate a variety of model flow rates. These particular capacities were selected to permit the use of simple multiplication factors on the direct reading square-root dial face scale of the Model 247 Barton ITT flow rate indicator which was used to monitor flow rate at the pump. The 1,000 GPM orifice plate was selected as the optimum size for the preliminary experimental program. A summary of data pertaining to all four of the available orifice plates is provided in Table 1. An effort was made to keep the orifice-to-pipe diameter ratios for all the orifice plates between 0.2 and 0.6 as recommended by Spink (Reference 8).

The Bailey Meter flow tube assembly shown in Figures 5 and 11 (See also Bailey Meter Co. Product Specification Sheet No. G23-3) has an overall length of 112-inches with the orifice flange union located 32-inches from the downstream end of the tube. The flow tube was fabricated by boring out a piece of schedule 40 carbon

TABLE 1

SUMMARY OF FLOW METER DATA

	Orifice Plate Data				Annubar Sensor Data**
Maximum Rated Flow Rate (GPM)	500	1000	1500	2000	2500
Minimum Recommended Flow Rate	100-500	200-300	300-450	400-600	200
Coefficient of discharge (C)*	18.99	37.98	56.97	75.96	150.09
Orifice I.D. (d)	2.362	3.314	4.015	4.574	-
Pipe I.D. (D)	7.981	7.981	7.981	7.981	5.065
Orifice-to-Pipe diameter (Beta) Ratios (d/D)	.296	.415	.503	.573	-
Pressure Differential at Maximum Rated Flow	25 psi	25 psi	25 psi	25 psi	10 psi
Material	304 SS	304 SS	304 SS	304 SS	316 SS

For a derivation of the empirical discharge coefficients see:

"Principles and Practice of Flow Meter Engineering," L. K. Spink, 9th Edition, p. 527 (Reference 8).

"Fluid Meters, Their Theory and Application," ASME Research Committee on Fluid Meters, (Reference 7).

* Flow Rate (GPM) = $C \cdot (\Delta P)^{1/2}$, where (ΔP) is expressed in inches of water

** Annubar Serial Number 46036, Model No. 741-316-SS, Calculation No. 5760-20587 steel pipe. At either end of the flow tube are standard 150 lb 1/16-inch raised face welding neck flanges. Flange type pressure taps are used on the 300 lb orifice flange union which possesses jacking screws to facilitate changing orifice plates.

To insure maximum flow measurement accuracy it is essential that the water enter the orifice plate with a fully developed turbulent velocity profile, free from swirls or vortices.* It is, therefore, common practice (Reference 10) to locate long lengths of straight pipe immediately ahead of the orifice. Physical constraints prevented the use of long straight pipe runs at the 36-inch water tunnel and, therefore, it was necessary to locate a flow straightener at the end of the flow tube assembly upstream from the orifice plate. The purpose of the flow straightener is to produce uniformly turbulent flow at the orifice regardless of the layout of the preceding piping. The use of flow straighteners is recognized as good practice in any laboratory metering section or testing installation where high accuracy water flow measurement is required. (Reference 11)

Two types of commercially available flow straighteners are on hand for use with the flow tube assembly. A 16-section carbon steel egg-crate (cross-plate) vane type flow straightener was used during the test program. A stainless steel multiplate type flow straightener arrived after the test program had been completed.

---

* Reference 9, p. 164

Although the multiplate flow straightener introduces a higher pressure loss, it has been shown to be superior to the egg-crate straightener in producing uniformly turbulent flow. Each passageway of the egg-crate straightener is continuous throughout its length and while the vanes break-up the whirl or swirl into 16-compartments, local swirls can still exist and be carried through.

The multiplate straightener consists of three perforated plates in series, spaced about one pipe diameter apart. Each plate has a large number of round holes arranged in a symmetrical pattern (Figure 12). As the flow stream passes through the series of perforated plates and the open areas between the plates, it is broken into small sections which tend to dissipate the helical motion of the swirl and a considerable loss of pressure occurs due to the transfer of pressure energy into kinetic energy. The superior performance of the multiplate flow staightener is experimentally documented in Reference 12.

The differential pressure across the orifice plate was measured simultaneously with a "Validyne"* 25 PSI reluctance-type differential pressure transducer (See Appendix C for calibration information) and a "Barton ITT" Model 247 portable flow indicator.**

---

* Validyne Engineering Corporation, Northridge, California

** Barton ITT, Monterey Park, California

The output of the Validyne transducer is read by the computer during data collection runs. The Barton flow meter provides a direct and continuous mechanical readout of the flow rate. It is used for setting system flow rates (IVR ratios), for observing unstable flow conditions caused by choking at the waterjet inlet, and as a secondary calibration standard for checking the accuracy of the flow measurements made with the computerized data acquisition system.

The Barton flow indicator is shown in Figure 13. The indicator is actuated by dual, rupture-proof beryllium copper bellows with integral temperature compensation. The bellows are liquid filled and can withstand repeated over-ranges without causing a calibration change. The instrument is accurate to 1/2 percent of full-scale differential pressure, requires no lubrication or regular maintenance, and intermittent operation does not affect accuracy of performance. A three-valve manifold on the flow meter is used for zero checks. Valves are also provided on the instrument housing for bleeding or venting. The meter face has a six-inch diameter dial for maximum readability and a square root scale for easy direct observation of the flow rate in gallons per minute.

Because of the importance of the flow rate measurement in the waterjet test loop facility, a redundant "Annubar" flow measuring element was installed at the bottom of the vertical 6-inch pipe run on the suction side of the pump. Normally flow metering elements are not placed on the suction side of a pump, however, it was desirable in this particular case due to the extremely low pressure drop caused by the Annubar sensing element and the extremely long straight run of pipe upstream from the pump. The vertical 6-inch pipe leg measures more than 24 feet in length and totally eliminates the need for any type of flow straightening device. The pressure drop across the Annubar sensor is only 1.6 PSI at a flow rate of 1000 GPM, as compared to the 25 PSI pressure differential across the orifice plate at the same 1000 GPM flow rate.

The Annubar sensor shown in Figure 14 is an inexpensive, relatively new, patented device which measures flow rate by means of a multiplicity of ports precisely located on the upstream side of a small diameter tube placed normal to the flow. The holes in the tube sense total pressure within different equal area annular segments across the flow stream, and produce an average flow rate regardless of flow profile. The small tube element pointing downstream measures static pressure, less the suction pressure of the flow.

The remarkably close correspondence of flow rate values read with the orifice plate and the Annubar sensor is shown in Figure 15. This figure indicates that if for any reason it should become either desirable or necessary to eliminate the pressure drop caused by the orifice plate on the discharge side of the pump, that the Annubar sensor could be relied upon to accurately measure flow rate in the test loop.

The differential pressure across the Annubar sensor was measured with a 5 PSI Validyne reluctance-type differential pressure transducer (See Appendix C for calibration information) and a second Barton Model 247 portable flow indicator. To optimize the meter's accuracy over the range of flow rates anticipated for most tests, full range on the dial face was selected as 1,500 GPM at 100-inches water column differential.

SIX-COMPONENT FORCE BALANCE DYNAMOMETER

A special six-component dynamometer (Figures 8 and 9) was designed for measuring the force and moment components acting on a strut-pod waterjet inlet. It is the first six-component force balance dynamometer of this type constructed for use inside the DTNSRDC 36-inch variable pressure water tunnel facility. Although the dynamometer possesses unique features which make it especially suited for waterjet testing, it obviously could be used for measuring the forces and moments on any body mounted in the open-jet test section of the tunnel. (See Appendix D for listing of manufacturing drawings.)

Flexible Coupling

One feature which distinguishes this dynamometer from others is the flexible coupling which permits passage of a six-inch diameter column of water through its center. This combination rolling diaphragm-"O"-ring type coupling causes minimal interaction between the various force and moment components, regardless of tunnel test pressure. This new coupling design represents a significant improvement over a previously used DTNSRDC towing carriage waterjet dynamometer which required pressure calibrations to obtain approximate correction factors for the lift and drag forces, (Reference 13).

To demonstrate that the flexible coupling has minimal influence on the measured forces irrespective of tunnel pressure, Figures 16 and 17 are presented. Each of these figures show negligible change in the measured drag coefficient for two different tunnel pressure and velocity conditions representing approximately the same cavitation number. The conditions in Figure 16 correspond to a prototype velocity of approximately 28-knots with fully wetted flow everywhere on the 50-knot subcavitating Lockheed model having faired trailing edge surfaces. The conditions in Figure 17 represent a prototype velocity of approximately 37-knots with the 76-knot supercavitating Lockheed model having blunt trailing edges on the strut and nacelle.

The frictional resistance of the sub and supercavitating models for each velocity condition was calculated to determine if the change in viscous drag with Reynolds Number was large enough to significantly influence the data presented in Figures 16 and 17. The Schoenherr frictional resistance coefficients were calculated using average chord lengths and approximate wetted surface areas, and were then referenced to the projected frontal areas of the models to permit a quantitative comparison of the viscous drag with the total measured drag coefficients plotted in Figures 16 and 17. At design IVR conditions the calculated differences in the frictional drag coefficients, resulting from changes in Reynolds

Number, were approximately 1.2 and 0.6 percent of the total drag coefficients for the sub and supercavitating models respectively. Since these Reynolds Number effects were smaller than the overall resolution of the force measuring system, it was concluded that the small difference in the measured drag for the two test conditions could not be explained by changes in viscous drag effects, but rather resulted from scatter of the experimental data. The resolution of the system does not permit measurement of extremely small changes in viscous drag. During future experimental programs the flexible coupling should be evaluated over a wider range of tunnel pressures and cavitation numbers.

A detail of the flexible coupling is shown in Figure 8 (DTNSRDC drawing E-3056-2). It has a circular shape and is located at the top of the transition section. A standard I.D. pipe size (6.065 inches) was selected for the flexible coupling to provide a cross-sectional area roughly approximating the ducting areas at the top of those model struts expected to be used with the facility.

Flexures

One of the outstanding features of the dynamometer is the low mechanical interaction, or cross-coupling, resulting from compound loading conditions. Flexures, which can be seen in Figures 9 and 18, effectively isolate each block-gage transducer element from all undesirable cross-coupling forces and moments. The two flexures shown in Figure 19 are normally hidden from view by the force-transmitting cylinder which can be seen in the foreground of Figure 18. The bottom flexure in Figure 19 is a special patented (Reference 14) universal flexure (Model UNF-MM4-10K) commercially available from Ormond, Inc., Santa Fe Springs, California. The flexure was manufactured from 17-4 PH-stainless steel, heat treated at 1000 degrees Fahrenheit for four hours and air cooled to provide optimum mechanical properties. The Ormond flexure functions in the same fashion as a universal ball-joint providing birotational (two-degree) freedom of motion. The two orthogonal axes of rotation are coincident, and thus the universal flexure movement, in all directions, takes place about a single central point. The universal flexure can transmit relatively large tension, compression, shear (side), or torsional forces.

The top flexure unit in Figure 19 is compliant in torsion and provides a third degree of freedom. This 8-leaf torsion flexure was manufactured at DTNSRDC (drawing E-3056-17) from 17-4PH stainless steel and heat treated in the same fashion as the Ormond flexure.

The Ormond universal flexure and DTNSRDC torsional flexure act in tandem to prevent any bending stresses from being transmitted up through the stack of block gages at the aft end of the dynamometer. As a result, only pure drag, lift, and side forces are imposed on the three aft gages. These 4-inch block-gage cubes (Figure 20) have demonstrated, through years of testing and evaluation at DTNSRDC, that they are extremely insensitive to large tension, compression, and transverse shear loadings.

Force-Measuring Block-Gage Elements

An excellent description of the "block-gage" is contained in NSRDC Hydromechanics Laboratory Test and Evaluation Report 2523 (Reference 15) and U.S. Patent 3,052,120 (Reference 16). It should be noted that the block-gage signal conditioning system, as described in Report 2523, has been changed. Originally, the variable-reluctance transducing elements were driven with a 400-hertz carrier frequency and 4.5-volt excitation. It has now become common practice to drive the block gages with a 3-kilohertz carrier and approximately one volt AC excitation using a commercially available "Endevco"* Model 4478.1A signal conditioning carrier amplifier unit which is modified at DTNSRDC to provide a measurement system with a gain that does not drift, superior linearity, and superior zero stability.

Calibration Matrices

Three six-by-six calibration matrices are presented in Table 2 to show both the small degree of mechanical interaction caused by compound loading conditions and the small amount of interaction

---

*ENDEVCO Corp., Dynamic Instrument Division, San Juan Capistrano, California

TABLE 2
INVERSE MATRIX CALIBRATION COEFFICIENTS FOR WATERJET DYNAMOMETER

With Flexible Coupling and Transition Piece for Supercavitating Model Installed

$$\text{DRAG} = 1.000 * F_D - .014 * F_S + .000 * F_L + .000 * M_Y + .000 * M_P + .000 * M_R$$

$$\text{SIDE F.} = .002 * F_D + 1.002 * F_S - .001 * F_L - .001 * M_Y + .000 * M_P - .003 * M_R$$

$$\text{LIFT} = .008 * F_D + .008 * F_S + 1.000 * F_L + .000 * M_Y + .002 * M_P + .001 * M_R$$

$$\text{YAW} = .020 * F_D + .000 * F_S + .016 * F_L + .973 * M_Y - .002 * M_P + .000 * M_R$$

$$\text{PITCH} = 1.097 * F_D - .134 * F_S + .000 * F_L - .007 * M_Y + 1.001 * M_P - .021 * M_R$$

$$\text{ROLL} = -.020 * F_D - .762 * F_S + .001 * F_L + .023 * M_Y + .007 * M_P + 1.024 * M_R$$

With Flexible Coupling and Transition Piece for Subcavitating Model Installed

$$\text{DRAG} = 1.000 * F_D - .005 * F_S + .000 * F_L + .000 * M_Y + .000 * M_P + .000 * M_R$$

$$\text{SIDE F.} = .000 * F_D + 1.001 * F_S - .001 * F_L - .001 * M_Y + .000 * M_P - .002 * M_R$$

$$\text{LIFT} = .003 * F_D - .001 * F_S + 1.000 * F_L + .000 * M_Y + .002 * M_P + .002 * M_R$$

$$\text{YAW} = -.003 * F_D - .001 * F_S + .016 * F_L + .981 * M_Y - .003 * M_P + .004 * M_R$$

$$\text{PITCH} = .916 * F_D - .094 * F_S + .000 * F_L - .010 * M_Y + .993 * M_P - .023 * M_R$$

$$\text{ROLL} = .008 * F_D - .465 * F_S + .001 * F_L + .024 * M_Y + .007 * M_P + 1.006 * M_R$$

With Flexible Coupling Removed

$$\text{DRAG} = 1.000 * F_D - .002 * F_S + .002 * F_L + .000 * M_Y + .000 * M_P + .000 * M_R$$

$$\text{SIDE F.} = -.002 * F_D + 1.000 * F_S + .001 * F_L + .001 * M_Y + .000 * M_P + .000 * M_R$$

$$\text{LIFT} = .015 * F_D + .000 * F_S + 1.000 * F_L + .000 * M_Y + .001 * M_P + .003 * M_R$$

$$\text{YAW} = .173 * F_D + .000 * F_S + .035 * F_L + 1.019 * M_Y - .001 * M_P + .000 * M_R$$

$$\text{PITCH} = .275 * F_D - .003 * F_S + .001 * F_L - .001 * M_Y + .997 * M_P - .036 * M_R$$

$$\text{ROLL} = -.004 * F_D - .127 * F_S + .000 * F_L + .000 * M_Y + .000 * M_P + .989 * M_R$$

generated by the flexible coupling. The extremely small interaction coefficients for the drag, lift, and side forces, in each of the three matrices, should be noted. The magnitude of the moment interaction coefficients cannot be totally explained without additional calibration checks. Inaccuracies in the loading points on the bar-type fixture used to apply pitching and rolling moments, might have affected the moment interaction coefficients. For further discussion of the dynamometer calibration, see the DYNAMOMETER CALIBRATION section of this report.

A comparison of the matrices, with and without the flexible coupling installed, shows a significant reduction in the influence of drag on pitching moment and side force on rolling moment with the flexible coupling removed. These interactions can easily be reduced by increasing a few clearances on the flexible coupling assembly. The influence of drag on yawing moment, evidenced with the flexible coupling removed, is likely the partial result of using only a one-hundred pound side force block-gage at the aft end of the dynamometer. A two-hundred pound gage (same capacity as forward side force gage number 3) would provide improved performance with no loss of measurement accuracy.

In spite of the interactions mentioned above, the overall performance of this dynamometer must be rated as very good. With a few minor modifications to the flexible coupling and the calibration stand,* it should be possible to reduce the interactions even further.

Equations for Computing Resultant Forces and Moments Applied to the Dynamometer

The sum and differencing equations used with the waterjet dynamometer to compute applied force and moment loading components are listed below (See Figures 18, 21, 22 and 23):

Drag Force = Gage #5

Side Force = Gage #3 + Gage #4

Lift Force = Gage #1 + Gage #2 + Gage #6

Pitching Moment = 14.0·[Gage #6 - Gage #1 - Gage #2]

Rolling Moment = 10.5·[Gage #1 - Gage #2]

Yawing Moment = 14.0·[Gage #3 - Gage #4]

The constants 14.0 and 10.5 are distances in inches from the dynamometer's center-of-moments to the flexure centerline locations where forces are transmitted to the block-gages. Block-gage numbers, 1, 3, 4, 5 and 6 are visible in Figure 18. Gage #1 is shown in the upper left-hand corner at the forward end of the dynamometer. Gage #3 is shown attached to the horizontal flexure at the forward end of the dynamometer. Gage numbers 4, 5, and 6 are located in the three-gage stack at the aft end of the dynamometer. Gage #4 is at the bottom, Gage #5 is in the middle, and Gage #6 is at the top. Gage #2 is opposite Gage #1 on the starboard side of

*See DYNAMOMETER CALIBRATION section of this report the dynamometer and is best shown in the upper right-hand corner of Figure 9 at the forward end of the dynamometer.

The equations presented above and the block-gage output polarities are arranged to produce force and moment sign conventions in accordance with a right-hand coordinate system where lift forces are positive in the upward direction, side forces are positive toward port, and drag forces are negative in the aft direction. The correct polarities are easily established with the dynamometer in the calibration stand.

Loading Capacities

The flexures used in the dynamometer were originally designed to withstand 33,000 pound-inches of pitch, 33,000 pound-inches of roll, 10,000 pound-inches of yaw, and 1000-pounds of drag, lift, and side force. Depending upon the locations where the force components are assumed to act, the block-gages could experience the following worst case of loadings: Gages 1 and 2 approximately 2,410 lbs, Gages 3 and 4 approximately 858 lbs, Gage 5-1,000 lbs, and Gage 6 approximately 1679 lbs. The actual loads experienced by individual block-gages can vary considerably since all the gages, with the exception of number 5 which experiences only pure drag, must transmit forces generated by a combination of the moments and forces acting on the dynamometer. Gages 1 and 2 simultaneously experience loads generated by lift force, pitching moment, and rolling moment. Gages 3 and 4 are affected by side force and yawing moment, while Gage 6 is influenced by lift force and pitching moment. Because of the complex manner in which the block-gages are loaded, care must be exercised during a test to ensure that none of the gages become overloaded.

It is good practice to always use gages with the same capacity (gage pairs) at locations 1 and 2 and locations 3 and 4. It is also advisable to yaw a model to port rather than starboard if large side loadings and yawing moments are anticipated. This will keep the forward horizontal flexure in a stable tension condition rather than placing the flexure in compression where column buckling becomes a consideration.

Calculation of Individual Block-Gage Loadings

To assist in calculating estimated block-gage loadings, schematic drawings of the dynamometer are presented in Figures 21, 22, and 23 in conjunction with the equations which follow. The arrows in the equations indicate the direction, up (↑) or down (↓), in which the forces act. The constants are determined by the dimensions between loading points on the dynamometer, and the percentage of each force component carried by the various block-gages. The drag, lift, and side forces are represented in the equations with the following symbols:

F_D = Drag Force

F_L = Lift Force

F_S = Side Force

Distances a, b, c, d, e, and f are identified in Figures 21, 22, and 23.

Equations for calculating block-gage loadings:

Force on Block-Gage 1 =

$$F_L/4\uparrow + \underbrace{(F_L \cdot a)/21\uparrow + (F_S \cdot b)/21\uparrow}_{\text{(Force components generated by rolling moment.)}} + \underbrace{(F_L \cdot c)/56\uparrow + (F_D \cdot d)/56\downarrow}_{\text{Force components generated by pitching moment.)}}$$

Force on Block-Gage 2 =

$$F_L/4\uparrow + \underbrace{(F_L \cdot a)/21\downarrow + (F_S \cdot b)/21\downarrow}_{\text{(Force components generated by rolling moment.)}} + \underbrace{(F_L \cdot c)/56\uparrow + (F_D \cdot d)/56\downarrow}_{\text{Force components generated by pitching moment.)}}$$

Force on Block-Gage 3 =

$$\overset{\text{Port}\ \rightarrow}{F_S/2} + \underbrace{\overset{\text{Port}\ \rightarrow}{(F_S \cdot e)/28} + \overset{\text{Port}\ \rightarrow}{(F_D \cdot f)/28}}_{\text{(Force components generated by yawing moment.)}}$$

Force on Block-Gage 4 =

$$\overset{\text{Port}\ \rightarrow}{F_S/2} + \underbrace{\overset{\text{Stbd.}\ \leftarrow}{(F_S \cdot e)/28} + \overset{\text{Stbd.}\ \leftarrow}{(F_D \cdot f)/28}}_{\text{(Force components generated by yawing moment.)}}$$

Force on Block-Gage 5 = F_D

Force on Block-Gage 6 =

$$F_L/2\uparrow + \underbrace{(F_L \cdot c)/28\downarrow + (F_D \cdot d)/28\uparrow}_{\text{(Force components generated by pitching moment.)}}$$

It is assumed that the drag, lift, and side forces are applied in the directions and approximate locations shown in the figures. Obviously, if the location where the resultant lift and side forces act is changed, such that the forces are applied on the opposite side of the dynamometer's center of moments, then the direction of each lift and side force term in the above equations will change. Also, if negative lift is assumed, the direction of all of the lift force terms should be reversed. Likewise, if the resultant side force acts toward starboard, instead of port, the direction of all side force terms should be reversed. If the yaw angle of the model is set equal to zero and the model is symmetrical in the plane perpendicular to the direction of flow, all side force, yawing moment, and rolling moment terms drop out of the above equations.

To simplify the procedure of applying the above equations and to determine equivalent pan weight loadings with the dynamometer in the calibration stand, a program was written for the mini-computer and is available on a "Tri-Data" magnetic tape cartridge. A copy of the program with sample output is contained in Appendices E and F.

Block-gage capacities for the test program described in this report were selected on the basis of the following worst case assumed dynamometer loading conditions:

Drag Force = 500 lbs.

Lift Force = 500 lbs. (acting upward)

Side Force = 200 lbs. (acting toward port)

The above forces were assumed to be located as per Figures 21, 22, and 23 with:

a = 2 inches	d = 25 inches
b = 22 inches	e = 8 inches
c = 5 inches	f = 4 inches

Inserting these values in the above equations yielded the following block-gage loadings:

$$\text{Force on Block-Gage 1} = \underbrace{125\uparrow}_{\text{Lift Force}} + \underbrace{47.6\uparrow + 209.5\uparrow}_{\text{Rolling Moment Forces}} + \underbrace{44.6\uparrow + 223.2\downarrow}_{\text{Pitching Moment Forces}}$$

$$= \underline{203.5\uparrow\ \text{lbs}}.\ \text{(Resultant Force)}$$

$$\text{Force on Block-Gage 2} = \underbrace{125\uparrow}_{\text{Lift Force}} + \underbrace{47.6\downarrow + 209.5\downarrow}_{\text{Rolling Moment Forces}} + \underbrace{44.6\uparrow + 223.2\downarrow}_{\text{Pitching Moment Forces}}$$

$$= \underline{310.7\downarrow\ \text{lbs}}.\ \text{(Resultant Force)}$$

$$\text{Force on Block-Gage 3} = \underbrace{\overrightarrow{100}}_{\text{Side Force}} + \underbrace{\overrightarrow{57.1} + \overrightarrow{71.4}}_{\text{Yawing Moment Forces}}$$

$$= \underline{\overrightarrow{228.5}\ \text{lbs}}.\ \text{(Resultant Force toward Port)}$$

Force on Block-Gage 4 = $\overrightarrow{100} + \overleftarrow{57.1} + \overleftarrow{71.4}$

(100 = Side Force; 57.1 + 71.4 = Yawing Moment Forces)

$= \overleftarrow{28.5}$ lbs. (Resultant Force toward Starboard)

Force on Block-Gage 5 = 500 lbs. (Drag in Aft Direction)

Force on Block-Gage 6 = $250^{\uparrow} + 89.3^{\downarrow} + 446.4^{\uparrow}$

(250 = Lift Force; 89.3 + 446.4 = Pitching Moment Forces)

$= 607.1^{\uparrow}$ lbs. (Resultant Force)

As a result of the above calculations and the availability of existing gage sizes, the following block-gage capacities were used:

Block-Gage Number 1 - 200 lb.

Block-Gage Number 2 - 200 lb.

Block-Gage Number 3 - 200 lb.

Block Gage Number 4 - 100 lb. (200 lb. gage would be preferable)

Block-Gage Number 5 - 500 lb.

Block-Gage Number 6 - 500 lb.

Yaw Adjustment

A convenient feature of the waterjet dynamometer is the ease with which the yaw angle can be changed in precise one degree increments through plus or minus 10 degrees. The yaw angle setting is established with a pin which is placed in the appropriate alignment hole in the top of the yaw plate (Figure 24). Once the pin is in place, the yaw plate is secured to the base plate by simply tightening the four one-half inch cap screws located in the slotted holes. Several large flat washers should be placed under the heads of these bolts.

Pitch Adjustment

The pitch angle of the model can be changed by placing wedge-shaped shims between the top of the strut and the bottom of the transition section. An opening must be machined in these shims which matches the duct configuration at the top of the strut. Slots must be provided at the ends of the shim pieces to accommodate any tubes or wires which extend down into the strut. A shim design for the supercavitating model is shown on DTNSRDC drawing E-3056-12. Fabrication of these shims was not completed after it was determined that time considerations would make it impossible to conduct pitch-angle evaluations as part of the preliminary experimental program.

Transition Sections

The purpose of the transition section is to change, with as low a pressure drop as possible, the cross-sectional shape of the duct at the top of the strut into a circular cross-section at the flexible coupling. The transition section is not designed to function as either a diffuser or a nozzle and, therefore, the circular cross-sectional area (28.89 square inches) was selected to roughly approximate the outlet duct areas of the models tested. The supercavitating model has an outlet area of 22.34 square inches and the subcavitating model an outlet area of 18.33 square inches.

The transition sections were molded out of fiber glass and epoxied to aluminum interface pieces at either end (DTNSRDC drawings E-3056-21 and E-3056-27). The internal shapes were established by means of wooden patterns which were contoured in accordance with DTNSRDC drawings (E-3056-20 and E-3056-28). Figures 25 and 26 show top, bottom, side, and end views of the transition pieces used with the sub and supercavitating models. It will be necessary to fabricate new transition sections for any models tested in the future, unless they are designed with the same strut-outlet dimensions as either of the two existing models.

Mounting of Dynamometer in Tunnel

To simplify mounting of the dynamometer in the tunnel test section, a special aluminum hatch cover was fabricated which replaces the top viewport of the open-jet test section. The entire dynamometer assembly is mounted beneath this special hatch cover. When the dynamometer is removed from the tunnel and placed in the calibration stand, it is reattached to the hatch cover.

Electrical and Pressure Feed-Throughs

In addition to supporting the dynamometer, the hatch cover contains three feed-through openings which can be used for either pressure tubes or electrical cables. The feed-through openings in the hatch cover are the same size as all the other tunnel feed-throughs and, therefore, they will accept the standard stuffing gland fittings used at the tunnel. For the program described in this report, the cables for the six block-gages were passed through a single stuffing gland. All the pressure measuring tubes were connected to two feed-through pieces which were fabricated specially for this test (DTNSRDC drawing E-3056-26). On the inside of the tunnel the fittings were designed for connection to either 3/32-inch or 1/8-inch I.D. "Tygon" tubing, while on the outside of the tunnel the fittings connect to 1/4-inch I.D. tubing.

DYNAMOMETER CALIBRATION

HARDWARE

The dynamometer was calibrated in the stand shown in Figures 27 and 28 (DTNSRDC drawings E-3056-24, 25, 29, and 30). Through an arrangement of cables and pulleys, the stand permits any combination of forces and moments to be applied to the dynamometer. In Figure 27 the dynamometer is shown loaded with all six force and moment components.

To make possible the application of pitching and rolling moments, a steel calibration bar was attached to the base plate of the dynamometer. The bottom half of this bar extends downward from the dynamometer and is clearly visible in Figure 27. The top half of the rod extends up through the transition piece and protrudes above the hatch cover as shown at the top of Figure 28. The calibration bar can also be seen in Figure 29, which shows the dynamometer undergoing final calibration checks inside the tunnel test section.

Attention is called to this calibration bar because of the simplified loading it provides, both in the calibration stand and in the tunnel. Most six-component dynamometers are not designed with an opening up through their center of moments and, therefore, calibration is more difficult and requires a greater number of fixtures.

The calibration rod permits the application of lift forces by pulling up on the dynamometer with either a dead weight pulley-cable system, or a ratchet tensioning device attached through a spring scale to the hook on the overhead crane. Without the calibration rod and the opening up through the center of the dynamometer, it would be necessary to apply lift forces by means of a jacking device and load cell mounted beneath the dynamometer. With such jacking arrangements, it becomes much more difficult to apply a pure axial force. The calibration bar also provides a simple means of applying pure moments to the dynamometer, either in the stand or in the tunnel. Because the calibration bar extends through the top of the tunnel, moments can be applied with fixtures mounted outside the tunnel test section.

Only drag, lift, side force, and pitching moment calibration checks were conducted with the dynamometer mounted inside the test section. Additional calibrations within the tunnel were not deemed necessary or important for a preliminary performance evaluation. If, in the future, extensive tunnel calibrations should be required, it would be desirable to fabricate a longer calibration rod which would extend a greater distance above the tunnel and have a greater number of loading points at either end. Pulley fixtures and support brackets for outside the tunnel would also be needed.

A small diameter (1-3/8 inches) calibration bar was used because of the narrow trapezoidal shaped opening in the transition section of the supercavitating model (Figure 26). The maximum side load that could be applied at the end of this rod was approximately 240 pounds with noticeable deflection. For transition sections with wider openings, or where greater calibration loads are necessary, larger diameter bars or tubes are recommended. If large pitching loads are anticipated, stiffening ribs should be welded along the fore and aft surfaces of the bar.

All calibration loadings were applied with dead weights, wire rope, and pulleys. For maximum strength and flexibility 3/32 inch diameter (7 x 19) stainless steel wire rope was used with thimbles and "Nicopress" sleeves. The rated breaking strength for this wire rope is 1,050 pounds. Two types of sheave assemblies were used: 1) four existing DTNSRDC 450 pound capacity ball bearing sheaves for use with 1/8 inch diameter wire rope maximum (DTNSRDC Y&D drawing 704517 or E-2657), and 2) six commercially available "Edson"* 1700 pound capacity needle bearing wire rope sheave assemblies for use with 3/8 inch diameter wire rope maximum.

---

* The Edson Corporation, New Bedford, Massachusetts

PROCEDURE

The same mini-computer data acquisition system used for collecting and analyzing the test data (Figures 2 and 3) was used for calibrating the dynamometer. The method of least squares (Reference 17) was used to compute the slope of the best fit straight line through the calibration data points. After determining the six-by-six matrix of measured interaction sensitivities, a matrix inversion routine was used to generate the final inverse matrix used for computing the applied loads.

Separate calibration matrices were generated with each of the two transition pieces installed and with no transition section installed. These three matrices are presented in Table 2 and discussed under the Calibration Matrices section of this report. The computer program used for calibration is listed in Appendices G and H.

To make it possible for the calibration matrix to convey some physical meaning in terms of interaction percentages, a normalizing procedure was used to convert the inverse matrix into a unit matrix having values approximately equal to one on the principal diagonal. The normalizing procedure consisted of setting the slope of each measured force and moment component equal to unity. This was done by using the method of least squares to determine the slopes or sensitivities of block-gages 1, 2, and 6 when subjected to a pure lift load, the slopes of block-gages 3 and 4 when subjected to a pure side load and the slope of block-gage 5 when subjected to a pure drag load, and then multiplying the reciprocal of these slopes by the constants shown in the following equations:

Normalizing Factor for Block-Gage #1 = (1/4)·(1/slope B.G. #1)

Normalizing Factor for Block-Gage #2 = (1/4)·(1/slope B.G. #2)

Normalizing Factor for Block-Gage #3 = (1/2)·(1/slope B.G. #3)

Normalizing Factor for Block-Gage #4 = (1/2)·(1/slope B.G. #4)

Normalizing Factor for Block-Gage #5 = (1/slope B.G. #5)

Normalizing Factor for Block-Gage #6 = (1/2)·(1/slope B.G. #6)

The multiplication factors (1/4 and 1/2) are determined by the percentage of the total applied load carried by each block-gage in the dynamometer.

The normalizing factors were then inserted into the computer's data collect program and used as permanent multiplication constants for each of the block-gages. The raw output voltage of the block-gages was multiplied by these constants before the calibration matrix was computed and, likewise, before the test data was operated upon by the inverse calibration matrix.

The block-gage sensitivities or slopes were set up with the "Endevco" signal conditioning units to produce approximately 2.0 volts output with maximum rated load applied to each gage. Increasing the gain of the amplifiers to produce higher output voltages does not increase the accuracy of the measurements. The computer records millivolt signals and, therefore, the resolution of the measuring system is approximately one part in 2000. This degree of resolution is quite adequate, since extensive calibration experience at DTNSRDC has shown the accuracy of the block-gages to fall somewhere between $\pm$ 1/2% and $\pm$ 1.0 %.

The calibration procedure consisted of incrementally applying one loading component (force or moment) at a time and recording the corresponding output from all six block-gages. After repeating this procedure for the three force and three moment components, a six-by-six matrix of interactions was obtained. The method of least squares was used to compute all interaction sensitivities.

Appendix H shows a typical computer printout of the least squares calibration data with a pure pitching moment applied to the dynamometer. Page 1 of Appendix H shows the actual loads applied to the dynamometer, the normalizing factors used, the output of each block-gage, and the resultant output of the dynamometer. Page 2 of Appendix H shows the interaction sensitivity (slopes) of the six block-gages and the gage outputs at all the loading points. For each block-gage, the slope between consecutive loading points is printed out to aid in locating slope changes which might not otherwise be obvious unless the data were plotted. These incremental slope values are extremely useful when checking for mechanical interferences in the flexible coupling assembly. Page 3 of Appendix H shows the slopes which are used in the formation of the six-by-six interaction matrix, and the resultant dynamometer outputs based on these slopes. The data in Appendix H are printed out to assist the experimenter with the evaluation of the dynamometer as the calibration procedure progresses.

To check the validity of the assumption that interaction sensitivities remain essentially constant regarless of compound loading conditions, a wide variety of complex force and moment loadings were applied to the dynamometer (Figures 27 and 28) while the block-gage outputs were recorded and analyzed with the same computer program used during actual tunnel testing operations. Similar calibration checks were made with the dynamometer mounted in the tunnel, as shown in Figure 29 and discussed under the Dynamometer Calibration HARDWARE section of this report. The loads computed with the data collect program were remarkably close to the actual applied loads and, therefore, it was concluded that the inverse calibration matrix was performing satisfactorily.

TEST PROCEDURE

After the dynamometer and model were installed in the tunnel test section and all calibrations were completed, the following testing procedure was followed:

1. The valve on the Ronningen-Petter pressure sensor was closed to protect the attached pressure transducer from overpressure during tunnel filling operations.

2. The tunnel was filled, vented, and referenced to barometric pressure in the usual fashion. The air vent valve at the top of the waterjet piping circuit (Figure 7) was opened at the conclusion of the tunnel filling operation to release entrapped air from the pipe loop.

The deaeration system was operated throughout the test program to keep the air content as low as possible. Due to the preliminary nature of the tests, no attempt was made to monitor air content levels. With regard to air bubbles in the test section, it should be noted that a significant difference existed in the bubble content between 2 and 4 PSIA. At 2 PSIA the bubble density often obscured the model, making it extremely difficult to photograph cavitation on the waterjet inlet.

3. The tunnel was then oeprated for about 15 minutes at a velocity of approximately 10 ft/sec to flush air pockets from the system. The waterjet pump was also operated at this time to flush out any entrapped air remaining in the waterjet piping system.

4. After purging the tunnel, the water velocity was brought to zero and atmospheric pressure was established at the tunnel

centerline. The valve to the Ronningen-Petter sensor was then opened and the transducer referenced to the atmoshperic tunnel pressure.

5. The tunnel pressure was then reduced to the predetermined testing level as water was slowly circulated through the test section at a rate of approximately 10 ft/sec. Circulating the water, as the pressure was being reduced, minimized the time required to reach test conditions (2 or 4 PSIA) at the tunnel centerline. The average time required to fill the tunnel test section and reach low pressure test conditions was approximately 45 minutes.

6. With the tunnel at test pressure, the water velocity in the tunnel was brought to zero and the butterfly valve in the piping loop was closed. At this point, the block-gages were zeroed and span checks were recorded for each block-gage signal conditioning module.

7. The tunnel pressure was then held constant as the tunnel velocity was slowly increased to the desired value. The butterfly valve in the loop was kept closed as the tunnel velcoity was increased. The waterjet inlet was carefully observed to determine at what tunnel velocity external cavitation would occur with a blocked flow condition at the inlet.

8. Having reached the desired cavitation-number scaling condition, as determined by tunnel pressure and velocity, data from all the transducers and block-gages was recorded with the butterfly valve still closed. At many of the test conditions a rather large

cavity enveloped the nose of the nacelle at zero inlet velocity ratio. (Figure 30(F)). The drag force was always at its lowest value with no flow through the inlet.

9. The butterfly valve was then opened and the flow meters were bled. The pump was started and flow through the loop increased until the cavity on the external surface of the inlet disappeared. Data was recorded at this point and the manometer boards were photographed. No data was recorded at points between this cavitation inception condition and the blocked flow condition, because IVR values in this low range were of little or no practical interest.

10. With the tunnel pressure and velocity held constant, the flow loop velocity was gradually increased until the maximum obtainable flow rate was reached. To guard against overloading the block-gages, especially when operating at high tunnel velocities, the block-gage outputs were carefully monitored as the flow rate through the inlet was increased. The maximum IVR condition was distinguished by the extremely unstable behavior of the Barton flow meter dials, and cavitation banging in the pump and in the piping on the suction side of the pump. Data was quickly recorded at this cavitating condition and then the pump speed was immediately reduced to the threshold condition where cavitation banging disappeared and the flow rate measurement became stable. Data was recorded at this maximum stable IVR condition. The flow rate was then decreased in equal increments,

and data recorded at each discrete IVR value, until external cavitation appeared on the inlet.

If in the future it should be decided to reduce the flow rate through the loop to zero and close the butterfly valve, caution should be exercised to avoid creating a hydraulic impact loading on the model by suddenly stopping the pump. The flow rate (pump RPM) should always be reduced slowly.

Approximately twenty data points were recorded over the range of IVR values between maximum flow rate and external cavitation. Frequently two data points were recorded at the same test condition to provide a check on the repeatability of the data acquisition system. The total number of data points that could be recorded over a range of IVR values was limited to twenty by the memory capacity of the computer.

11. After the last IVR test condition was recorded, the tunnel velocity was brought to zero and the pump was stopped. With the tunnel pressure still maintained at the test condition, zero readings were again recorded for all the transducer elements.

12. After recording post test zeros, the computer proceeded to print out a preliminary analysis of all the data from the series of test runs just completed.

13. Immediately after the computer completed the preliminary analysis, the raw test data was written on a "Tri-Data" magnetic tape cartridge for preservation and future analysis.

14. If no more tests were to be run, the tunnel would be brought back up to atmospheric pressure and vented while the computer printout was in progress. Otherwise, after the test data was written on magnetic tape, a new set of tunnel test conditions would be established and the test procedure repeated - starting with step 6.

15. To protect the block-gage electrical cables from water leakage, the tunnel test section was drained at the end of each day to a level beneath the dynamometer. No transducer wetting problems were encountered during the test program.

SUMMARY OF WATERJET TEST FACILITY CAPABILITY

A new DTNSRDC waterjet inlet cavitation testing facility, including a new six-component force balance dynamometer, was successfully designed, fabricated, and experimentally evaluated. The preliminary test program conducted with both sub and supercavitating strut-pod inlets demonstrated the system's capability to characterize the performance of waterjet inlets by:

- Simulating, through cavitation number scaling, speeds of approximately 84 knots.
- Measuring the six force and moment components acting on the strut-pod inlet.
- Measuring inlet forces and moments free of interaction effects.
- Determining the location where the resultant drag force acts on the strut-pod assembly.
- Permitting easy variation of yaw angle in precise one degree increments.
- Permitting determination of minimum IVR limits by visual observation of cavity growth on the external surface of the inlet.
- Determining maximum IVR (choking) conditions for the inlet-strut-transition section assembly.
- Measuring pressure distributions at the inlet and at the top of the strut.

- Rapidly collecting and analyzing large quantities of force and pressure data on a mini-computer system.

As a result of this developmental effort, the Navy now has the ability to thoroughly evaluate the cavitation and drag characteristics of strut-pod waterjet inlets, such as those used on the PHM hydrofoil craft and the SES 100-A surface effect vehicle.

RECOMMENDATIONS FOR FUTURE IMPROVEMENTS

This section contains recommendations for improving the performance of the waterjet inlet testing facility.

1. Invert the dynamometer and the model in the tunnel test section, so that the water will flow downward in the strut and pass through the bottom hatch cover. It should be possible to accomplish this change by simply modifying the external aluminum piping circuit. The dynamometer will function equally as well in an "upside-down" position.

This change is necessary to make possible the positive identification of those IVR conditions at low tunnel pressures which cause inlet choking. With the present piping configuration, the elevation of the pipe above the inlet limits the minimum total inlet pressure required to sustain flow through the pipe loop. As a result of the limiting condition imposed by the elevation of the pipe, it was not always certain whether the no-flow condition resulted from inlet choking due to cavitation, or flow breakdown due to insufficient pressure. This problem of determining the cause of the no-flow condition was most acute when trying to simulate low craft speeds at 2 PSIA tunnel pressure.

The decreasing static head above the tunnel centerline also makes it impossible to use tubes, run out through the top of the tunnel, to sense vapor pressures on the model. The lowest pressure that the tubes in this configuration can accurately transmit is approximately 2

PSIA. By inverting the model, the lowest pressure in the system would occur at the waterjet inlet. It would then be possible to sense cavitation vapor pressures with the same tubes extending downward, rather than upward, from the anticipated cavitation inception points. Measuring pressures outside the water tunnel is preferable, whenever possible, to avoid the expense and difficulty associated with mounting a multitude of miniature electromechanical pressure transducers inside the shell of the model.

Although it may be necessary to invert the model to conclusively identify the maximum obtainable IVR condition free of inlet choking, force and moment data can be reliably measured with the existing arrangement. Likewise, the present test setup can be used to locate the external cavitation inception point on an inlet, and to examine inlet-strut pressure losses over a broad range of IVR values, which for each of the models tested encompassed the design cruise conditions. The design IVR takeoff condition (1.12) for the subcavitating model was also achieved.

2. Increase the clearances between the mating flexible coupling pieces to minimize the possibility of any future mechanical interaction problems, such as those which occurred on one series of the preliminary test runs. With the present dimensions, alignment of the flexible coupling and the top of the transition section is rather critical. The dimensions of the "O"-ring groove around the top of the transition section should also be increased to accommodate low-friction teflon "O"-rings.

3. Properly anchor the first 8-inch pipe elbow on the discharge side of the pump to prevent movement of the elbow at high flow rates. The simplest method of accomplishing this would be to remove the flexible pipe coupling just ahead of the elbow and replace it with a solid spool piece. The flexible coupling and the ball joint beneath the elbow were originally installed to accommodate small motions of the tunnel with respect to the ground. After completing the preliminary test program, it was concluded that the movement of the lower horizontal section of the tunnel was not significant enough to warrant the use of this flexible joint. Furthermore, the U-shaped piping configuration between the pump and the hatch cover would permit a small amount of flexing to occur if the tunnel happened to move a slight amount.

4. Check the alignment of the wire rope calibration cables used to apply drag forces and lift forces. The sheaves over which these cables pass are located very close to the applied loading points on the dynamometer and, therefore, it is difficult to ensure proper cable alignment. This problem could be alleviated by modifying the pulley mounting brackets to increase the length of cable between the loading points on the dynamometer and the sheaves.

If for future test programs the required calibration loads increase significantly, it may become necessary to apply calibration forces through lever arms which create a mechanical advantage.

5. Write all test data collected by the mini-computer onto a nine-track tape which can be directly interfaced with the DTNSRDC CDC

6700 computer system. At the time this test program was conducted, equipment did not exist for conveniently transferring digital data from the "Tri-Data" magnetic tape cartridges to the CDC 6700 system.

6. Measure the frequency and amplitude of the unsteady hydrodynamic forces acting on the strut-pod model. Although tunnel velocity and pressure were always held constant as the test data was recorded, the models pulsated noticeably at the higher flow rates due to the buffeting action of the water. It is likely that the frequency and amplitude of these forces can be measured by simply monitoring the ouput of the force balance block-gages with a strip chart recorder. The 3-kilohertz carrier frequency used with the block-gages should permit the accurate measurement of frequencies up to 300-hertz.

7. Use pressure transducers instead of manometer boards for measuring total and static pressures on future models. The cost of additional transducers and signal conditioning equipment will be offset by eliminating the labor required to read and process large quantities of manometer board data. The use of transducers will permit data collection with the mini-computer system, and immediate analysis of the internal pressure loss coefficients.

8. Determine the pressure drop between the tunnel centerline and the top of the transition section with a differential pressure transducer connected directly between the Ronningen-Petter sensor (see the section of this report entitled, Static Pressure Sensor Above Test

Section) and the primary water tunnel test section pressure measuring system.

9. Manufacture the inlets of future models from plexiglass to permit visual observation of internal cavitation inception.

10. With each new model fabricate a faired plug which can be used to cover the inlet opening. Such a plug would make it possible to experimentally compare the hydrodynamic forces acting on a model, both with and without a waterjet inlet. This comparative data would be extremely useful for relating existing experimental and theoretical work on solid streamlined strut-pod bodies (References 18 and 19) to the drag of strut-pod waterjet inlets.

ACKNOWLEDGMENTS

The author wishes to acknowlege the assistance of all Center personnel who contributed to the successful design, fabrication and performance evaluation of the new waterjet inlet testing facility. Deserving of special recognition are Mr. George J. Norman who designed the six-component dynamometer and flexible coupling, Mr. Dennis R. Mullinix who set up the instrumentation system and programmed all the data collect and anlysis programs on the mini-computer, and Mr. Richard F. Lach who assembled the dynamometer, the calibration stand, and the two inlet models. Appreciation is expressed to Elizabeth C. Waksmunski and Patricia A. Wollaver for typing the manuscript of this report.

REFERENCES

1. Brownell, W.F., "Two New Hydromechanics Research Facilities at the David Taylor Model Basin," DTMB Report 1690 (Dec 1962).

2. Vincent, M., "The Naval Ship Research and Development Center," NSRDC Report 3039 (Jun 1969).

3. "Horizontal Split-Case Centrifugal Pumps Types LR-LLR," Worthington Pump International publication 2036-B1D.

4. "Instructions for Installation, Operation and Maintenance and List of Parts, Centrifugal Pumps Types LR, LLR, and Fire Pumps LRG," Worthington Pump International publication 2036-E1D.

5. "Type LR Volute Pumps Double Suction," Worthington Pump International Dimension Sheet Drawing No.RW-148724R2.

6. "Speed Variator Instructions," General Electric Company, Manual GEK-23968 for SP200 SCR Drive Model 6V75F3178, furnished by General Electric Company, Washington, D.C. (Aug 1972).

7. "Fluid Meters - Their Theory and Application," ASME Research Committee on Fluid Meters Report, Fifth Edition (1959).

8. Spink, L.K., "Principles and Practice of Flow Meter Engineering," The Foxboro Company, Foxboro, Massachusetts, Ninth Edition (1967).

9. "Flowmeter Computation Handbook," ASME Research Committee on Fluid Meters Report (1961).

10. Sprenkle, R.E., "Piping Arrangements for Acceptable Flowmeter Accuracy," ASME Transactions Vol. 67, No. 5, pp. 345-360 (Jul 1945).

11. "Aero-Space Applied Thermodynamics Manual," Society of Automotive Engineers, Inc, New York (1962) (Part G, Paragraph 4 - Test Instrumentation and Measurement, Fluid Flow Measurement).

12. Sprenkle, R.E. and N.S. Courtright, "Straightening Vanes for Flow Measurement," ASME Paper No. 57-A-76 (Dec 1957); also published in Mechanical Engineering (the Journal of the ASME) Vol. 80, No. 2, pp. 71-73, (Feb 1958).

13. Huang, T.T. and G.S. Belt, "Development of a Hydrofoil Waterjet Propulsion System Test Facility," Naval Ship Research and Development Center Report 3318 (May 1970).

14. Ormond, A.N., "Universal Flexure Joint," U.S. Patent 2,966,049 (Dec 27, 1960).

15. Gertler, M., "The DTMB Planar-Motion-Mechanism System," NSRDC Report 2523 (Jul 1967).

16. Goodman, A. and M. Gertler, "Planar-Motion-Mechanism and System," U.S. Patent 3,052,120 (Sep 4, 1962).

17. Fuller, G., "Analytic Geometry," Addison-Wesley Publishing Company, Inc., Cambridge, Massachusetts (1954).

18. Hoerner, S.F., "Fluid-Dynamic Drag," published by author, Midland Park, New Jersey (1965).

19. Johnson, R.S., "Prediction of Lift and Cavitation Characteristics of Hydrofoil-Strut Arrays," Marine Technology, Vol. 2, No. 1, pp. 57-69 (Jan 1965).

20. Brown, J.R. and J. Traksel, "Waterjet Propulsion System Study - Report No. 4, External Flow Tests," Lockheed California Company Report LR 17885-4 (1965).

21. Brown, J.R. and J. Traksel, "Waterjet Propulsion System Study - Report No. 5, System Design and Analysis," Lockheed California Company Report, LR 17885-5(1965).

22. Brown, J.R. and J. Traksel, "Waterjet Propulsion System Study - Report No. 3, Internal Flow Test," Lockheed California Company Report LR 17885-3 (1965).

23. Kinkel, J.F., "Force Balance Measuring Device," U.S. Patent 2,780,101 (Feb 5, 1957).

24. "Pressure-Volume Controls, Principle of Operation," Volumetrics, Inglewood, California, Technical Memorandum No. 101.

25. "Use of Pressure-Volume Controls as Vacuum/Pressure Generators," Volumetrics, Inglewood, California, Technical Memorandum No. 102.

26. "Use of Pressure-Volume Controls as Vernier Pressure Controls," Volumetrics, Inglewood, California, Technical Memorandum No. 103.

APPENDIX A

DESCRIPTION OF MODELS TESTED

The performance of the new waterjet inlet test facility was evaluated with two existing strut-pod ram-type waterjet inlets which had been previously evaluated in high-speed towing basins at the Lockheed Underwater Missile Facility in Sunnyvale, California (Reference 20) and the David W. Taylor Naval Ship Research and Development Center, Bethesda, Maryland (Reference 13). Both models were designed and constructed by Lockheed and are described fully in References 20 and 21, including the coordinates and shapes of the struts and nacelles.

Although the two inlet-strut designs investigated have never been used on a Navy hydrofoil craft, they represent the product of a rather extensive development effort by the Lockheed Corporation which was intended to produce the final waterjet ducting design for a hardware application. The ducting system components for these models resulted from an internal-flow model test program conducted at the Hydraulic Laboratory of Byron Jackson Pumps, Inc., Los Angeles, California (Reference 22). This test program consisted of more than 300 test runs during which important design variables, such as turning vane configuration and inlet shape, were systematically investigated over a large number of operating conditions. As a result of these tests, it was concluded that two turning vanes represented the optimum configuration for turning the flow from the nacelle into the strut based on the criteria of pressure recovery, flow distribution downstream from the elbow, and cavitation on the vanes. Two vanes minimized flow separation around the inside of the turn, and the presence of the vanes more than halved the pressure loss which resulted with no vanes installed. The nacelle elbow was identified as the most critical ducting element in regard to internal flow cavitation.

Circular axially symmetric inlets were used because it was believed they would produce less drag, higher pressure recovery, and more uniform inlet flow than elliptical, rectangular, or other cross-sectional shapes. A summary of important model dimensions is presented in Table 3.

Figures 31 and 32 show the model designed for supercavitating operation on an *80-knot hydrofoil ship*. *This* supercavitating model has blunt trailing edges on the strut and nacelle. The cross-sectional shape of the strut is a modified parabola and the leading edge makes an angle of 7.5 degrees with the vertical. The chord tapers from 12.26 inches at the nacelle to 19.27 inches at the top of the strut. The internal and external elliptical contours of the inlet lip and nacelle were established by a Lockheed computer program. The flow through the strut is divided into three channels by two splitter vanes which extend well forward into the nacelle (Figure 33). The location of the splitters is such that the diffusion rate is the same for each channel.

The second model, shown in Figures 34 and 35 was design for subcavitating flow at 50-knots and all trailing edge surfaces are faired. The original design for the subcavitating strut-pod

TABLE 3

SUMMARY OF MODEL DATA

	SUBCAVITATING MODEL	SUPERCAVITATING MODEL
Total projected model area normal to flow discharging from tunnel nozzle	48.42 in^2* (.336 ft^2)	52.47 in^2* (.364 ft^2)
Design cruise speed	50 knots**	76 knots**
Design takeoff hump speed	30 knots**	40 knots**
Design IVR at cruise speed	.7	.65
Design IVR at takeoff speed	1.12	-
<u>Nacelle</u>		
Overall external length	23.74 in	20.575 in
Maximum external diameter ahead of leading edge of strut	4.40 in*	5.77 in*
Distance from inlet lip to leading edge of strut	6.00 in	8.312 in
Inlet lip diameter	3.194 in	3.235 in
Inlet lip area	8.01 in^2	8.22 in^2
Throat diameter	3.024 in*	2.923 in*
Throat area	7.18 in^2*	6.71 in^2*
Throat area occupied by tips of total pressure tap tubes	.074 in^2*	.074 in^2*
Throat area occupied by total pressure tap tubes	.37 in^2*	.35 in^2*
Inlet diffuser length	2.94 in	4.638 in
Diffuser inlet diameter	3.024 in*	2.923 in*
Diffuser inlet area	7.18 in^2*	6.71 in^2*
Diffuser outlet diameter	3.46 in*	3.742 in

*DTNSRDC measured or calculated values
** Full-scale values
No asterik - Lockheed values from references 20, 21, and 22

Diffuser outlet area	9.40 in^{2*}	10.99 in^2
Total included diffuser angle	8.5°*	10.07°
Diffusion ratio	1.31*	1.64
Elbow		
Inlet area	9.40 in^{2*}	10.99 in^2
Outlet area	9.65 in^2	8.06 in^2
Contraction ratio	——	.27
Strut		
Overall height (perpendicular distance from top of nacelle to top of mounting flange)	27.84 in*	27.22 in*
Angle of leading edge with vertical	0°	7.5°
Angle of trailing edge with vertical	0°	21.27°
Chord length at nacelle (parallel to waterline)	14.1 in*	12.26 in
Chord length at top of strut (parallel to waterline)	14.1 in*	19.27 in
Maximum thickness to chord ratio at nacelle intersection (parallel to waterline)	11.3%	10.08%
Maximum thickness to chord ratio at top of strut (parallel to waterline)	19.8%	10.08%
Inlet area	9.65 in^2	8.06 in^{2*}
Outlet area	18.33 in^{2*}	22.34 in^{2*}
Diffusion ratio	1.9	2.77*

*DTNSRDC measured or calculated values
** Full-scale values
No asterik - Lockheed values from references 20, 21, and 22

configuration was for a propeller-drive unit. The design was subsequently modified to accommodate a waterjet duct system. The subcavitating model, therefore, represents a compromise waterjet strut-pod inlet design rather than an optimized design.

The external shape of the subcavitating nacelle was established by a Lockheed computer program based on the criteria of cavitation free flow and minimum drag over the entire range of operating speeds. The strut has no sweep. The nacelle contains a straight wall conical diffuser, having a total included angle of 12 degrees and a diffusion ratio of 1.4, to reduce the flow velocity approximately 40 percent prior to entering the elbow. The area in the elbow is uniformly converged to minimize pressure losses. The flow in the strut is diffused with an area ratio of 1.9. The strut is divided into three channels by two splitter vanes which extend forward into the nacelle to induce turning of the flow prior to entering the elbow. The splitters are located such that the diffusion rate for each channel is the same.

Figures 31 and 34 show each of the models mounted in the DTNSRDC 36-inch variable pressure water tunnel beneath the six-component force-balance. These figures clearly show the "Tygon" tubes which transmit the total and static pressures measured at the top of the strut.

The L-shaped total pressure taps at the top of the supercavitating strut are shown in Figure 36. These adjustable 1/8-inch diameter tubes and mounting chucks were obtained commercially from United Sensor and Control Corporation, Watertown, Massachusetts.

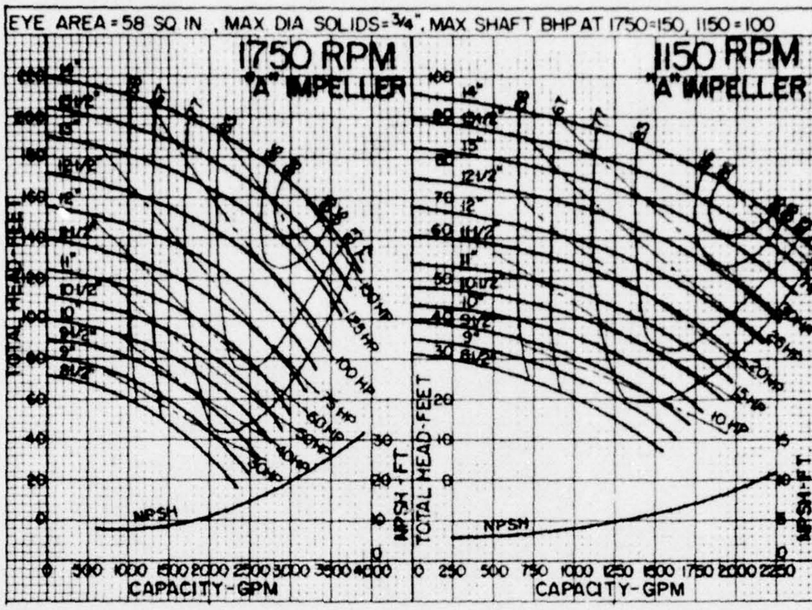

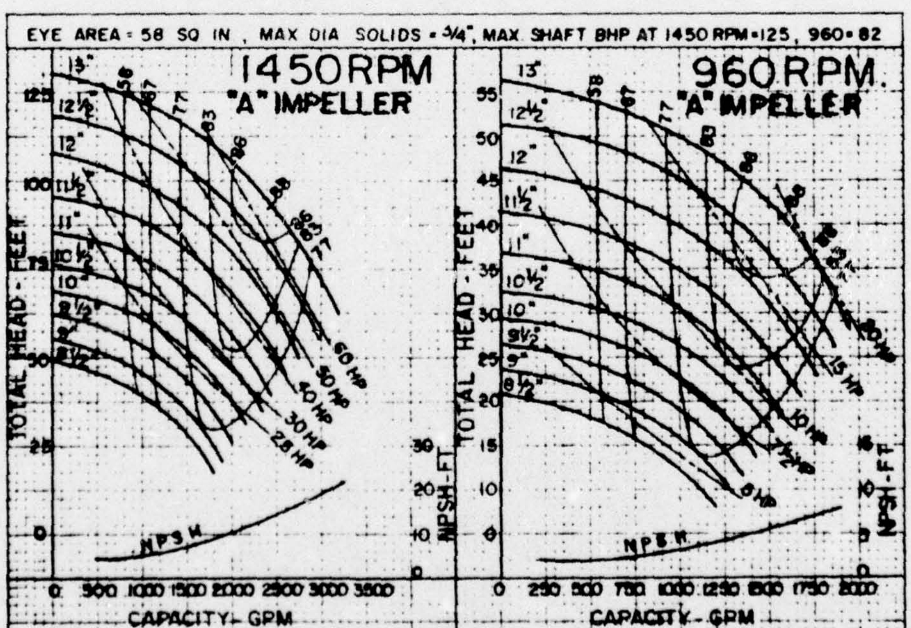

APPENDIX B – Worthington Corporation – Rating Curves for Horizontal Split Case Double Suction Centrifugal Pump Type 8 LR-13 "A"

APPENDIX C

PRESSURE TRANSDUCER CALIBRATION

HARDWARE

The pressure transducers used with the orifice-plate flow meter, the "Annubar" flow meter, and the "Ronningen-Petter" pressure sensor were calibrated with a "Consolidated Electrodynamics (CEC)" Electromanometer system which is shown mounted in a portable aluminum carrying case in Figure 37. This precision pressure measuring system is used at DTNSRDC as a secondary calibration standard and its calibration accuracy has been verified by the National Bureau of Standards. The system consists of a "CEC" Force Balance Pressure Transducer, a "CEC" Type 1-156 Servo Amplifier, a "Fluke" Type 8100A Digital Multimeter, a "Volumetrics" Pressure-Volume (P-V) Controller, and a manifold of "Whitey" needle valves.

The patented force balance pressure transducer (Reference 23) is the heart of the system and operates on the non-displacement force balance principle. Applied pressure is sensed by a pressure-summing bellows which converts pressure to force. The resulting displacement, or movement of the bellows, is detected by a linear differential transformer, which sends an error signal to the Servo Amplifier. The Servo Amplifier acts on the error signal and supplies a proportional current to the force coil of the balance linkage. The current flowing through the force coil creates an electromagnetic force which precisely balances the force applied by the pressure summing bellows. The amount of current flowing through the coil produces a measure of the applied pressure.* The force balance pressure measuring system is designed to measure differential, gage, or absolute pressures. The pressure range of the unit shown in Figure 37 is ±30 PSI differential. Its published accuracy is 0.05% of full-scale output over a 5-minute duration, including nonlinearity, hysteresis, resolution, zero drift, and zero set.

PROCEDURE

Pressures were applied to the transducers with the "Volumetrics" Pressure-Volume (P-V) controller (Figure 37). A zero leak piston compresses the trapped air in the system. For detailed information on the design and operation of this vernier pressure controller, consult References 24,25, and 26. Although the P-V controller was used as the pressure source for the low range transducers calibrated in this test program, an external compressed air supply or vacuum pump could be used in conjunction with the P-V controller to generate higher pressures or vacuums.

The outputs of both the pressure transducer under calibration and the "Fluke" digital multimeter mounted in the "CEC" calibration unit (Figure 37) were recorded with the mini-computer data acquisition system. After all the pressure calibration points were recorded, the computer applied a least squares program and computed the slope of the best-fit straight line calibration curve. Separate slopes were

* CEC Bulletins 1547C, 1156A, 1164

computed for both increasing and decreasing pressure calibrations. The program printout for the 5 PSID "Validyne" gage used with the "Annubar" flow meter is shown in Appendix J. A listing of this computer program is contained in Appendix I.

The computerized pressure calibration procedure offers several advantages. In addition to eliminating the need for manually recording calibration data and manually plotting curves to determine transducer sensitivities, the computer permits the simultaneous calibration of almost an unlimited number of pressure transducers. This feature is expected to be of special value in future test programs which may employ large numbers of transducers to determine pressure distributions on waterjet inlets. The computer also eliminates the need or desirability of establishing precise calibration pressure levels as a means of simplifying manual plotting procedures.

APPENDIX D – LISTING OF DTNSRDC MANUFACTURING DRAWINGS FOR WATERJET INLET TESTING FACILITY

DTNSRDC Drawing No.	Drawing Title
E-3056-1	General Arrangement (Overall Facility)
Six-Component Balance	
E-3056-2, Rev I	General Arrangement
E-3056-3	Sub-Assembly
E-3056-4, Rev II	Loading Point Assembly (Various Sub-Assemblies)
E-3056-5	Details
E-3056-6, Rev II	Mounting Plate Detail
E-3056-7, Rev III	Yaw Plate Detail
E-3056-8	Lift Gage Bracket (Weldment)
E-3056-9, Rev I	Hatch Cover Plate Detail
E-3056-10, Rev I	Loading Point Socket and Strut Details (Flexures)
E-3056-11	(Drawing deleted from series)
E-3056-12, Rev II	Shim Details (Supercavitating Model)
E-3056-13	(Drawing deleted from series)
E-3056-14, Rev II	Block Gage Mounting Plate Details
E-3056-15, Rev I	Water Disconnect Details (Flexible Coupling Pcs.)
E-3056-16	Bolting Flange and Gaskets Details
E-3056-17	Torque Flexure, Block Gage Bracket, Lift Loading Channel Details
E-3056-18	Details (Flexible Coupling Pcs. and Mounting Plate Sub-Assembly)
E-3056-20	Lines for Transition Duct (Supercavitating Model)
E-3056-21	Transition Duct Sub-Assembly and Details (Supercavitating Model)
E-3056-26	Details (Flat Mounting Shim for Subcavitating Model and Pressure Tap Feed Through Fittings)

DTNSRDC Drawing No.	Drawing Title
E-3056-27	Details (Transition Duct Sub-Assembly for Subcavitating Model)
E-3056-28	Details (Lines for Transition Duct - Subcavitating Model)
E-3056-31	Subcavitating Strut Modification (Mounting Flange)

Piping System External to Tunnel Test Section

E-3056-19, Rev I	Details
E-3056-22	Pump-Motor Mounting Sub-Assembly
E-3056-23	Weldment Details

Pump Drive System - Electrical Drawings

C-477-1, Rev I	Schematic
B-922-1	Control Box Details

(Also see Reference 31)

Calibration Stand and Fixtures

E-3056-24, Rev I	Details
E-3056-25, Rev II	Details
E-3056-29, Rev I	Assembly
E-3056-30	Pulley Modification

Original Dynamometer Design Drawings Prepared by G. J. Norman

E-3056-32	Section View (General Arrangement)
E-3056-33	Section and Details (Sub-Assembly and Flexure)
E-3056-34	Section and Details (Mounting Brackets)
E-3056-35	Sub-Assembly (Loading Point Flexure Assembly and Detail)

APPENDIX E — LISTING OF COMPUTER PROGRAM FOR DETERMINING CALIBRATION LOADING CONDITIONS AND RESULTANT FORCES ACTING ON BLOCK-GAGES

<u>SUBR PR</u>

```
      SUBR PR
      X=2
      WRIT X
      X=4
      WRIT X,'USED FOR PRELIMINARY DETERMINATION'
      WRIT X,' OF CALIBRATION LOADING CONDITIONS '
      X=1
      WRIT X,'& RESULTANT FORCES ACTING ON BLOCK GAGES'
      WRIT X,' '
      WRIT X,'   (CALL PR)'
      WRIT X,' '
      CC=0
      TYPE 'CALIBRATION LOADS'
      TYPE 'LOCATION OF RESULTANT FORCES'
      TYPE 'LIFT FORCE X,Y'
      ACCE XL,YL
      TYPE 'DRAG FORCE Y,Z'
      ACCE YD,ZD
      TYPE 'SIDE FORCE X,Z'
      ACCE XS,ZS
      BB=ZS
      DD=ZD
      I=1
      TYPE 'LIFT,DRAG,SIDE FORCES (-LIFT STOPS INPUT)'
 1    ACCE FL(I),FD(I),FS(I)
      IF (FL(I)) 3,2,2
 2    I=I+1
      IF (I-15) 1,1,3
 3    JI=I-1
      X=1
      WRIT X,'LOCATION OF RESULTANT FORCES (IN)'
      WRIT X,' '
      X=4
      WRIT X,'            LIFT FORCE                          '
      WRIT X,' DRAG FORCE                         '
      X=1
      WRIT X,'SIDE FORCE'
      X=4
      WRIT X,'   X                Y                 Y'
      WRIT X,'               Z                 X'
      X=1
      WRIT X,'               Z'
      X=3
      WRIT X,XL,YL,YD,ZD
      X=1
      WRIT X,XS,ZS
      WRIT X,' '
      WRIT X,' '
      X=4
      WRIT X,'LOADING CONDITION     LIFT FORCE
      X=1
      WRIT X,'DRAG FORCE        SIDE FORCE'
      WRIT X,' '
      DO 6 I=1,JI
      WRIT X,I,FL(I),FD(I),FS(I)
 6    CONT
      WRIT X,' '
      WRIT X,' '
      X=4
      WRIT X,'LOADING CONDITION LIFT COMP       DRAG'
      WRIT X,' COMP          SIDE COMP        TOTAL MOMENT'
      X=1
      WRIT X,'        REQUIRED PAN WT.'
      WRIT X,' '
      WRIT X,'ROLLING MOMENT'
      WRIT X,' '
      DO 10 I=1,JI
      A=FL(I)*YL
      B=-FS(I)*BB
      X=3
      WRIT X,I,A,CC,B
      X=1
      WRIT X,A+B,(A+B)/52.6
 10   CONT
      WRIT X,' '
      WRIT X,'PITCHING MOMENT'
      WRIT X,' '
      DO 11 I=1,JI
      A=-FL(I)*XL
      B=FD(I)*DD
      X=3
      WRIT X,I,A,B,CC
      X=1
      WRIT X,A+B,(A+B)/52.6
 11   CONT
      WRIT X,' '
      WRIT X,'YAWING MOMENT'
      WRIT X,' '
      DO 12 I=1,JI
      A=FS(I)*XS
      B=-FD(I)*YD
      X=3
      WRIT X,I,CC,B,A
      X=1
      WRIT X,A+B,(A+B)/28
 12   CONT
      WRIT X,' '
      WRIT X,' '
      WRIT X,'LOADS APPLIED TO BLOCK GAGES'
      DO 13 I=1,2
      WRIT X,' '
      WRIT X,'BLOCK GAGE NO. ',I,' (200 LB)'
      WRIT X,' '
      X=4
      WRIT X,'LOADING CONDITION  1/4 OF TOTAL               '
      WRIT X,'     ROLLING MOMENT                     '
      X=1
      WRIT X,' PITCHING MOMENT                 TOTAL FORCE'
      X=4
      WRIT X,'                           LIFT FORCE        '
      WRIT X,'LIFT COMP             SIDE COMP              '
      X=1
      WRIT X,'LIFT COMP             DRAG COMP'
      WRIT X,' '
      DO 13 L=1,JI
      A=(FL(L)*YL)/21
      B=-(FS(L)*BB)/21
      IF (I-1) 14,15,14
 14   A=-A
      B=-B
 15   C=(FL(L)*XL)/56
      D=-(FD(L)*DD)/56
      X=3
      WRIT X,L,FL(L)/4,A,B
      E=FL(L)/4+A+B+C+D
 16   X=1
      WRIT X,C,D,E
 13   CONT
      XX=200
      DO 18 I=3,4
      WRIT X,' '
      WRIT X,'BLOCK GAGE NO. ',I,' (',XX,' LB)'
      WRIT X,' '
      X=4
      WRIT X,'LOADING CONDITION  1/2 OF TOTAL
      WRIT X,'    YAWING MOMENT                    TOTAL
      X=1
      WRIT X,' FORCE'
      X=4
      WRIT X,'                        SIDE FORCE        SIDE
      X=1
      WRIT X,' COMP            DRAG COMP'
      WRIT X,' '
      DO 20 L=1,JI
      A=(FS(L)*XS)/28
      B=-(FD(L)*YD)/28
      IF (I-3) 21,23,21
 21   A=-A
      B=-B
 23   X=3
      WRIT X,L,FS(L)/2,A,B
 22   C=FS(L)/2+A+B
      X=1
      WRIT X,C
 20   CONT
      XX=100
 18   CONT
      X=1
      WRIT X,' '
      WRIT X,'BLOCK GAGE NO. 6 (500 LB)'
      WRIT X,' '
      X=4
      WRIT X,'LOADING CONDITION  1/2 OF TOTAL
      X=1
      WRIT X,'PITCHING MOMENT                 TOTAL FORCE'
      X=4
      WRIT X,'                          LIFT FORCE        '
      X=1
      WRIT X,'LIFT COMP             DRAG COMP'
      WRIT X,' '
      DO 25 L=1,JI
      A=-(FL(L)*XL)/28
      B=(FD(L)*DD)/28
      X=3
      WRIT X,L,FL(L)/2,A,B
      X=1
      WRIT X,FL(L)/2+A+B
 25   CONT
      WRIT X,' '
      X=2
      WRIT X
      END
```

COPY AVAILABLE TO DDC DOES NOT PERMIT FULLY LEGIBLE PRODUCTION

Copy available to DDC does not permit fully legible reproduction

APPENDIX F – OUTPUT OF COMPUTER PROGRAM FOR DETERMINING CALIBRATION LOADING CONDITIONS AND RESULTANT FORCES ACTING ON BLOCK GAGES

USED FOR PRELIMINARY DETERMINATION OF CALIBRATION LOADING CONDITIONS & RESULTANT FORCES ACTING ON BLOCK GAGES

(CALL PR)

LOCATION OF RESULTANT FORCES (IN)

LIFT FORCE		DRAG FORCE		SIDE FORCE	
X	Y	Y	Z	X	Z
5	2	4	-25	8	-22

LOADING CONDITION	LIFT FORCE	DRAG FORCE	SIDE FORCE
1	10	-20	6
2	20	-40	12
3	30	-60	18
4	40	-80	24
5	50	-100	30
6	60	-120	36
7	70	-140	42
8	80	-160	48
9	90	-180	54
10	100	-200	60

LOADING CONDITION	LIFT COMP	DRAG COMP	SIDE COMP	TOTAL MOMENT	REQUIRED PAN WT.
ROLLING MOMENT					
1	20	0	132	152	2.88973
2	40	0	264	304	5.77947
3	60	0	396	456	8.6692
4	80	0	528	608	11.5589
5	100	0	660	760	14.4486
6	120	0	792	912	17.3383
7	140	0	924	1064	20.2281
8	160	0	1056	1216	23.1178
9	180	0	1188	1368	26.0076
10	200	0	1320	1520	28.8973
PITCHING MOMENT					
1	-50	500	0	450	8.55513
2	-100	1000	0	900	17.1102
3	-150	1500	0	1350	25.6654
4	-200	2000	0	1800	34.2205
5	-250	2500	0	2250	42.7756
6	-300	3000	0	2700	51.3308
7	-350	3500	0	3150	59.8859
8	-400	4000	0	3600	68.4411
9	-450	4500	0	4050	76.9962
10	-500	5000	0	4500	85.5513
YAWING MOMENT					
1	0	80	48	128	4.57143
2	0	160	96	256	9.14286
3	0	240	144	384	13.7142
4	0	320	192	512	18.2857
5	0	400	240	640	22.8571
6	0	480	288	768	27.4285
7	0	560	336	896	32
8	0	640	384	1024	36.5714
9	0	720	432	1152	41.1428
10	0	800	480	1280	45.7143

COPY AVAILABLE TO DDC DOES NOT PERMIT FULLY LEGIBLE PRODUCTION

LOADS APPLIED TO BLOCK GAGES

BLOCK GAGE NO. 1 (200 LB)

LOADING CONDITION	1/4 OF TOTAL LIFT FORCE	ROLLING MOMENT LIFT COMP	ROLLING MOMENT SIDE COMP	PITCHING MOMENT LIFT COMP	PITCHING MOMENT DRAG COMP	TOTAL FORCE
1	2.5	.952381	6.28571	.892857	-8.92857	1.70238
2	5	1.90476	12.5714	1.785 1	-17.8571	3.40475
3	7.5	2.85714	18.8571	2.67857	-26.7857	5.10711
4	10	3.80952	25.1428	3.57143	-35.7143	6.80951
5	12.5	4.7619	31.4285	4.46428	-44.6428	8.51189
6	15	5.71428	37.7143	5.35714	-53.5714	10.2142
7	17.5	6.66667	44	6.25	-62.5	11.9166
8	20	7.61905	50.2857	7.14286	-71.4286	13.619
9	22.5	8.57143	56.5714	8.03571	-80.3571	15.3214
10	25	9.52381	62.8571	8.92857	-89.2857	17.0238

BLOCK GAGE NO. 2 (-00 LB)

LOADING CONDITION	1/4 OF TOTAL LIFT FORCE	ROLLING MOMENT LIFT COMP	ROLLING MOMENT SIDE COMP	PITCHING MOMENT LIFT COMP	PITCHING MOMENT DRAG COMP	TOTAL FORCE
1	2.5	-.952381	-6.28571	.892857	-8.92857	-12.7738
2	5	-1.90476	-12.5714	1.785 1	-17.8571	-25.5476
3	7.5	-2.85714	-18.8571	2.67857	-26.7857	-38.3214
4	10	-3.80952	-25.1428	3.57143	-35.7143	-51.0952
5	12.5	-4.7619	-31.4285	4.46428	-44.6428	-63.8691
6	15	-5.71428	-37.7143	5.35714	-53.5714	-76.6429
7	17.5	-6.66667	-44	6.25	-62.5	-89.4167
8	20	-7.61905	-50.2857	7.14286	-71.4286	-102.19
9	22.5	-8.57143	-56.5714	8.03571	-80.3571	-114.964
10	25	-9.52381	-62.8571	8.92857	-89.2857	-127.738

BLOCK GAGE NO. 3 (200 LB)

LOADING CONDITION	1/2 OF TOTAL SIDE FORCE	YAWING MOMENT SIDE COMP	YAWING MOMENT DRAG COMP	TOTAL FORCE
1	3	1.71428	2.85714	7.57143
2	6	3.42857	5.71428	15.1428
3	9	5.14286	8.57143	22.7143
4	12	6.85714	11.4285	30.2857
5	15	8.57143	14.2857	37.8571
6	18	10.2857	17.1428	45.4285
7	21	12	20	53
8	24	13.7142	22.8571	60.5714
9	27	15.4286	25.7143	68.1429
10	30	17.1428	28.5714	75.7143

BLOCK GAGE NO. 4 (100 LB)

LOADING CONDITION	1/2 OF TOTAL SIDE FORCE	YAWING MOMENT SIDE COMP	YAWING MOMENT DRAG COMP	TOTAL FORCE
1	3	-1.71428	-2.85714	-1.57142
2	6	-3.42857	-5.71428	-3.14285
3	9	-5.14286	-8.57143	-4.71428
4	12	-6.85714	-11.4285	-6.28571
5	15	-8.57143	-14.2857	-7.85714
6	18	-10.2857	-17.1428	-9.42856
7	21	-12	-20	-11
8	24	-13.7142	-22.8571	-12.5714
9	27	-15.4286	-25.7143	-14.1428
10	30	-17.1428	-28.5714	-15.7142

BLOCK GAGE NO. 6 (500 LB)

LOADING CONDITION	1/2 OF TOTAL LIFT FORCE	PITCHING MOMENT LIFT COMP	PITCHING MOMENT DRAG COMP	TOTAL FORCE
1	5	-1.78571	17.8571	21.0714
2	10	-3.57143	35.7143	42.1428
3	15	-5.35714	53.5714	63.2143
4	20	-7.14286	71.4286	84.2857
5	25	-8.92857	89.2857	105.3 7
6	30	-10.7142	107.142	126.428
7	35	-12.5	125	147.5
8	40	-14.2857	142.857	168.571
9	45	-16.0714	160.714	189.643
10	50	-17.8571	178.571	210.714

COPY AVAILABLE TO DDC DOES NOT
PERMIT FULLY LEGIBLE PRODUCTION

APPENDIX G – LISTING OF COMPUTER PROGRAM FOR DETERMINING INVERSE CALIBRATION MATRIX OF INTERACTION EFFECTS BY METHOD OF LEAST SQUARES

SUBR DC

```
    SUBR DC
    X=2
    WRIT X
    X=4
    WRIT X,'USED FOR COLLECTION OF CALIBRATION'
    X=1
    WRIT X,' DATA WITH COMPOUND LOADING CONDITIONS'
    WRIT X,' '
    WRIT X,'    (CALL DC)'
    WRIT X,' '
    TYPE 'MONTH,DAY,YEAR'
    ACCE M1,M2,M3
    TYPE 'START TIME, TEMP'
    ACCE M4,M6
    TYPE 'VARIED 1-DRAG 2-LIFT 3-SIDE 4-ROLL 5-PITCH 6-YAW'
    ACCE FF
    JT=1
    CALL CC
    K=1
    TYPE 'DRAG,LIFT,SIDE,ROLL,PITCH,YAW'
2   ACCE DR(K),LI(K),SI(K),RO(K),PI(K),YA(K)
    IF (DR(K)-999) 3,4,3
3   X=1
    FUNC (X,NC,BU)
    DO 1 I=1,6
    DA(K,I)=BU(I+1)/819.2
1   CONT
    DA(K,1)=-DA(K,1)
    DA(K,2)=-DA(K,2)
    DA(K,3)=-DA(K,3)
    DA(K,4)=-DA(K,4)
    K=K+1
    IF (K-26) 2,4,4
4   TYPE 'NO. DATA PTS. UP'
    ACCE KK
    JT=2
    CALL CC
    TYPE 'STOP TIME'
    ACCE M5
    K=K-1
    X=1
    WRIT X,M1,'-',M2,'-',M3
    WRIT X,'STARTED AT ',M4,'    STOPPED AT ',M5
    WRIT X,'TEMPERATURE = ',M6,' DEGREES'   -
    WRIT X,' '
    X=4
    WRIT X,'   SPAN                GAGE 1
    WRIT X,'GAGE 2              GAGE 3
    WRIT X,'GAGE 4              GAGE 5
    X=1
    WRIT X,'GAGE 6'
    WRIT X,' '
    WRIT X,'START CAL'
    WRIT X,' '
    DO 11 J=1,2
    X=4
    WRIT X,' + SPAN
    X=3
    WRIT X,PS(J,1),PS(J,2),PS(J,3),PS(J,4)
    X=1
    WRIT X,PS(J,5),PS(J,6)
    X=4
    WRIT X,' - SPAN            '
    X=3
    WRIT X,MS(J,1),MS(J,2),MS(J,3),MS(J,4)
    X=1
    WRIT X,MS(J,5),MS(J,6)
    DO 10 I=1,6
    AS(I)=(PS(J,I)-MS(J,I))/2
10  CONT
    X=4
    WRIT X,'AVG SPAN           '
    X=3
    WRIT X,AS(1),AS(2),AS(3),AS(4)
    X=1
    WRIT X,AS(5),AS(6)
    WRIT X,' '
    IF (J-1) 11,12,11
12  X=1
    WRIT X,'STOP CAL'
    WRIT X,' '
11  CONT
    WRIT X,' '
    X=1
    WRIT X,'APPLIED CALIBRATION LOADS'
    WRIT X,' '
    X=4
    WRIT X,'LOADING CONDITION   DRAG FORCE
    X=1
    WRIT X,'LIFT FORCE          SIDE FORCE'
    WRIT X,' '
    DO 20 I=1,K
    WRIT X,I,DR(I),LI(I),SI(I)
20  CONT
    WRIT X,' '
    WRIT X,'PAN WEIGHT (LB)'
    WRIT X,'MOMENT     (IN-LB)'
    WRIT X,' '
    X=4
    WRIT X,'LOADING CONDITION          ROLLING'
    WRIT X,' MOMENT
    WRIT X,'PITCHING MOMENT
    X=1
    WRIT X,'YAWING MOMENT'
    X=4
    WRIT X,'                     PAN WEIGHT        '
    WRIT X,'MOMENT            PAN WEIGHT           '
    WRIT X,'MOMENT            PAN WEIGHT           '
    X=1
    WRIT X,'MOMENT'
    WRIT X,' '
    DO 21 I=1,K
    X=3
    WRIT X,I,RO(I),RO(I)*52.6,PI(I)
    X=1
    WRIT X,PI(I)*52.6,YA(I),YA(I)*88
21  CONT
    WRIT X,' '
    WRIT X,'RAW DATA FROM EACH BLOCK GAGE'
    WRIT X,' '
    X=4
    WRIT X,'LOADING CONDITION     GAGE 1            GAGE 2'
    WRIT X,'                   GAGE 3          GAGE 4'
    X=1
    WRIT X,'                   GAGE 5          GAGE 6'
    WRIT X,' '
    DO 6 I=1,K
    X=3
    WRIT X,I,DA(I,1),DA(I,2),DA(I,3)
    X=1
    WRIT X,DA(I,4),DA(I,5),DA(I,6)
6   CONT
    TR=1
    TX=K
    TW=0
    X=1
    WRIT X,' '
    X=4
    WRIT X,'RESULTANT FORCES & MOMENTS FROM RAW '
    X=1
    WRIT X,'BLOCK GAGE DATA'
    WRIT X,' '
    OT=0
    CALL TT
    CALL AZ
    X=2
    WRIT X
    END
```

SUBR CC

```
    SUBR CC
    TYPE 'COLLECT CALS'
    DO 1 I=1,6
    TYPE 'GAGE ',I
    TYPE 'PLUS 0-Y'
    ACCE YE
    IF (YE) 99,4,99
4   X=1
    FUNC (X,NC,BU)
    PS(JT,I)=BU(I+1)/819.2
    TYPE 'MINUS 0-Y'
    ACCE YE
    IF (YE) 99,5,99
5   X=1
    FUNC (X,NC,BU)
    MS(JT,I)=BU(I+1)/819.2
1   CONT
99  CONT
    END
```

SUBR DI

```
    SUBR DI
    DIME PS(2,6),MS(2,6),AS(2,6)
    DIME DR(25),LI(25),SI(25),RO(25)
    DIME PI(25),YA(25),FL(15),FD(15)
    DIME FS(15),DA(25,6),M(6),B(6)
    DIME NT(6),BT(6),N(2,6)
    DIME BU(7),WT(25)
    END
```


COPY AVAILABLE TO DDC DOES NOT PERMIT FULLY LEGIBLE PRODUCTION

SUBR TT

```
    SUBR TT
    IF (OT) 5,4,5
5   L=1
    DO 2 I=1,3
    CALL G
    N(L,1)=F5
    N(L,2)=F3+F4
    N(L,3)=F1+F2+F6
    N(L,4)=14*(F3-F4)
    N(L,5)=14*(F6-F1-F2)
    N(L,6)=10.5*(F1-F2)
    L=L+1
    I=I+1
2   CONT
    DO 3 I=1,6
    NT(I)=(N(1,I)-N(2,I))/(WT(1)-WT(3))
3   CONT
    DO 4 I=1,6
    BT(I)=N(1,I)-(NT(I)*WT(1))
4   CONT
    X=1
    WRIT X,'EQUATIONS'
    WRIT X,' '
    WRIT X,'DRAG FORCE       = GAGE 5'
    WRIT X,'SIDE FORCE       = GAGE 3 + GAGE 4'
    WRIT X,'LIFT FORCE       = GAGE 1 + GAGE 2 + GAGE 6'
    WRIT X,'YAWING MOMENT    = 14 * (GAGE 3 - GAGE 4)'
    X=4
    WRIT X,'PITCHING MOMENT = 14 * (GAGE 6 - GAGE 1 - '
    X=1
    WRIT X,'GAGE 2)'
    WRIT X,'ROLLING MOMENT   = 10.5 * (GAGE 1 - GAGE 2)'
    IF (OT) 6,7,6
6   X=1
    WRIT X,' '
    X=4
    WRIT X,'                         SLOPE
    X=1
    WRIT X,'           Y-INTERCEPT'
    WRIT X,' '
    WRIT X,'  DRAG FORCE            ',NT(1),BT(1)
    WRIT X,'  SIDE FORCE            ',NT(2),BT(2)
    WRIT X,'  LIFT FORCE            ',NT(3),BT(3)
    WRIT X,'  YAWING MOMENT         ',NT(4),BT(4)
    WRIT X,'  PITCHING MOMENT       ',NT(5),BT(5)
    WRIT X,'  ROLLING MOMENT        ',NT(6),BT(6)
    WRIT X,' '
    TYPE '1-DRAG 2-SIDE 3-LIFT 4-YAW 5-PITCH 6-ROLL'
    ACCE RE
    BE=RE
    RE=(RE*6)-5
    J=1
    DO 10 I=RE,RE+5
    IF (TV) 12,13,12
13  C7(J,BE)=NT(J)
    GO 14
12  C8(J,BE)=NT(J)
14  J=J+1
10  CONT
7   CONT
    END
```

SUBR AZ

```
    SUBR AZ
    X=1
    WRIT X,' '
    WRIT X,' '
    WRIT X,' '
    X=4
    WRIT X,'LOADING CONDITION    DRAG FORCE        SIDE'
    WRIT X,' FORCE           LIFT FORCE        YAWING'
    WRIT X,' MOMENT          PITCHING MOMENT'
    X=1
    WRIT X,'  ROLLING MOMENT'
    WRIT X,' '
    DO 1 I=TR,TX
    IF (TV) 3,4,3
3   CALL G
    GO 5
4   CALL F
5   X=3
    WRIT X,I,F5,F3+F4,F1+F2+F6
    X=1
    WRIT X,14*(F3-F4),14*(F6-F1-F2),10.5*(F1-F2)
1   CONT
    X=1
    WRIT X,' '
    END
```

SUBR F

```
    SUBR F
    F1=DA(I,1)
    F2=DA(I,2)
    F3=DA(I,3)
    F4=DA(I,4)
    F5=DA(I,5)
    F6=DA(I,6)
    END
```

SUBR G

```
    SUBR G
    F1=M(1)*WT(I)+B(1)
    F2=M(2)*WT(I)+B(2)
    F3=M(3)*WT(I)+B(3)
    F4=M(4)*WT(I)+B(4)
    F5=M(5)*WT(I)+B(5)
    F6=M(6)*WT(I)+B(6)
    END
```

SUBR LS

```
    SUBR LS
    X=2
    WRIT X
    X=4
    WRIT X,'USED FOR CALCULATING MATRIX OF BEST'
    WRIT X,' FIT STRAIGHT LINE INTERACTION '
    X=1
    WRIT X,'EFFECTS BY METHOD OF LEAST SQUARES'
    WRIT X,' '
    WRIT X,'      (CALL LS)'
    WRIT X,' '
    WRIT X,M1,'-',M2,'-',M3
    WRIT X,'STARTED AT ',M4,'  STOPPED AT ',M5
    WRIT X,' '
    GO (20,21,22,26,27,28),FF
26  DO 29 I=1,25
    WT(I)=RO(I)*52.6
29  CONT
    GO 25
27  DO 30 I=1,25
    WT(I)=PI(I)*52.6
30  CONT
    GO 25
28  DO 31 I=1,25
    WT(I)=YA(I)*28
31  CONT
    GO 25
20  DO 23 I=1,25
    WT(I)=DR(I)
23  CONT
    GO 25
21  DO 24 I=1,25
    WT(I)=LI(I)
24  CONT
    GO 25
22  DO 25 I=1,25
    WT(I)=SI(I)
25  CONT
    TYPE 'NO. PTS. UP'
    ACCE KK
    NP=KK
    NP=KK
    TR=1
    TX=KK
    KT=1
    X=1
    WRIT X,'***INCREASING LOAD***'
    WRIT X,' '
    TV=0
95  X=4
    WRIT X,'LEAST SQUARES BEST FIT STRAIGHT LINE'
    X=1
    WRIT X,' CALCULATION FROM RAW BLOCK GAGE DATA'
8   DO 3 I=1,6
    Y(I)=0
    XY(I)=0
3   CONT
    X=0
    X2=0
    DO 1 I=KT,KK
    X=X+WT(I)
    X2=X2+(WT(I)*WT(I))
    DO 1 L=1,6
    Y(L)=Y(L)+DA(I,L)
    XY(L)=XY(L)+(WT(I)*DA(I,L))
1   CONT
```

COPY AVAILABLE TO DDC DOES NOT PERMIT FULLY LEGIBLE PRODUCTION

```
      DO 8 I=1,6
      M(I)=((NP*XY(I))-(X*Y(I)))/((NP*X2)-(X*X))
      B(I)=((X2*Y(I))-(X*XY(I)))/((NP*X2)-(X*X))
8     CONT
      X=1
      WRIT X,' '
      WRIT X,' '
      WRIT X,' '
      X=4
      WRIT X,'BLOCK GAGE          SLOPE  (VOLTS/LB)'
      X=1
      WRIT X,'     Y-INTERCEPT'
      WRIT X,' '
      DO 5 I=1,6
      WRIT X,I,M(I),B(I)
5     CONT
      X=1
      WRIT X,' '
      WRIT X,' '
      WRIT X,' '
      X=4
      WRIT X,'
      WRIT X,'                                         CONSECUT'
      X=1
      WRIT X,'IVE CONDITIONS'
      X=4
      WRIT X,'LOADING CONDITION     ACTUAL DATA        BEST'
      WRIT X,' FIT             DEVIATION'
      X=1
      WRIT X,'            DIFFERENCE          SLOPE'
      WRIT X,' '
      DO 6 I=1,6
      X=1
      WRIT X,' BLOCK GAGE ',I
      WRIT X,' '
      V1=DA(KT,I)
      V2=VT(KT)
      DO 7 L=KT,KK
      EZ=M(I)*VT(L)+B(I)
      X=3
      WRIT X,L,DA(L,I),EZ,EZ-DA(L,I)
      X=1
      WRIT X,DA(L,I)-V1,(DA(L,I)-V1)/(VT(L)-V2)
      V1=DA(L,I)
      V2=VT(L)
7     CONT
      WRIT X,' '
6     CONT
      TV=1
      X=1
      WRIT X,' '
      X=4
      WRIT X,'CALCULATION OF RESULTANT FORCE & '
      WRIT X,'MOMENT CALIBRATION CURVES FROM '
      WRIT X,'BEST FIT STRAIGHT LINE DATA FOR '
      X=1
      WRIT X,'EACH BLOCK GAGE'
      WRIT X,' '
      OT=1
      CALL TI
      CALL AZ
      IF (TV) 99,10,99
10    X=1
      WRIT X,' '
      WRIT X,' '
      WRIT X,'***DECREASING LOAD***'
      WRIT X,' '
      KT=K-KK+1
      KK=K
      TV=1
      TR=KT
      TX=K
      NP=KK-KT+1
      GO 95
99    X=2
      WRIT X
      END
```

SUBR MA

```
      SUBR MA
      TYPE 'UP-0 DOWN-1 AVERAGE-2'
      ACCE UP
      IF (UP-1) 91,90,93
90    DO 92 I=1,6
      DO 92 J=1,6
      A(I,J)=C8(I,J)
92    CONT
      GO 94
91    DO 95 I=1,6
      DO 95 J=1,6
      A(I,J)=C7(I,J)
95    CONT
      GO 94
93    DO 21 I=1,6
      DO 21 J=1,6
      A(I,J)=(C7(I,J)+C8(I,J))/2
21    CONT
94    X=2
      WRIT X
      X=4
      WRIT X,'THE MATRIX OF CALIBRATION IS'
      X=1
      IF (UP-1) 97,96,24
96    WRIT X,' DOWN'
      GO 98
97    WRIT X,' UP'
      GO 98
24    WRIT X,' AVERAGED'
98    WRIT X,' '
      CALL OU
      N1=6
      DE=1
      DO 1 J=1,N1
      IN(J,3)=0
1     CONT
      DO 38 I=1,N1
      AM=0
      DO 3 J=1,N1
      IF (IN(J,3)-1) 4,3,4
4     DO 5 K=1,N1
      IF (IN(K,3)-1) 6,5,60
6     IF (A(J,K)) 10,11,11
10    AT=-A(J,K)
      GO 12
11    AT=A(J,K)
12    IF (AM-AT) 15,5,5
15    IR=J
      IC=K
      AM=AT
5     CONT
3     CONT
      IN(IC,3)=IN(IC,3)+1
      IN(I,1)=IR
      IN(I,2)=IC
      IF (IR-IC) 20,25,20
20    DE=-DE
      DO 23 L=1,N1
      SV=A(IR,L)
      A(IR,L)=A(IC,L)
      A(IC,L)=SV
23    CONT
25    PI=A(IC,IC)
      DE=DE*PI
30    A(IC,IC)=1
      DO 32 L=1,N1
      A(IC,L)=A(IC,L)/PI
32    CONT
34    DO 38 L1=1,N1
      IF (L1-IC) 40,38,40
40    T=A(L1,IC)
      A(L1,IC)=0
      DO 42 L=1,N1
      A(L1,L)=A(L1,L)-A(IC,L)*T
42    CONT
38    CONT
      DO 50 I=1,N1
      L=N1+1-I
      IF (IN(L,1)-IN(L,2)) 51,50,51
51    JR=IN(L,1)
      JC=IN(L,2)
      DO 53 K=1,N1
      SW=A(K,JR)
      A(K,JR)=A(K,JC)
      A(K,JC)=SW
53    CONT
50    CONT
      DO 55 K=1,N1
      IF (IN(K,3)-1) 60,61,60
61    CONT
55    CONT
      ID=1
      GO 99
60    ID=2
99    CONT
      X=1
      WRIT X,' '
      WRIT X,' '
      WRIT X,'THE DETERMINANT IS ',DE
      WRIT X,' '
      WRIT X,'THE INDICATOR IS ',ID
      WRIT X,' '
      WRIT X,' '
      WRIT X,'THE INVERSE MATRIX IS'
      WRIT X,' '
      CALL OU
      X=2
      WRIT X
      END
```

SUBR OU

```
      SUBR OU
      DO 8 I=1,6
      X=4
      WRIT X,'CH. ',I
      X=3
      WRIT X,A(I,1),A(I,2),A(I,3),A(I,4)
      X=1
      WRIT X,A(I,5),A(I,6)
8     CONT
      END
```


COPY AVAILABLE TO DDC DOES NOT PERMIT FULLY LEGIBLE PRODUCTION

APPENDIX H — OUTPUT OF COMPUTER PROGRAM FOR DETERMINING CALIBRATION MATRIX OF INTERACTION EFFECTS BY METHOD OF LEAST SQUARES

(CALL DC)

STARTED AT 1435 STOPPED AT 1520
TEMPERATURE = 68 DEGREES

APPLIED CALIBRATION LOADS

LOADING CONDITION	DRAG FORCE	LIFT FORCE	SIDE FORCE
1	0	0	0
2	0	0	0
3	0	0	0
4	0	0	0
5	0	0	0

PAN WEIGHT (LB)
MOMENT (IN-LB)

LOADING CONDITION	ROLLING MOMENT		PITCHING MOMENT		YAWING MOMENT	
	PAN WEIGHT	MOMENT	PAN WEIGHT	MOMENT	PAN WEIGHT	MOMENT
1	0	0	0	0	0	0
2	0	0	25	1315	0	0
3	0	0	50	2630	0	0
4	0	0	75	3945	0	0
5	0	0	100	5260	0	0

RAW DATA FROM EACH BLOCK GAGE
MULTIPLIED BY FOLLOWING NORMALIZING FACTORS

BLOCK GAGE NO.	NORMALIZING FACTORS
1	59.194
2	96.7511
3	79.6004
4	39.5041
5	171.688
6	183.924

LOADING CONDITION	GAGE 1	GAGE 2	GAGE 3	GAGE 4	GAGE 5	GAGE 6
1	0	0	0	0	0	0
2	-24.1342	-23.3846	0	-.626895	0	46.2504
3	-49.2801	-47.596	0	-.72334	0	92.9503
4	-73.7753	-71.4531	0	-.964453	0	138.976
5	-98.2709	-94.6016	0	-1.20556	0	184.552

RESULTANT FORCES & MOMENTS FROM RAW BLOCK GAGE DATA

EQUATIONS

DRAG FORCE = GAGE 5
SIDE FORCE = GAGE 3 + GAGE 4
LIFT FORCE = GAGE 1 + GAGE 2 + GAGE 6
YAWING MOMENT = 14 * (GAGE 3 - GAGE 4)
PITCHING MOMENT = 14 * (GAGE 6 - GAGE 1 - GAGE 2)
ROLLING MOMENT = 10.5 * (GAGE 1 - GAGE 2)

LOADING CONDITION	DRAG FORCE	SIDE FORCE	LIFT FORCE	YAWING MOMENT	PITCHING MOMENT	ROLLING MOMENT
1	0	0	0	0	0	0
2	0	-.626895	-1.2684	8.77653	1312.77	-7.87084
3	0	-.72334	-3.9259	10.1267	2657.97	-17.6836
4	0	-.964453	-6.25204	13.5023	3978.86	-24.3831
5	0	-1.20556	-8.32056	16.8779	5283.94	-38.5279

COPY AVAILABLE TO DDC DOES NOT PERMIT FULLY LEGIBLE PRODUCTION

USED FOR CALCULATING MATRIX OF BEST FIT STRAIGHT LINE INTERACTION EFFECTS BY METHOD OF LEAST SQUARES

(CALL LS)

STARTED AT 1435 STOPPED AT 1520

INCREASING LOAD

LEAST SQUARES BEST FIT STRAIGHT LINE CALCULATION FROM RAW BLOCK GAGE DATA

BLOCK GAGE	SLOPE (VOLTS/LB)	Y-INTERCEPT
1	-.187211E-01	.144442
2	-.180434E-01	.472317E-01
3	0	0
4	-.209026E-03	-.154312
5	0	0
6	.351201E-01	.179783

LOADING CONDITION	ACTUAL DATA	BEST FIT	DEVIATION	CONSECUTIVE CONDITIONS DIFFERENCE	SLOPE
BLOCK GAGE 1					
1	0	.144442	.144442	0	.723704E76
2	-24.1342	-24.4738	-.339599	-24.1342	-.18353E-01
3	-49.2801	-49.0921	.188049	-25.1459	-.191223E-01
4	-73.7753	-73.7104	.648956E-01	-24.4951	-.186274E-01
5	-98.2709	-98.3287	-.577545E-01	-24.4956	-.186278E-01
BLOCK GAGE 2					
1	0	.472317E-01	.472317E-01	0	.723704E76
2	-23.3846	-23.6799	-.295303	-23.3846	-.17783E-01
3	-47.596	-47.4071	.188904	-24.2113	-.184116E-01
4	-71.4531	-71.1343	.318832	-23.8571	-.181422E-01
5	-94.6016	-94.8614	-.259826	-23.1485	-.176034E-01
BLOCK GAGE 3					
1	0	0	0	0	.723704E76
2	0	0	0	0	0
3	0	0	0	0	0
4	0	0	0	0	0
5	0	0	0	0	0
BLOCK GAGE 4					
1	0	-.154312	-.154312	0	.723704E76
2	-.626895	-.429181	.197713	-.626895	-.476726E-03
3	-.72334	-.704051	.192892E-01	-.96445E-01	-.733421E-04
4	-.964453	-.97892	-.144664E-01	-.241113	-.183356E-03
5	-1.20556	-1.25379	-.482225E-01	-.241113	-.183356E-03
BLOCK GAGE 5					
1	0	0	0	0	.723704E76
2	0	0	0	0	0
3	0	0	0	0	0
4	0	0	0	0	0
5	0	0	0	0	0
BLOCK GAGE 6					
1	0	.179783	.179783	0	.723704E76
2	46.2504	46.3628	.112304	46.2504	.351714E-01
3	92.9503	92.5458	-.404495	46.6998	.355131E-01
4	138.976	138.728	-.247589	46.0261	.350008E-01
5	184.552	184.911	.359787	45.5756	.346582E-01

COPY AVAILABLE TO DDC DOES NOT
PERMIT FULLY LEGIBLE PRODUCTION

CALCULATION OF RESULTANT FORCE & MOMENT CALIBRATION CURVES FROM BEST FIT STRAIGHT LINE DATA FOR EACH BLOCK GAGE

EQUATIONS

DRAG FORCE = GAGE 5
SIDE FORCE = GAGE 3 + GAGE 4
LIFT FORCE = GAGE 1 + GAGE 2 + GAGE 6
YAWING MOMENT = 14 ÷ (GAGE 3 - GAGE 4)
PITCHING MOMENT = 14 ÷ (GAGE 6 - GAGE 1 - GAGE 2)
ROLLING MOMENT = 10.5 ÷ (GAGE 1 - GAGE 2)

	SLOPE	Y-INTERCEPT
DRAG FORCE	0	0
SIDE FORCE	-.209026E-03	-.154312
LIFT FORCE	-.164445E-02	.371458
YAWING MOMENT	.292636E-02	2.16037
PITCHING MOMENT	1.00638	-.166472
ROLLING MOMENT	-.711533E-02	1.02071

LOADING CONDITION	DRAG FORCE	SIDE FORCE	LIFT FORCE	YAWING MOMENT	PITCHING MOMENT	ROLLING MOMENT
1	0	-.154312	.371458	2.16037	-.166472	1.02071
2	0	-.429181	-1.791	6.00854	1323.23	-8.33595
3	0	-.704051	-3.95344	9.85671	2646.63	-17.6926
4	0	-.97892	-6.1159	13.7049	3970.02	-27.0495
5	0	-1.25379	-8.27835	17.553	5293.42	-36.4062

COPY AVAILABLE TO DDC DOES NOT PERMIT FULLY LEGIBLE PRODUCTION

APPENDIX I – LISTING OF COMPUTER PROGRAM FOR LEAST SQUARES CALIBRATION OF PRESSURE TRANSDUCERS USING CEC ELECTROMANOMETER SYSTEM

```
    SUBR DC
    X=2
    WRIT X
    X=4
    WRIT X,'PRESSURE GAGE CALIBRATION BY METHOD OF '
    X=1
    WRIT X,'LEAST SQUARES'
    WRIT X,' '
    WRIT X,'  CALL DC'
    WRIT X,' '
    TYPE 'MONTH,DAY,YEAR'
    ACCE M1,M2,M3
    TYPE 'TIME'
    ACCE TI
    TYPE '   ** INSTRUCTIONS **'
    TYPE 'A/D CH. 2 = CALIBRATOR'
    TYPE 'A/D CH. 3 = FIRST GAGE'
    TYPE 'A/D CH. 4 = NEXT GAGE'
    TYPE 'MAX NO. GAGES = 8'
    TYPE 'MAX NO. PTS. = 31'
    TYPE 'NO. GAGES'
    ACCE NG
    X=1
    WRIT X,M1,'-',M2,'-',M3
    WRIT X,'  TIME = ',TI
    WRIT X,' '
    WRIT X,' '
    X=1
    WRIT X,'SPANS BEFORE CALIBRATION'
    WRIT X,' '
    CALL CC
    K=1
    TYPE 'COLLECT DATA 0-Y'
4   ACCE YE
    IF (YE) 1,2,1
2   X=1
    FUNC (X,NC,BU)
    DO 3 I=1,NG
    DA(K,I)=BU(I+2)/819.2
3   CONT
    DT(K)=(BU(2)/819.2)*3
    K=K+1
    IF (K-32) 4,1,1
1   K=K-1
    X=1
    WRIT X,' '
    WRIT X,' '
    WRIT X,'SPANS AFTER CALIBRATION'
    WRIT X,' '
    CALL CC
    WRIT X,' '
    WRIT X,'RAW DATA OF CALIBRATION'
    WRIT X,' '
    DO 10 I=1,NG
    X=1
    WRIT X,'   PSI                    GAGE NO. ',I
    WRIT X,' '
    DO 11 J=1,K
    WRIT X,DT(J),DA(J,I)
11  CONT
    WRIT X,' '
10  CONT
    TYPE 'NO. PTS. UP'
    ACCE KK
    END


    SUBR CC
    TYPE 'COLLECT SPANS'
    DO 1 I=1,NG
    TYPE 'GAGE NO. ',I
    TYPE 'PLUS 0-Y'
    ACCE YE
    IF (YE) 5,3,5
3   X=1
    FUNC (X,NC,BU)
    PS(I)=BU(I+2)/819.2
    TYPE 'MINUS 0-Y'
    ACCE YE
    IF (YE) 5,4,5
4   X=1
    FUNC (X,NC,BU)
    MS(I)=BU(I+2)/819.2
1   CONT
    X=4
    WRIT X,' GAGE NO.                    PLUS
    X=1
    WRIT X,'MINUS                  AVERAGE'
    WRIT X,' '
    DO 5 I=1,NG
    WRIT X,I,PS(I),MS(I),(PS(I)-MS(I))/2
5   CONT
    END

    SUBR DI
    NC=10
    DIME PS(8),MS(8),BU(10),DA(31,8)
    DIME DT(31),Y(8),XY(8),M(8),B(8)
    END
```

```
    SUBR LS
    X=2
    WRIT X
    X=1
    WRIT X,'   CALL LS'
    WRIT X,' '
    WRIT X,M1,'-',M2,'-',M3
    WRIT X,'  TIME = ',TI
    WRIT X,' '
    NP=KK
    KT=1
    TV=0
    X=1
    WRIT X,'   *** INCREASING LOAD ***'
    WRIT X,' '
95  X=4
    WRIT X,'LEAST SQUARES BEST FIT STRAIGHT LINE CALCU'
    X=1
    WRIT X,'LATIONS FROM RAW PRESSURE GAGE DATA'
    WRIT X,' '
    DO 3 I=1,NG
    Y(I)=0
    XY(I)=0
3   CONT
    X=0
    X2=0
    DO 1 I=KT,KK
    X=X+DT(I)
    X2=X2+(DT(I)*DT(I))
    DO 1 L=1,NG
    Y(L)=Y(L)+DA(I,L)
    XY(L)=XY(L)+(DT(I)*DA(I,L))
1   CONT
    DO 2 I=1,NG
    M(I)=((NP*XY(I))-(X*Y(I)))/((NP*X2)-(X*X))
    B(I)=((X2*Y(I))-(X*XY(I)))/((NP*X2)-(X*X))
2   CONT
    WRIT X,' '
    X=4
    WRIT X,' GAGE NO.              SLOPE (VOLTS/PSI)
    WRIT X,'SLOPE (PSI/VOLT)   '
    X=1
    WRIT X,'Y-INTERCEPT'
    WRIT X,' '
    DO 5 I=1,NG
    WRIT X,I,M(I),1/M(I),B(I)
5   CONT
    WRIT X,' '
    WRIT X,' '
    X=4
    WRIT X,'    PSI                    ACTUAL DATA
    X=1
    WRIT X,'  BEST FIT                 DEVIATION'
    WRIT X,' '
    DO 6 I=1,NG
    X=1
    WRIT X,' GAGE NO. ',I
    WRIT X,' '
    DO 7 L=KT,KK
    EZ=M(I)*DT(L)+B(I)
    WRIT X,DT(L),DA(L,I),EZ,EZ-DA(L,I)
7   CONT
    WRIT X,' '
6   CONT
    WRIT X,' '
    WRIT X,' '
    TYPE 'MAX PSI, INCREMENT'
    ACCE MP,IN
    X=1
    WRIT X,'CALCULATED VALUES FROM SLOPES'
    WRIT X,' '
    WRIT X,'   PSI                    VOLTS'
    WRIT X,' '
    DO 8 I=1,NG
    X=1
    WRIT X,'GAGE NO. ',I
    WRIT X,' '
    X8=(MP/IN)+1
    X9=0
    DO 9 L=1,X8
    WRIT X,X9,M(I)*X9+B(I)
    X9=X9+IN
9   CONT
    WRIT X,' '
8   CONT
    IF (TV) 99,10,99
10  X=1
    WRIT X,' '
    WRIT X,' '
    WRIT X,'   *** DECREASING LOAD ***'
    WRIT X,' '
    KT=KK
    KK=K
    TV=1
    NP=KK-KT+1
    GO 95
99  X=2
    WRIT X
    END
```


COPY AVAILABLE TO DDC DOES NOT PERMIT FULLY LEGIBLE PRODUCTION

APPENDIX J — OUTPUT OF COMPUTER PROGRAM USED FOR LEAST SQUARES CALIBRATION OF PRESSURE TRANSDUCERS USING CEC ELECTROMANOMETER SYSTEM

PRESSURE GAGE CALIBRATION BY METHOD OF LEAST SQUARES

CALL DC

11-12-73
TIME = 1645

SPANS BEFORE CALIBRATION

GAGE NO.	PLUS	MINUS	AVERAGE
1	.26123	-.27832	.269775

SPANS AFTER CALIBRATION

GAGE NO.	PLUS	MINUS	AVERAGE
1	.263671	-.272216	.267944

RAW DATA OF CALIBRATION

PSI	GAGE NO. 1
0	-.366211E-02
.600586	.366211
1.18286	.736084
1.77612	1.12426
2.40966	1.51489
2.98095	1.8811
3.57788	2.25952
4.17846	2.65014
4.77905	3.0249
4.19311	2.67578
3.59985	2.30957
2.98095	1.91284
2.39135	1.54785
1.80175	1.17553
1.19018	.783691
.593261	.397949
0	.12207E-02

COPY AVAILABLE TO DDC DOES NOT PERMIT FULLY LEGIBLE PRODUCTION

COPY AVAILABLE TO DDC DOES NOT PERMIT FULLY LEGIBLE PRODUCTION

CALL LS

11-12-73
TIME = 1645

*** INCREASING LOAD ***

LEAST SQUARES BEST FIT STRAIGHT LINE CALCULATIONS FROM RAW PRESSURE GAGE DATA

GAGE NO.	SLOPE (VOLTS/PSI)	Y-INTERCEPT	
1	.635225	-.105239E-01	1.5742 PSI/VOLT

PSI | ACTUAL DATA | BEST FIT | DEVIATION

GAGE NO. 1

PSI	ACTUAL DATA	BEST FIT	DEVIATION
0	-.366211E-02	-.105239E-01	-.686179E-02
.600586	.366211	.370983	.477266E-02
1.18286	.736084	.740859	.477534E-02
1.77612	1.12426	1.11771	-.65527E-02
2.40966	1.51489	1.52015	.526619E-02
2.98095	1.8811	1.88305	.195217E-02
3.57788	2.25952	2.26223	.271415E-02
4.17846	2.65014	2.64374	-.640297E-02
4.77905	3.0249	3.02525	.348091E-03

CALCULATED VALUES FROM SLOPES

GAGE NO. 1

PSI	VOLTS
0	-.105239E-01
1	.624701
2	1.25992
3	1.89515
4	2.53038

*** DECREASING LOAD ***

LEAST SQUARES BEST FIT STRAIGHT LINE CALCULATIONS FROM RAW PRESSURE GAGE DATA

GAGE NO.	SLOPE (VOLTS/PSI)	Y-INTERCEPT	
1	.632549	.234335E-01	1.5809 PSI/VOLT

GAGE NO. 1

PSI	ACTUAL DATA	BEST FIT	DEVIATION
4.77905	3.0249	3.04641	.21513E-01
4.19311	2.67578	2.67578	0
3.59985	2.30957	2.30051	-.905609E-02
2.98095	1.91284	1.90903	-.380897E-02
2.39135	1.54785	1.53608	-.117683E-01
1.80175	1.17553	1.16313	-.124044E-01
1.19018	.783691	.776283	-.74079E-02
.593261	.397949	.3987	.751197E-03
0	.12207E-02	.234335E-01	.222128E-01

CALCULATED VALUES FROM SLOPES

GAGE NO. 1

PSI	VOLTS
0	.234335E-01
.5	.339708
1	.655982
1.5	.972256
2	1.28853
2.5	1.6048
3	1.92108
3.5	2.23735
4	2.55362
4.5	2.8699
5	3.18617

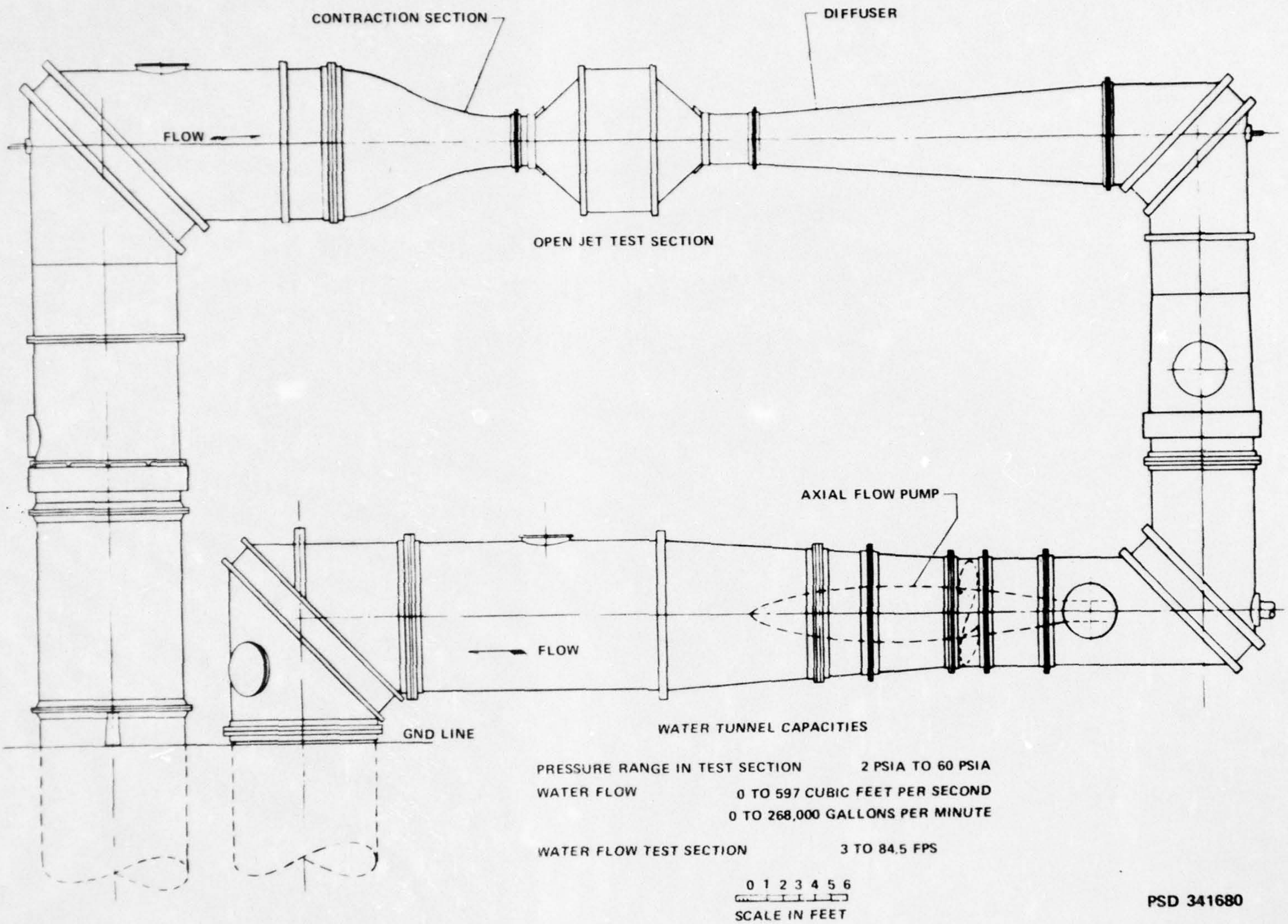

Figure 1– Schematic Drawing of DTNSRDC 36-Inch Variable Pressure Water Tunnel

AD-A031 746 DAVID W TAYLOR NAVAL SHIP RESEARCH AND DEVELOPMENT CE--ETC F/G 20/4
A NEW EXPERIMENTAL FACILITY FOR THE PERFORMANCE EVALUATION OF S--ETC(U)
DEC 75 S E CALLANEN

UNCLASSIFIED SPD-671-01 NL

2 OF 2
AD
A031746

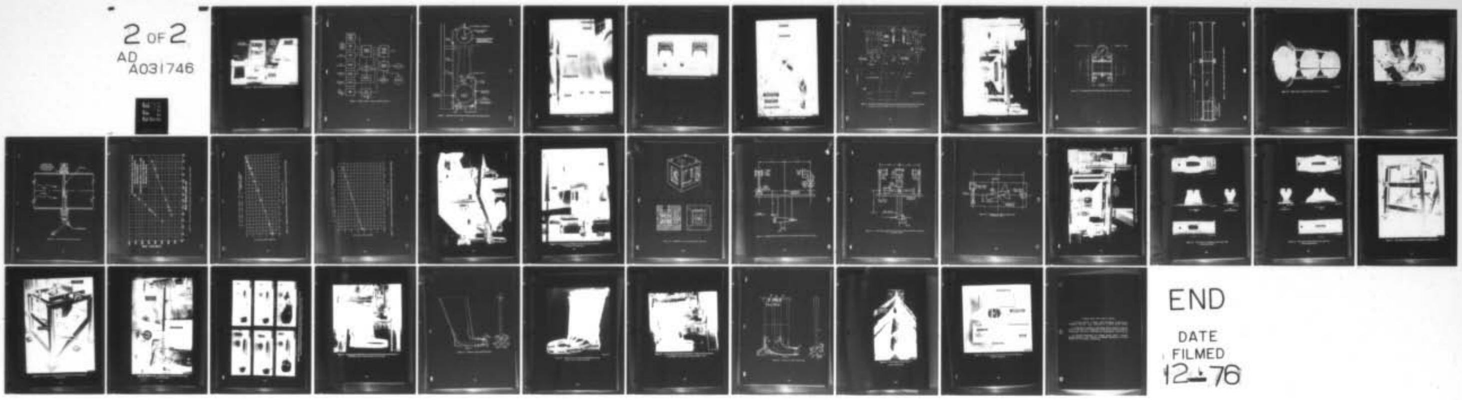

END
DATE
FILMED
12-76

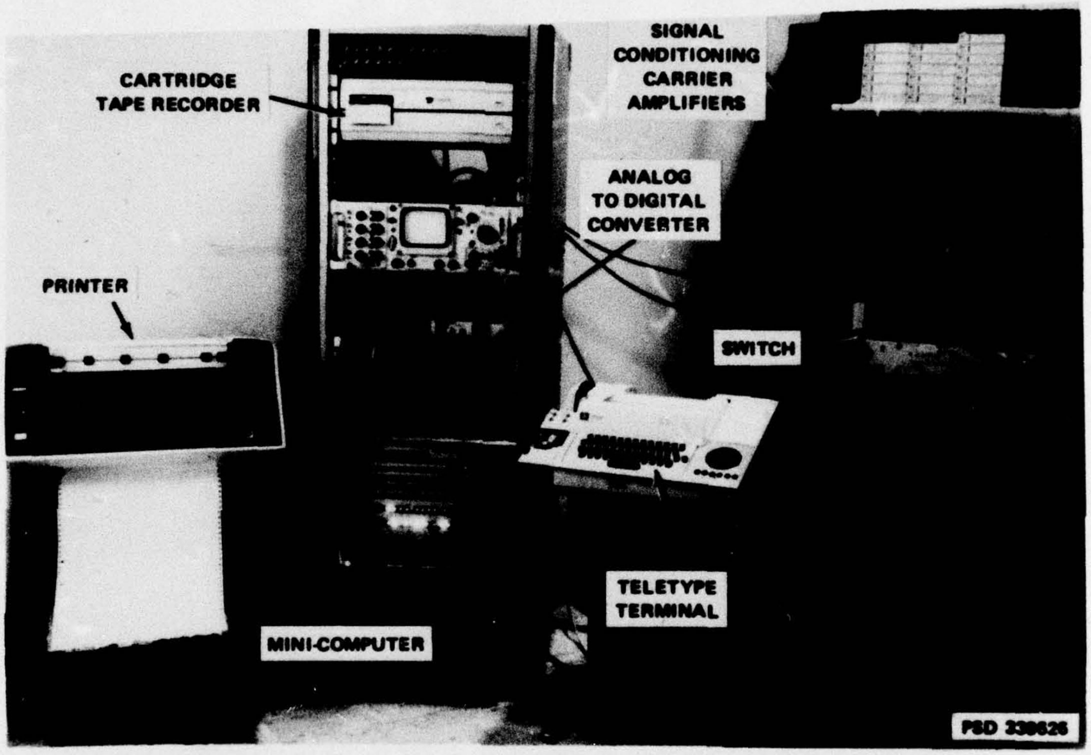

Figure 2 – Mini-Computer Data Acquisition System

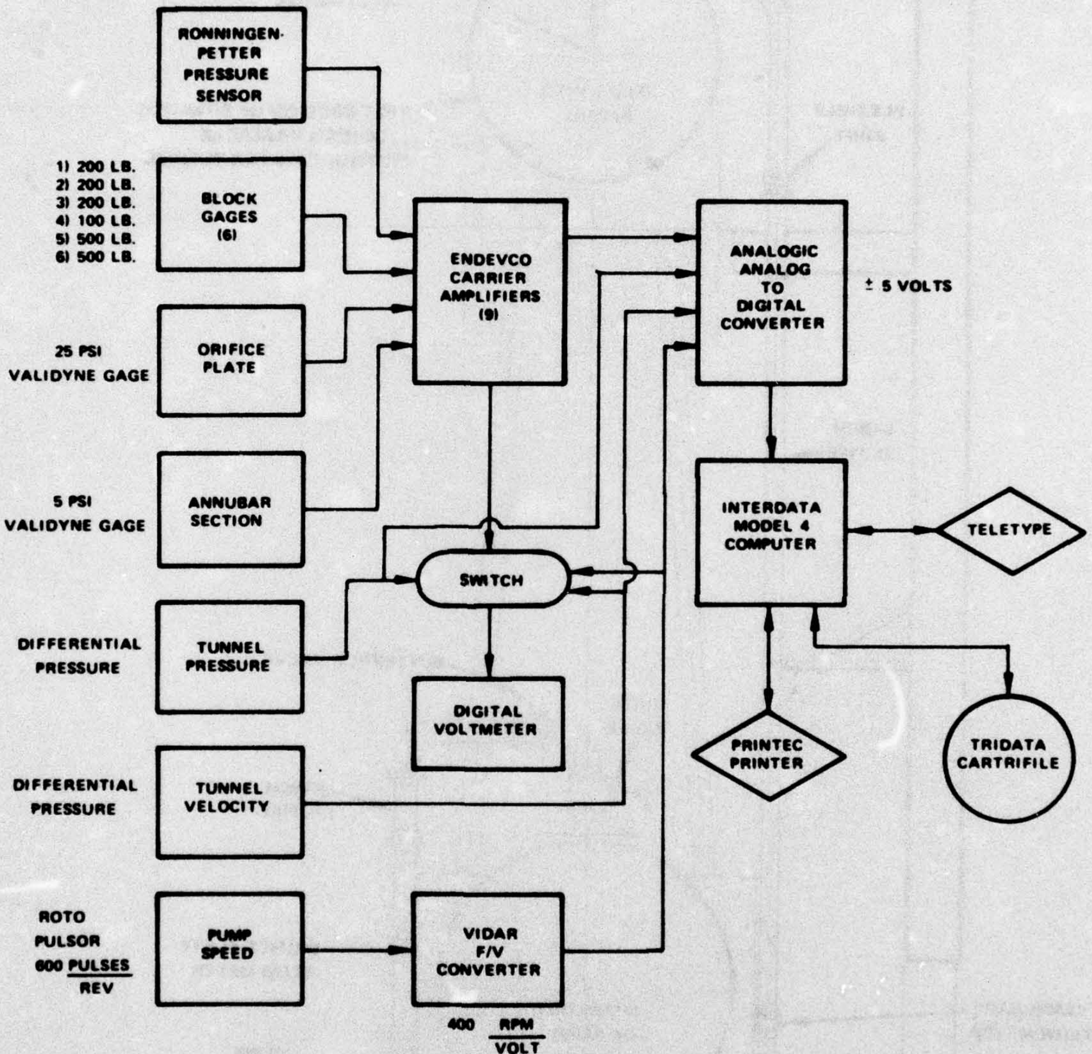

Figure 3 – Block Diagram of Data Acquisition System

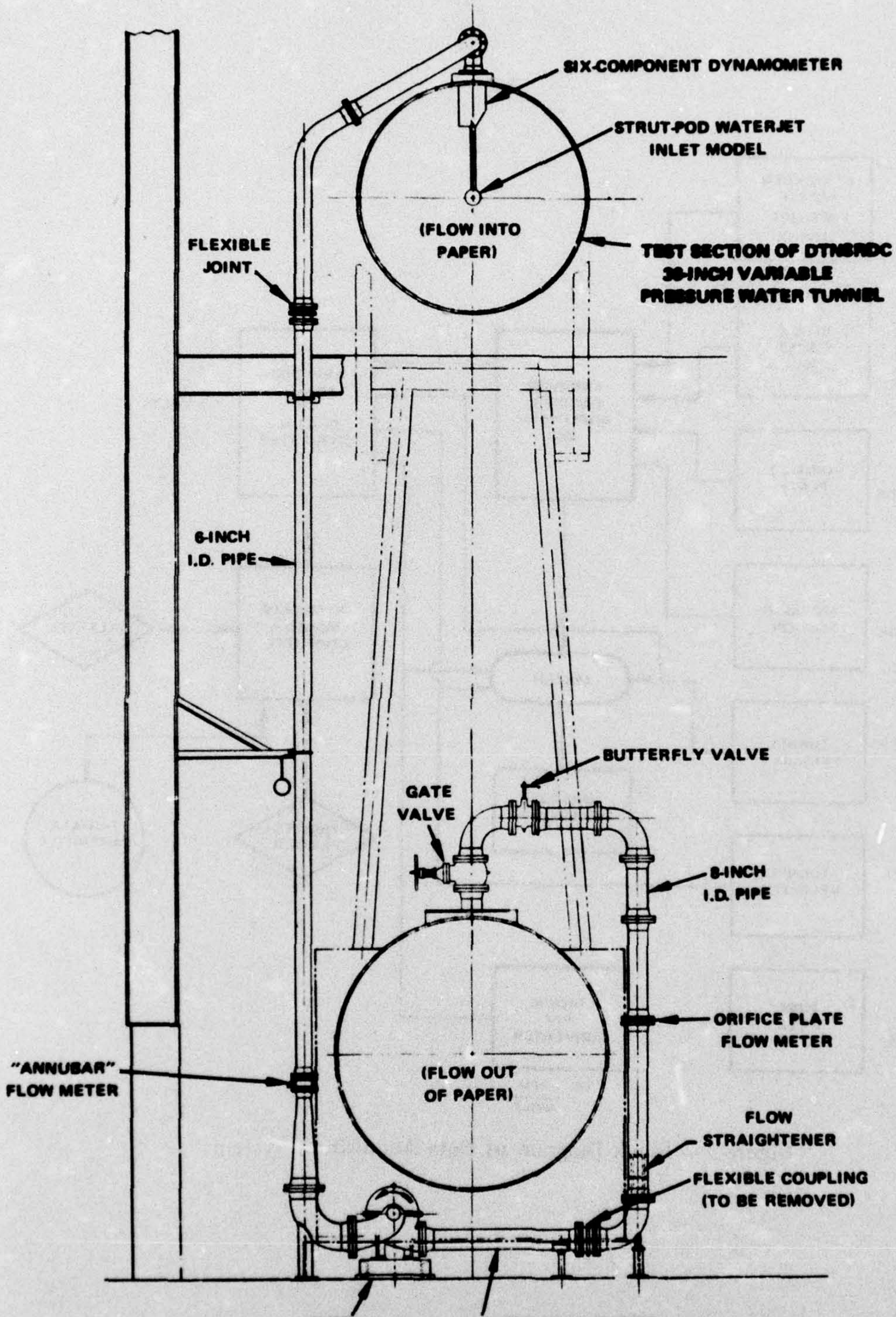

Figure 4 – Schematic Cross Section of Waterjet Test Loop Piping Circuit

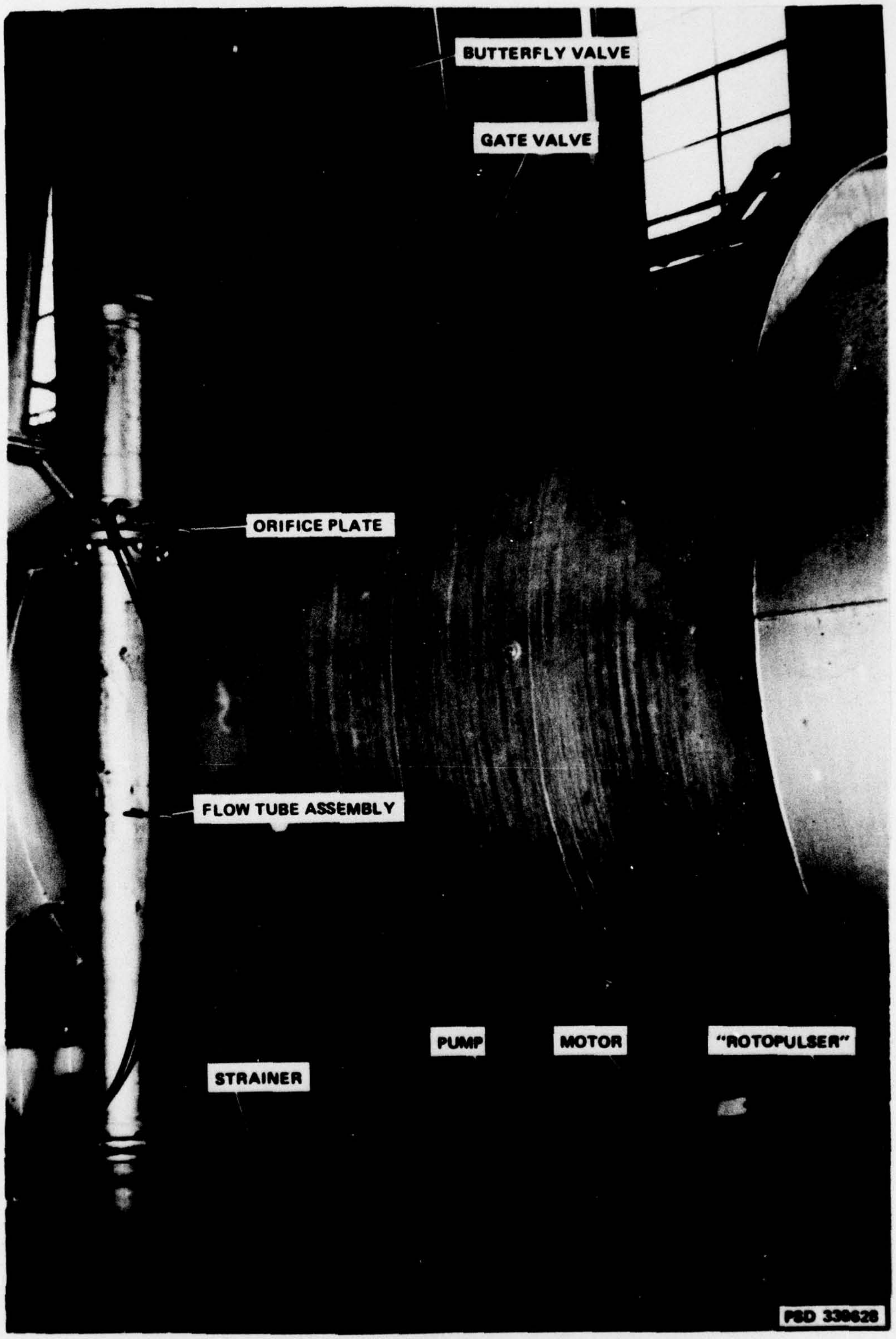

Figure 5 – Piping on Discharge Side of Pump

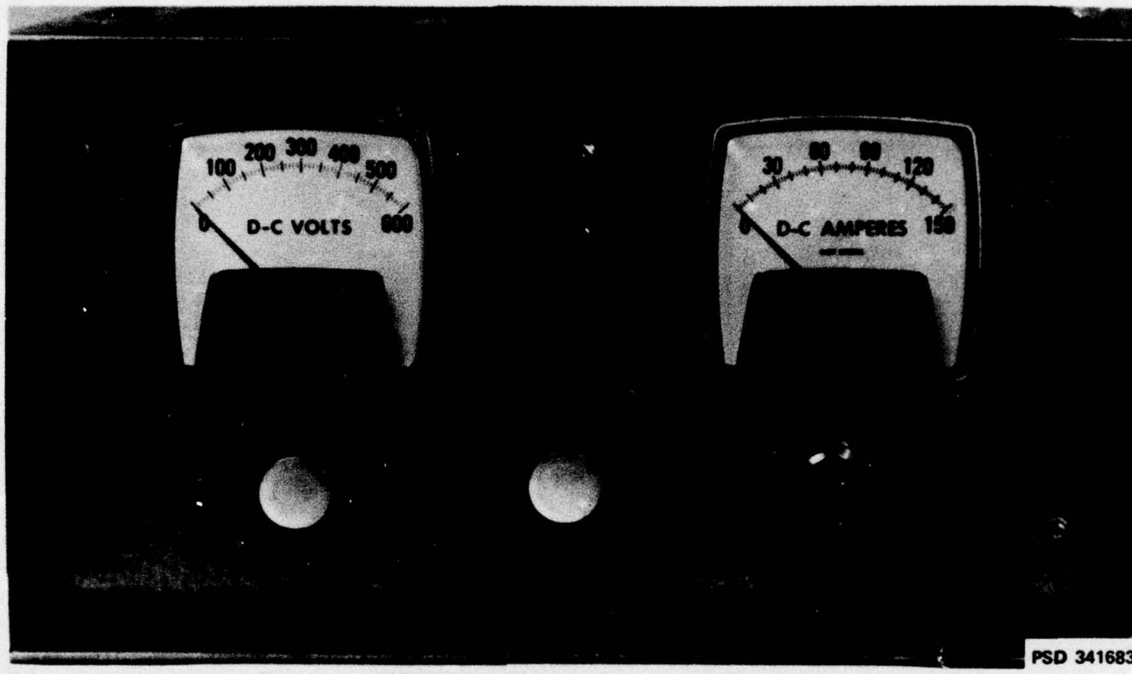

Figure 6 – Control Unit for Variable Speed Pump Drive System

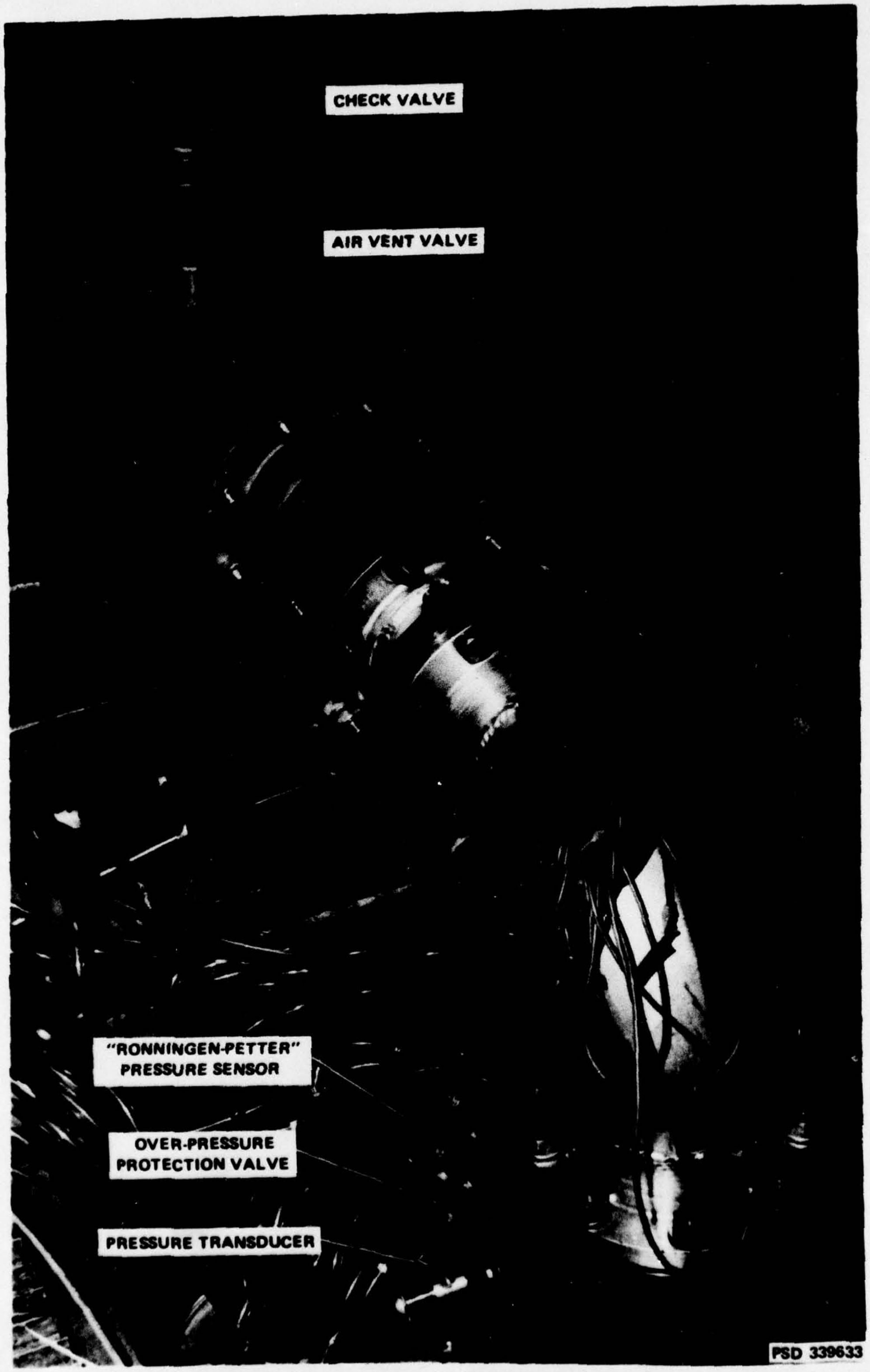

Figure 7 – Piping at Top of Tunnel Test Section

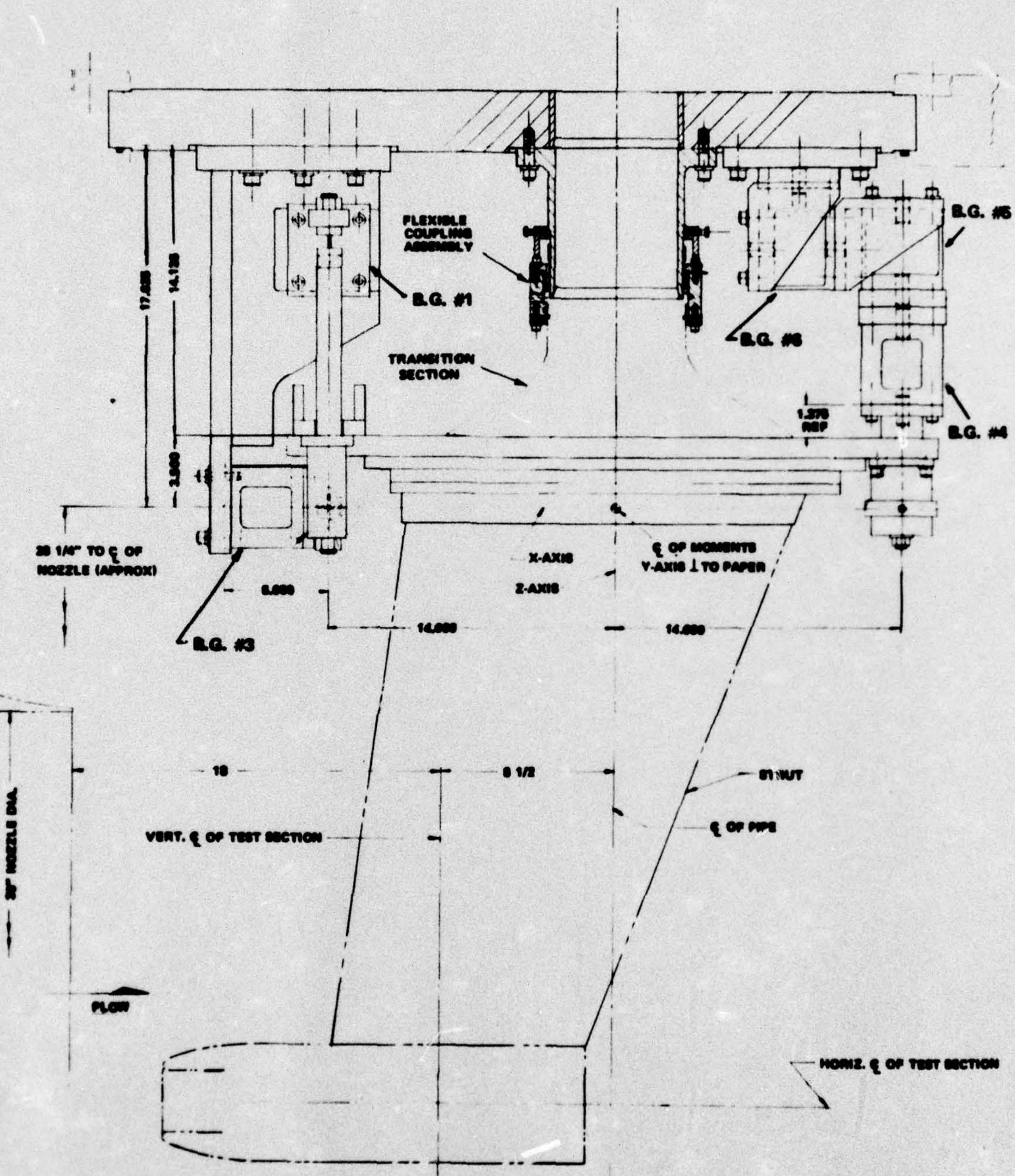

Figure 8 – Schematic Drawing of Supercavitating Model Mounted Beneath 6-Component Dynamometer in DTNSRDC 36-Inch Variable Pressure Water Tunnel

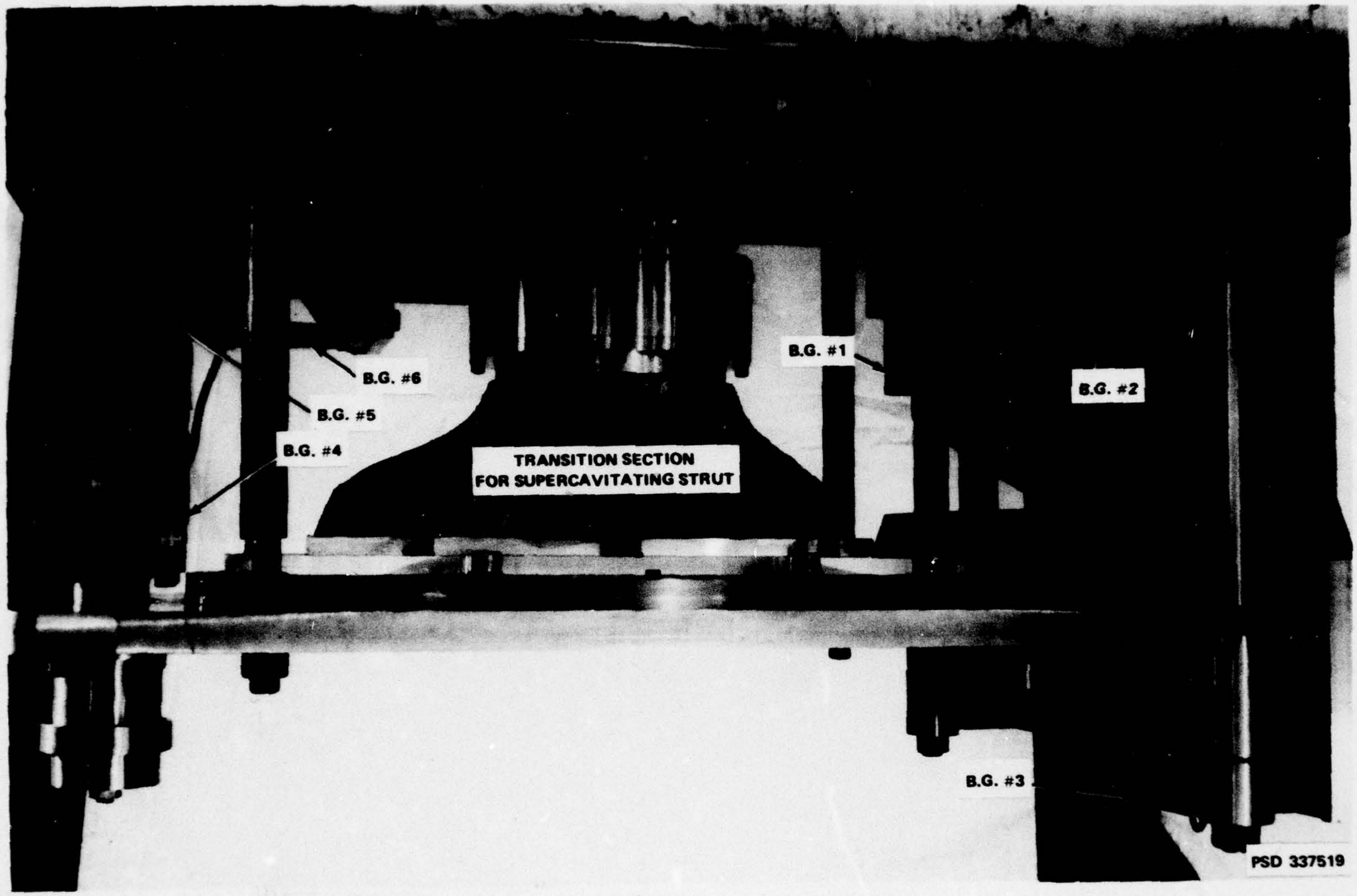

Figure 9 – 6-Component Dynamometer with Transition Section for Supercavitating Model Installed

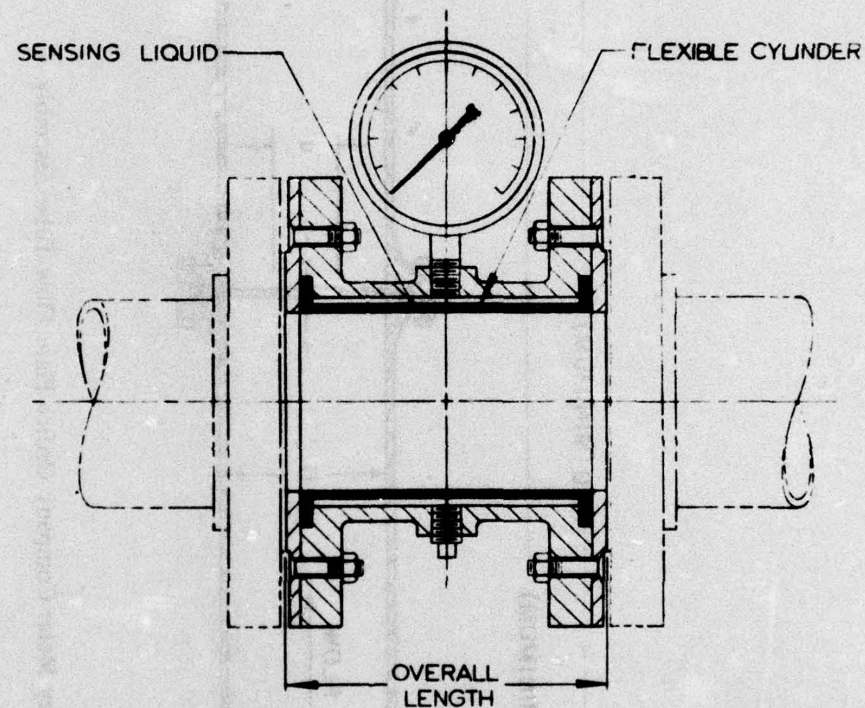

Figure 10 – Ronningen-Petter Ful-Stream Pressure Sensor Shown in Cross Section

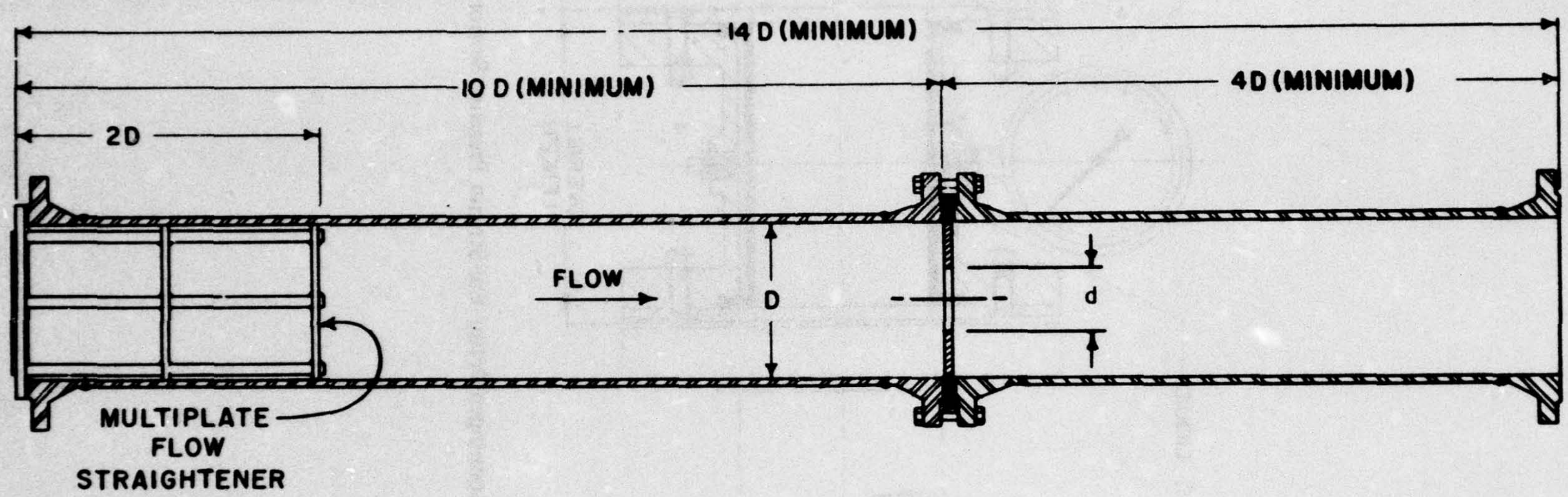

Figure 11 – Bailey Meter Company Orifice Plate Flow Tube Assembly

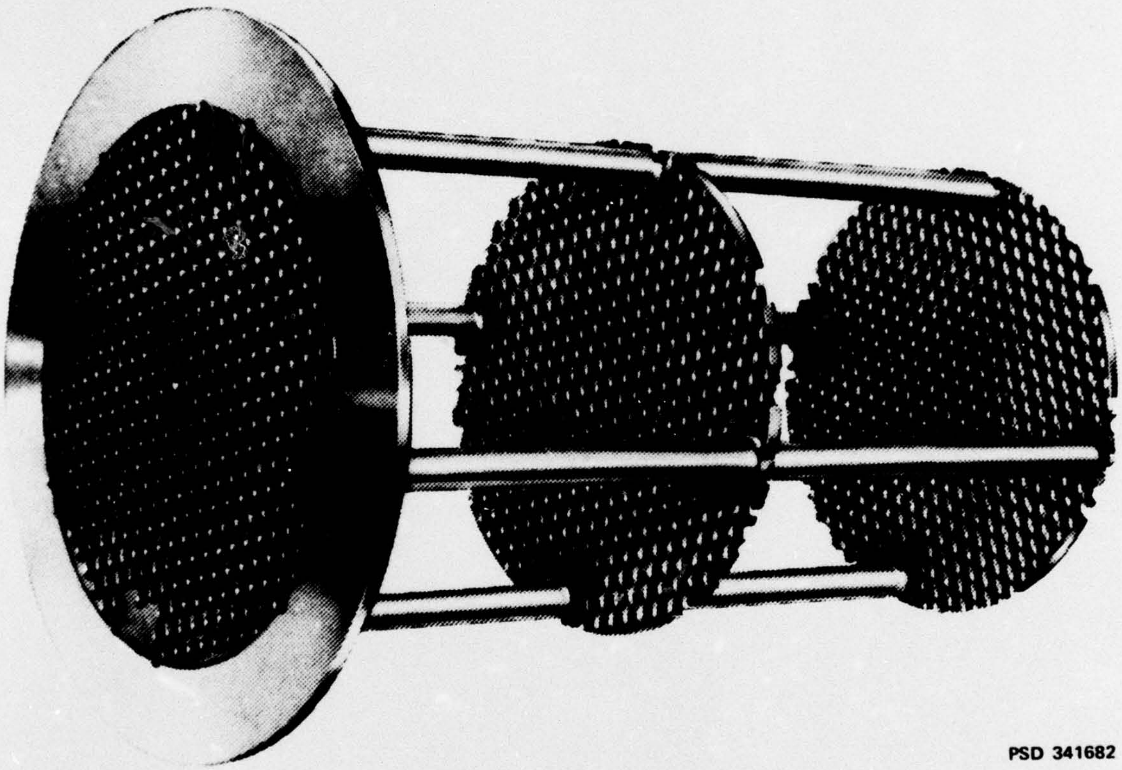

PSD 341682

Figure 12 – Bailey Meter Company Multiplate Flow Straightener

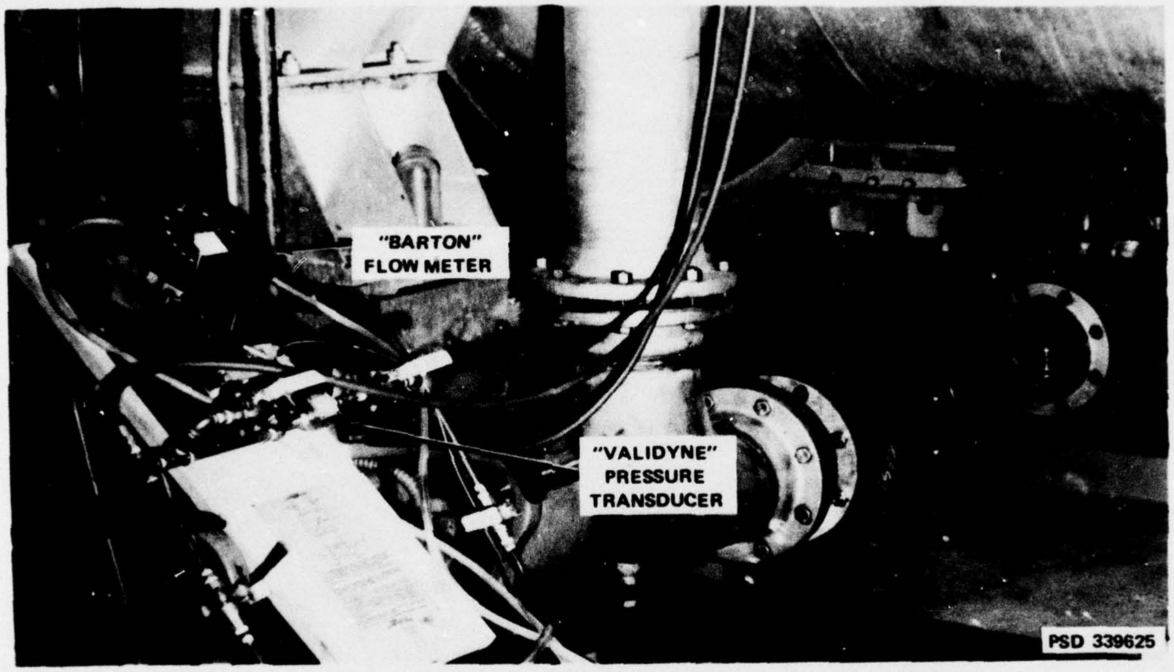

Figure 13 – ITT Barton Portable Flow Indicator with Differential Pressure Transducer Attached

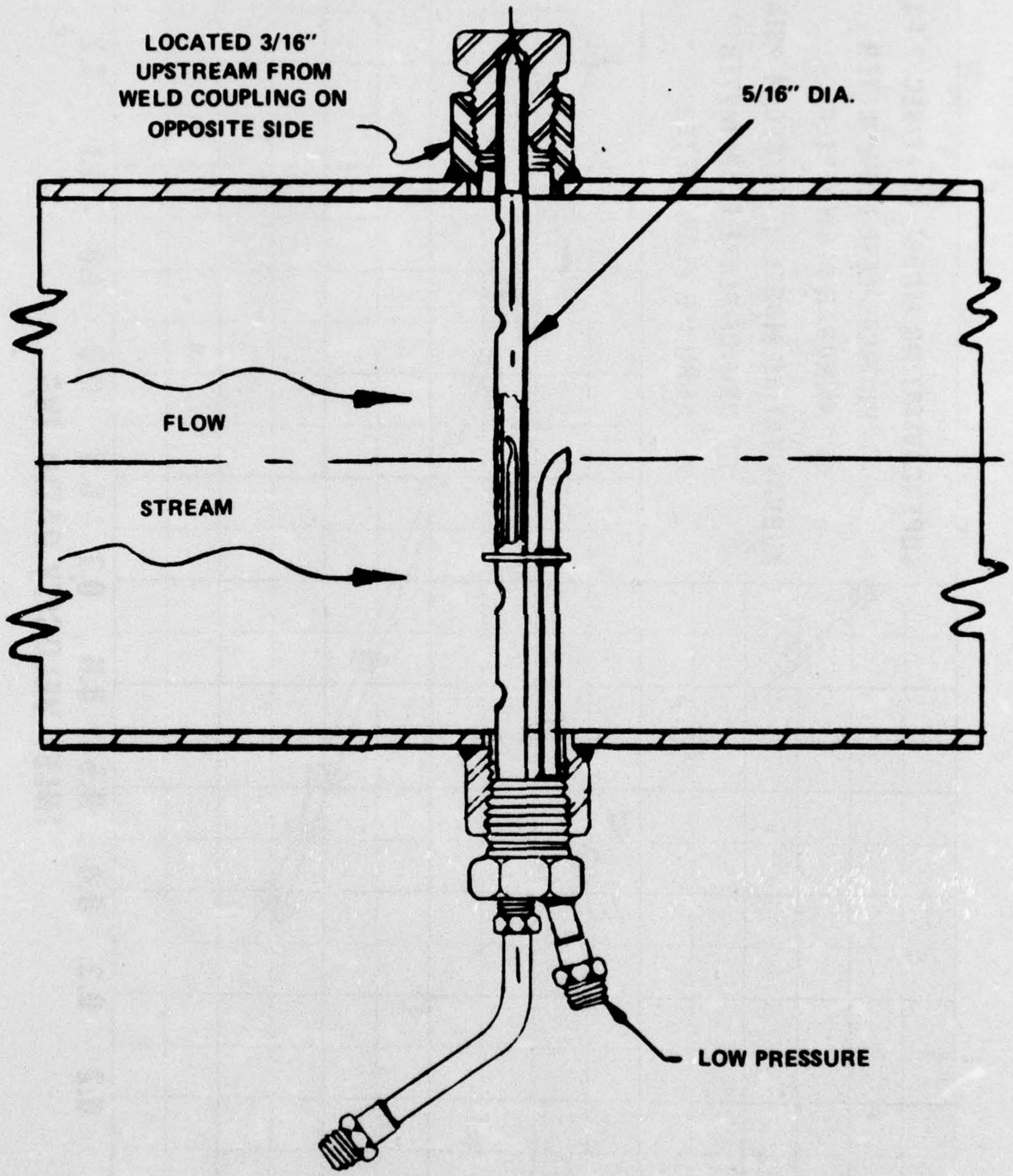

Figure 14 – Annubar Flow Measuring Element

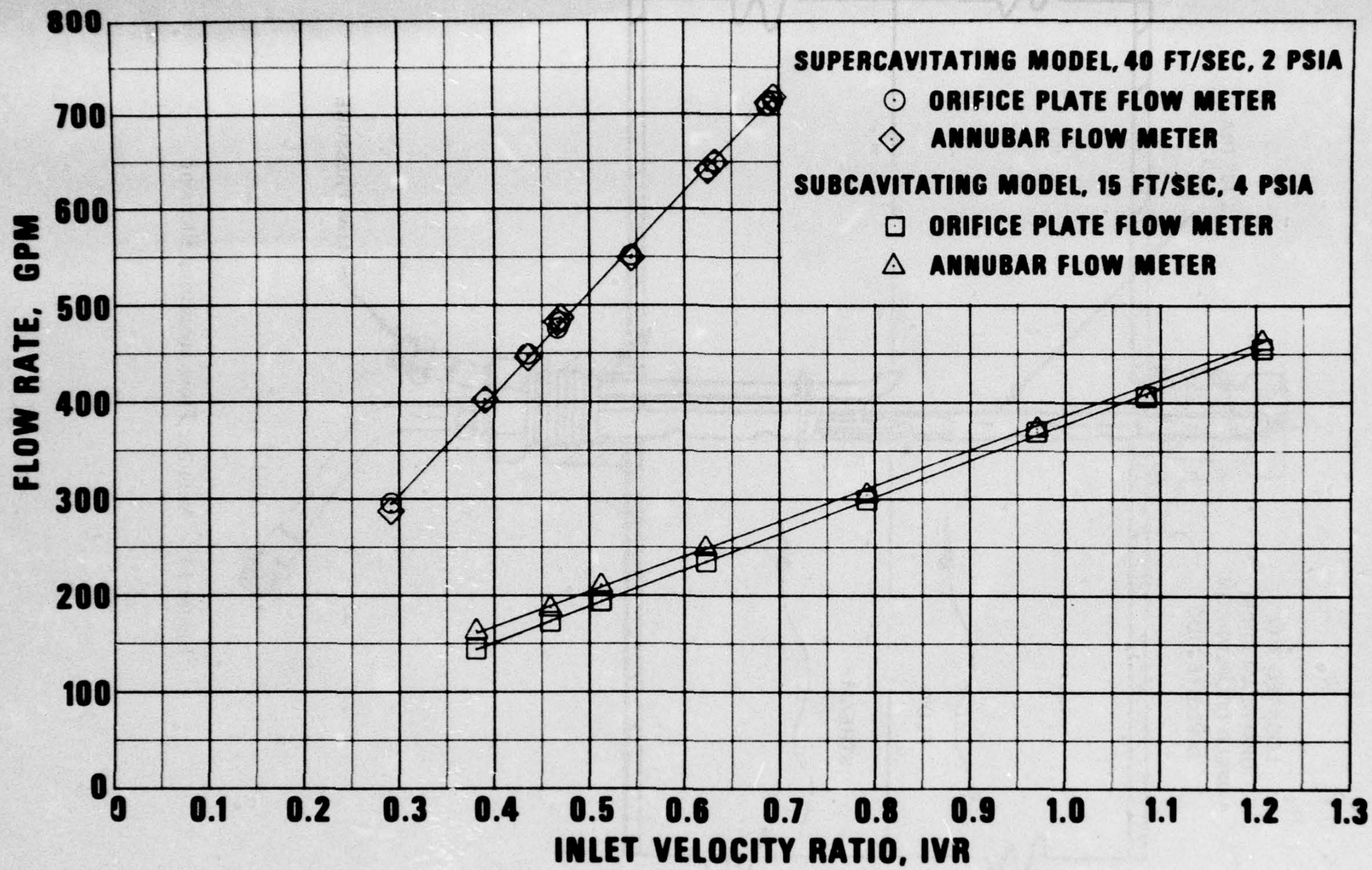

Figure 15 – Comparison of Flow Rates Measured with Orifice Plate and Annubar Sensor

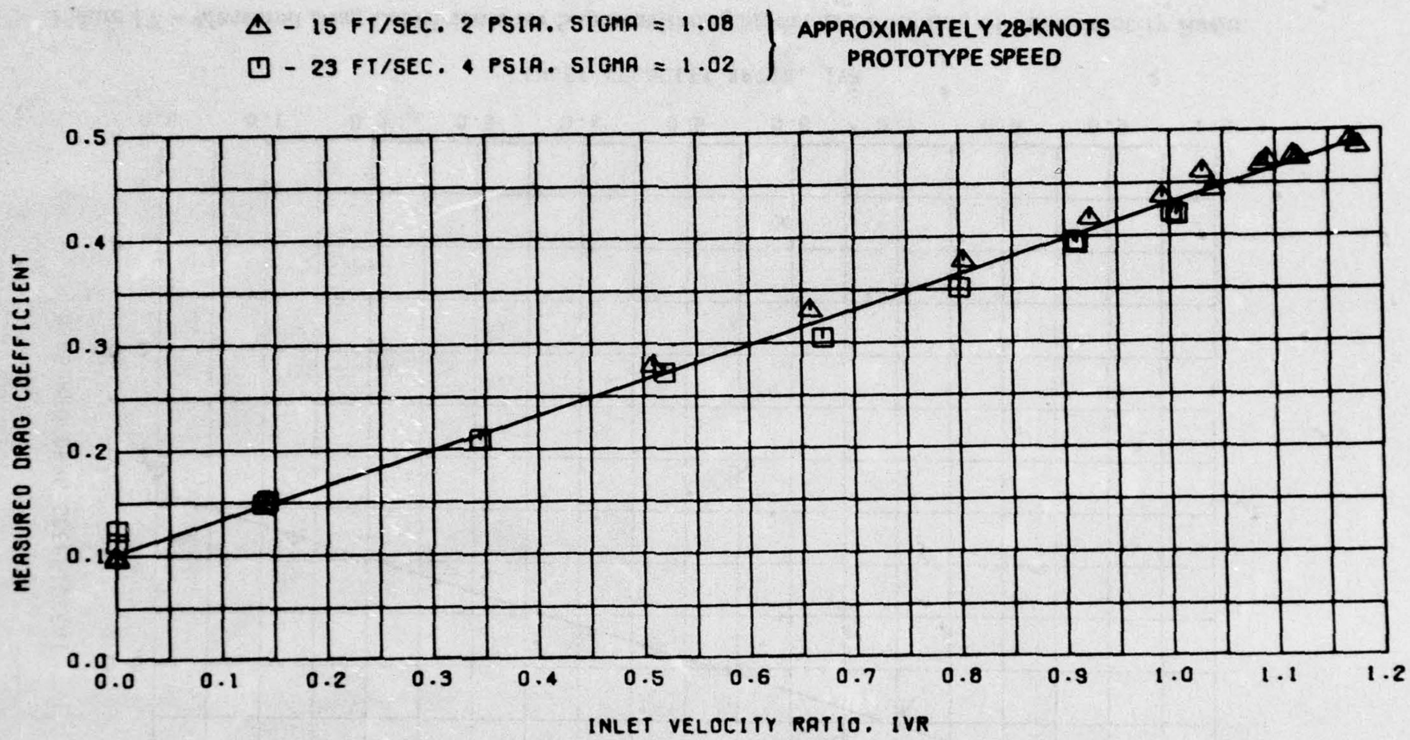

Figure 16 – Measured Drag Coefficients for Subcavitating Model as a Function of Inlet Velocity Ratio

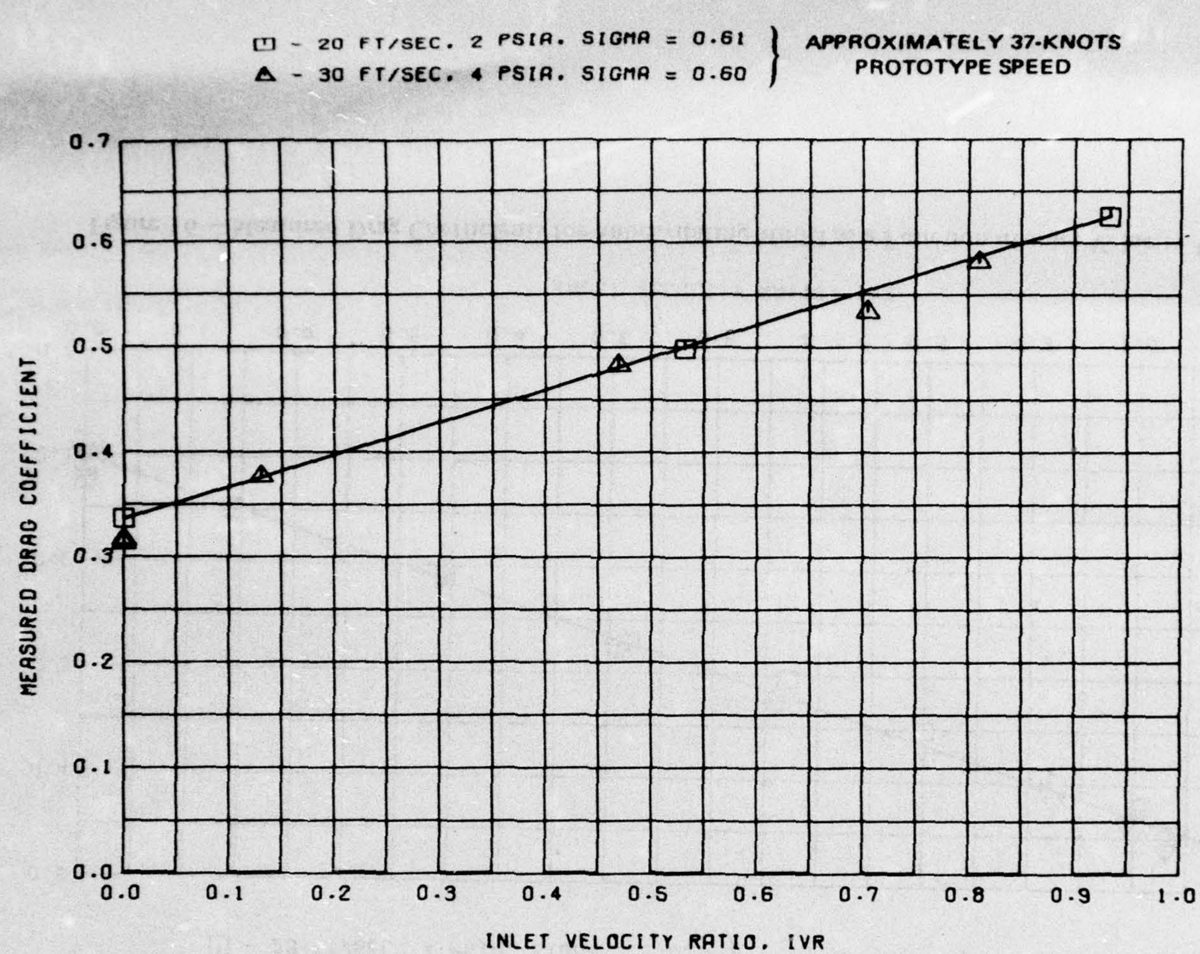

Figure 17 – Measured Drag Coefficients for Supercavitating Model as a Function of Inlet Velocity Ratio

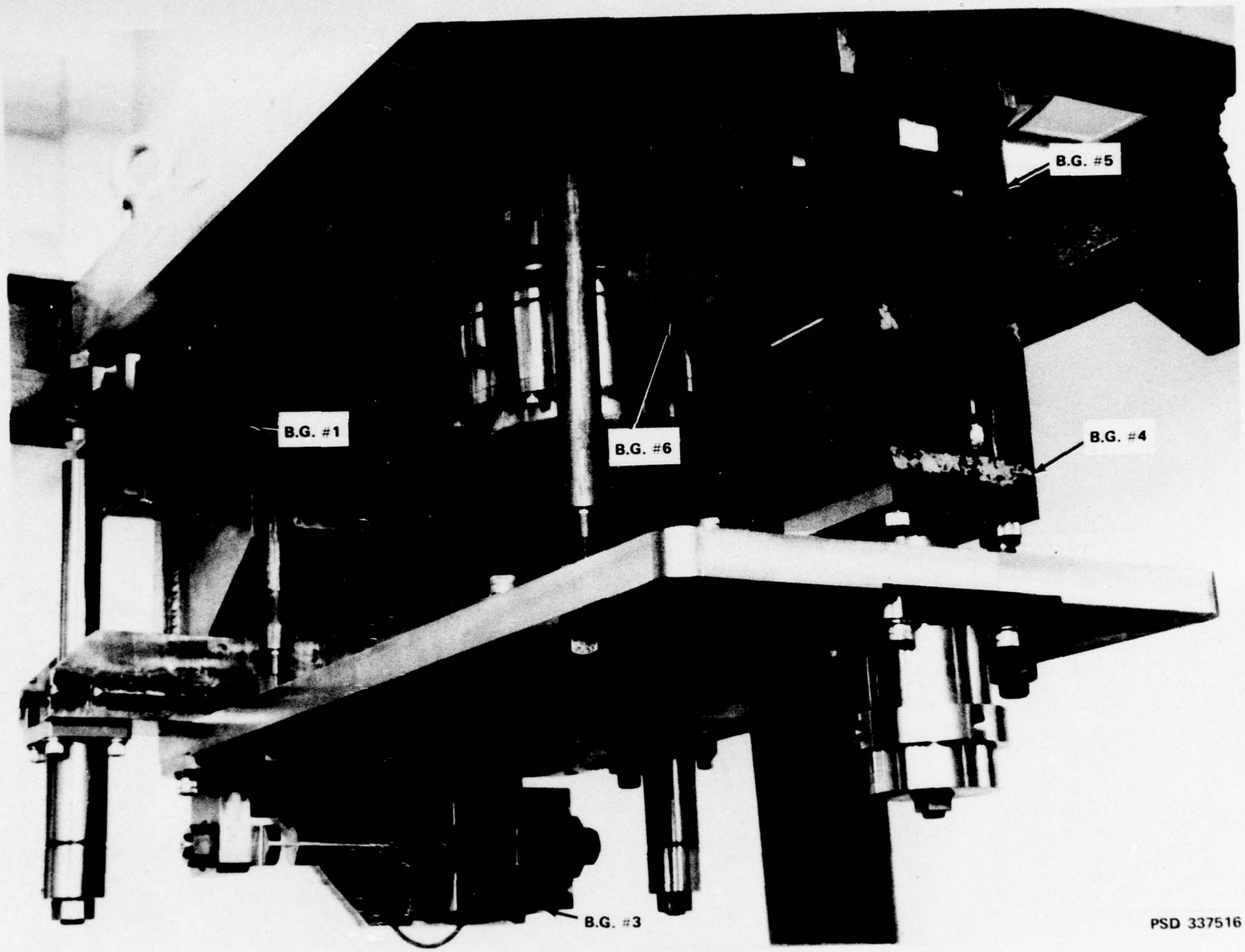

PSD 337516

Figure 18 – 6-Component Dynamometer–Looking Forward

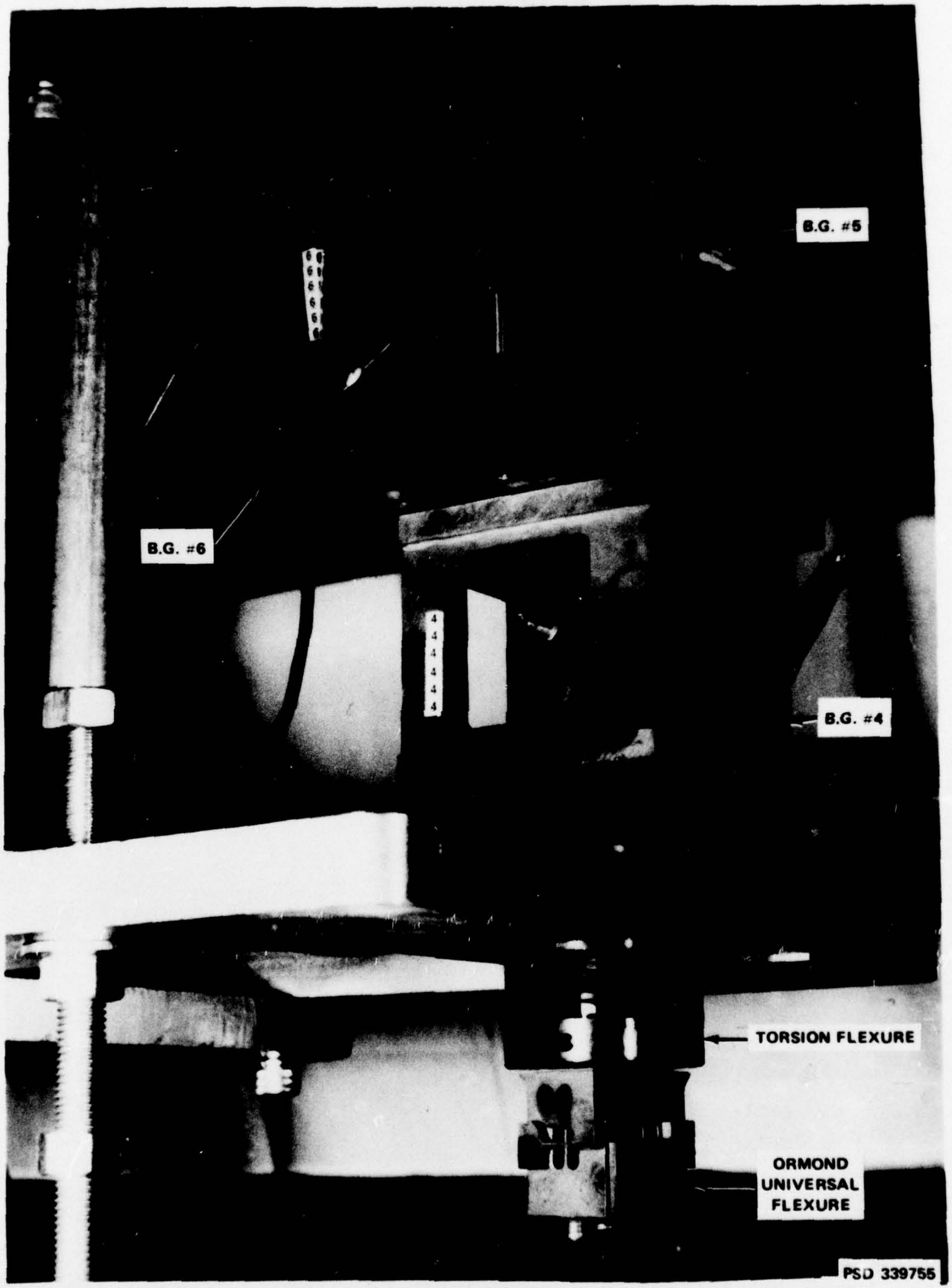

Figure 19 – Ormond and DTNSRDC Isolation Flexures at Aft End of 6-Component Dynamometer

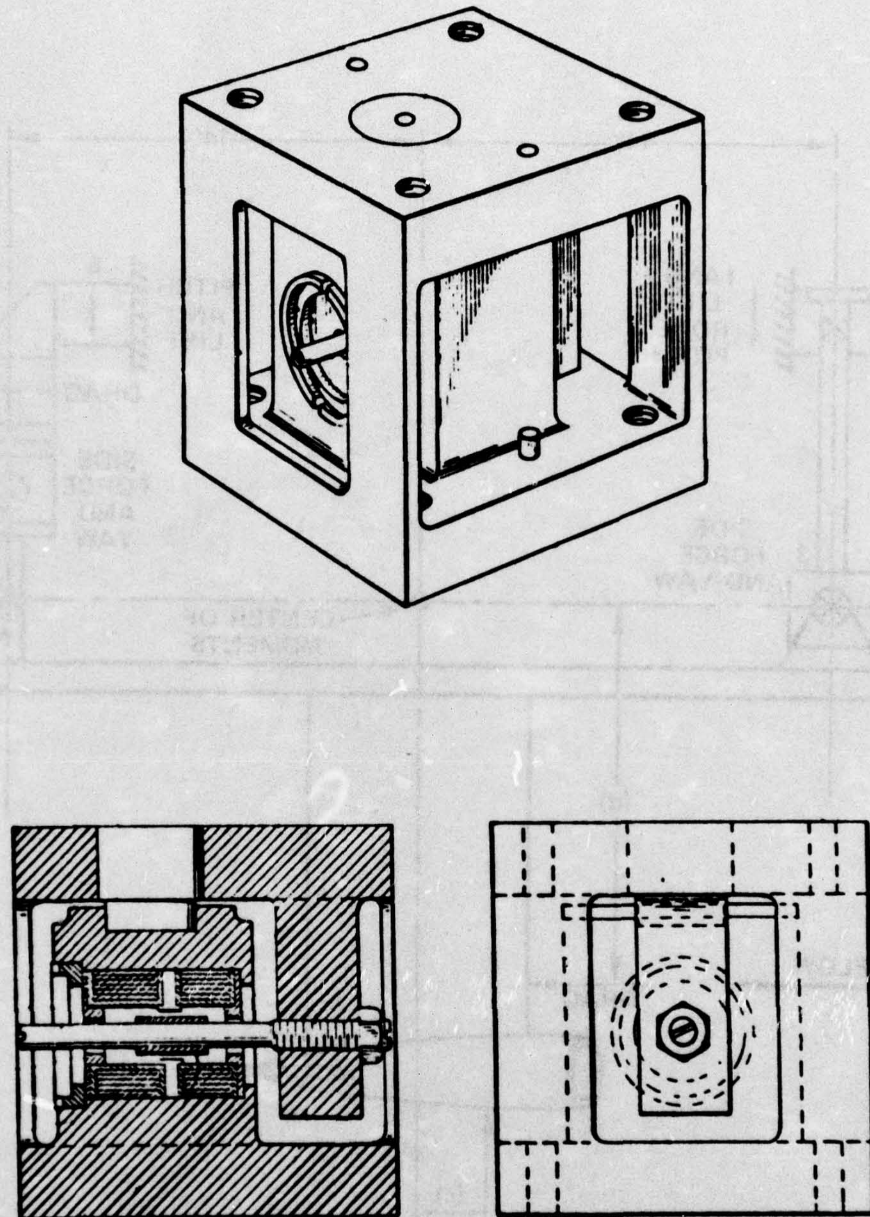

Figure 20 – DTNSRDC Force Measuring Block-Gage Cube

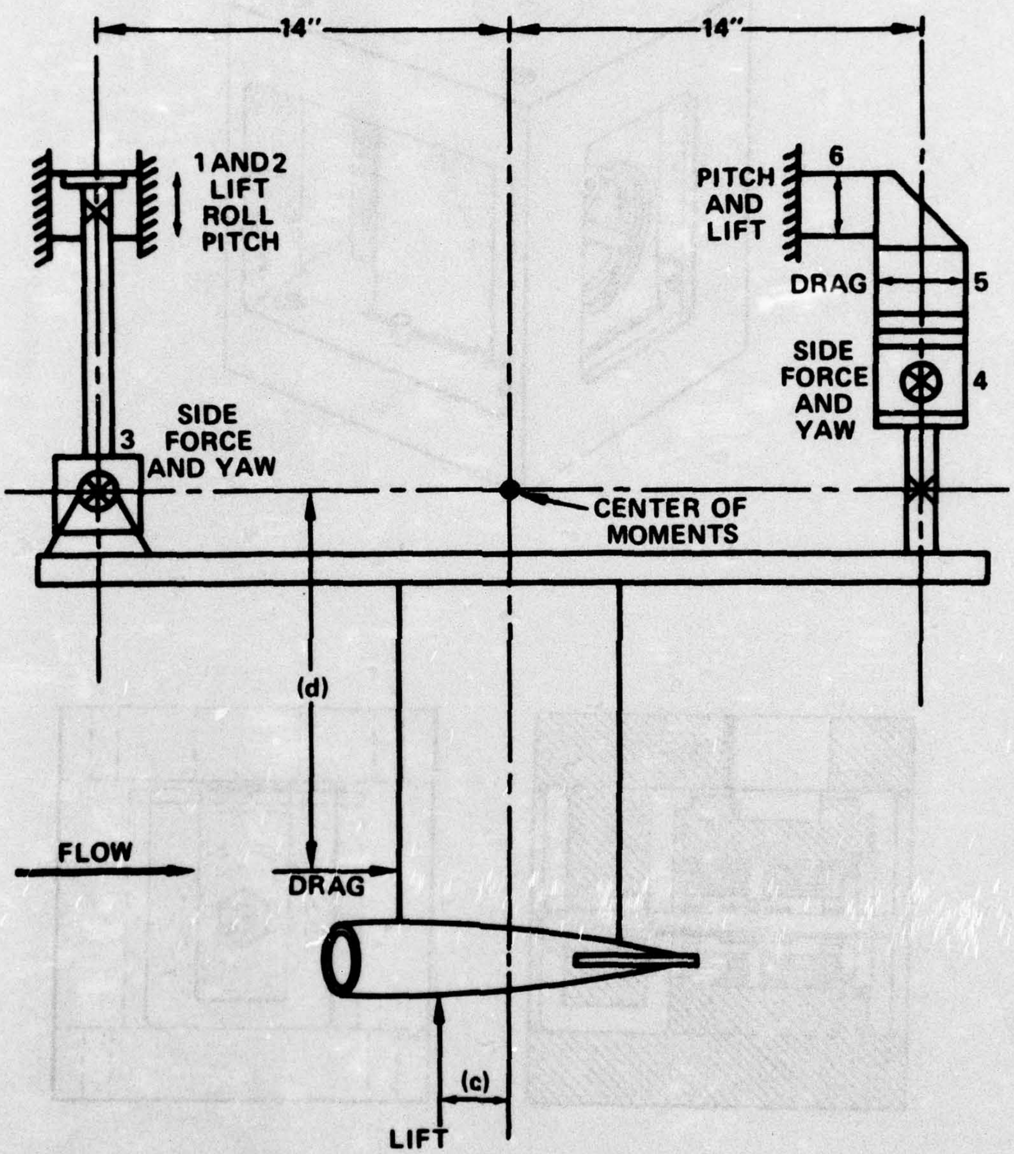

Figure 21 – Dynamometer Schematic Side View Elevation (Model Shown Yawed)

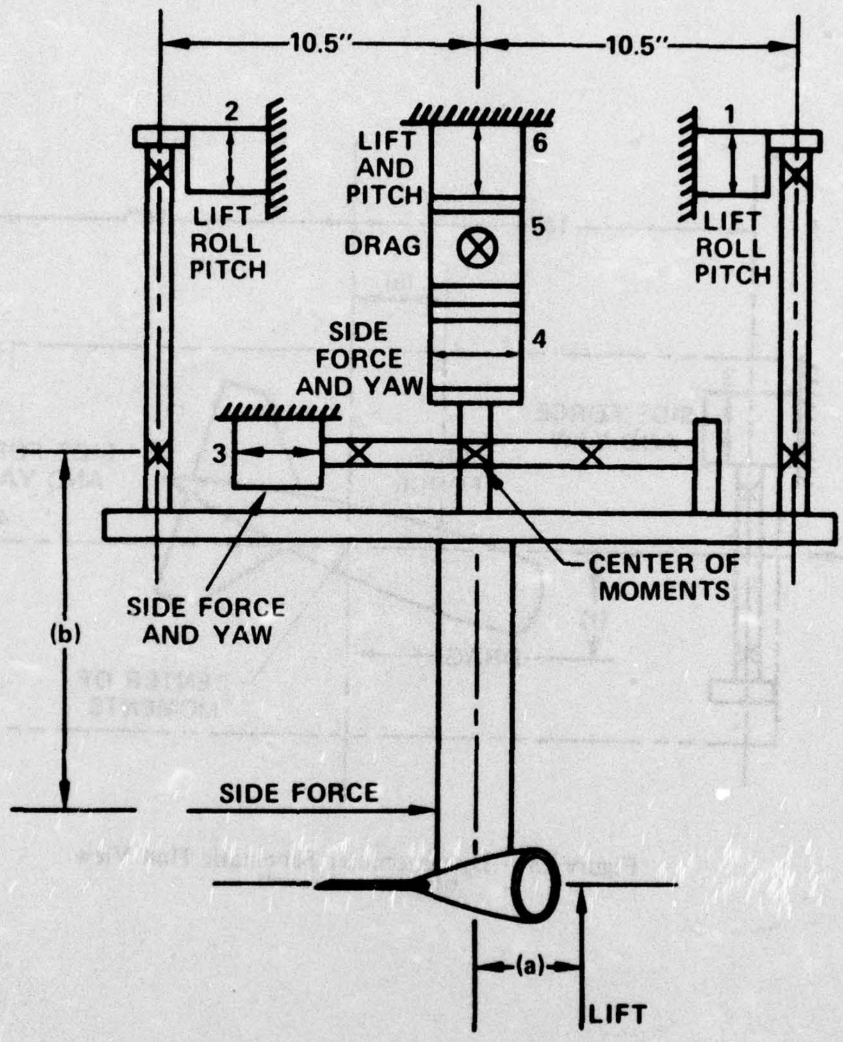

Figure 22 – Dynamometer Schematic End View Looking Aft (Flow into Paper) (Model Shown Yawed)

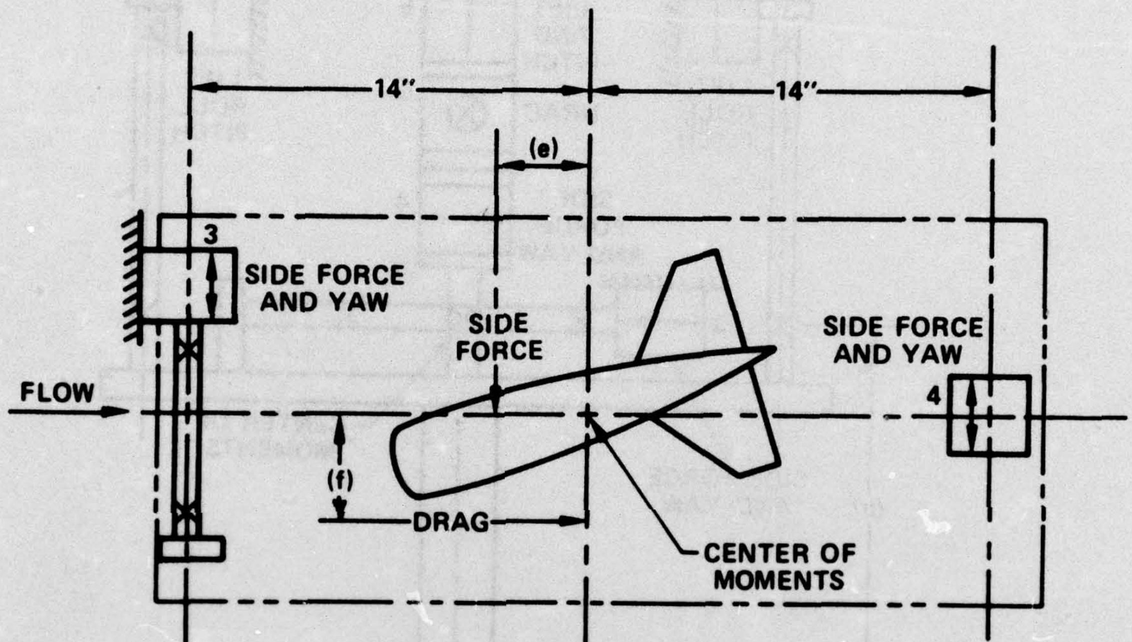

Figure 23 – Dynamometer Schematic Plan View
(Model Shown Yawed)

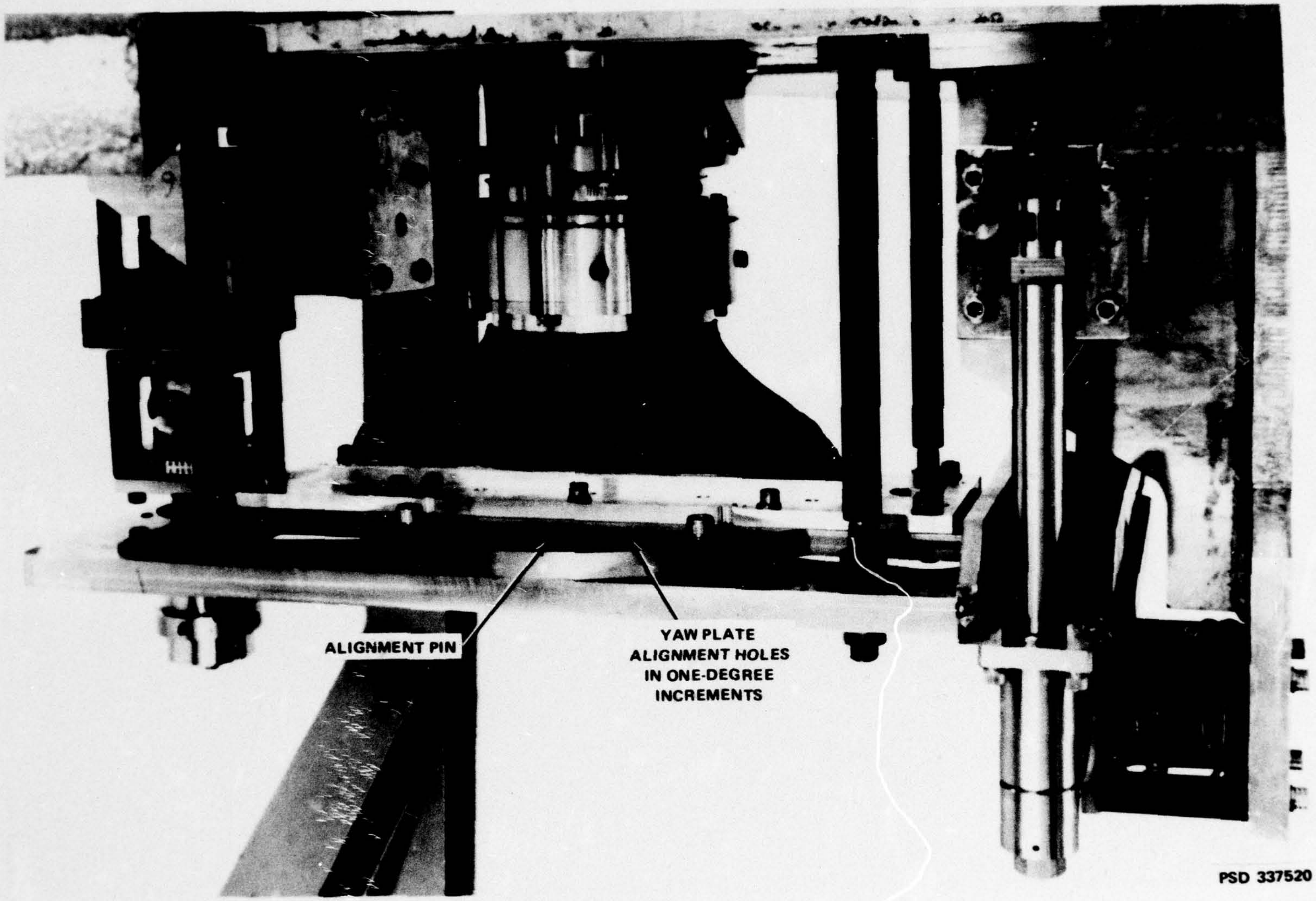

Figure 24 – 6-Component Dynamometer Showing Yaw Plate Alignment Holes

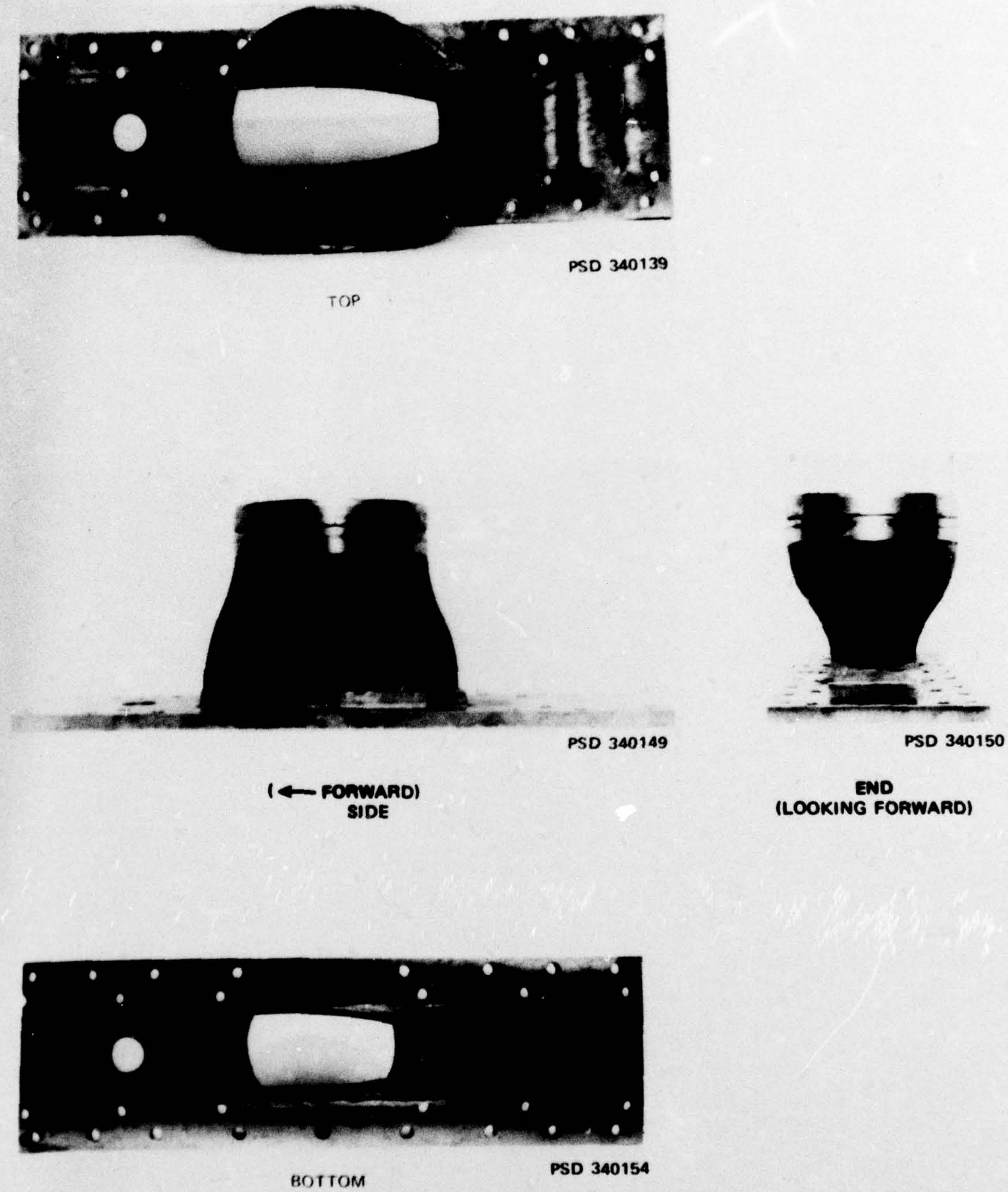

Figure 25 – Four Views of Transition Section Used with Subcavitating Model

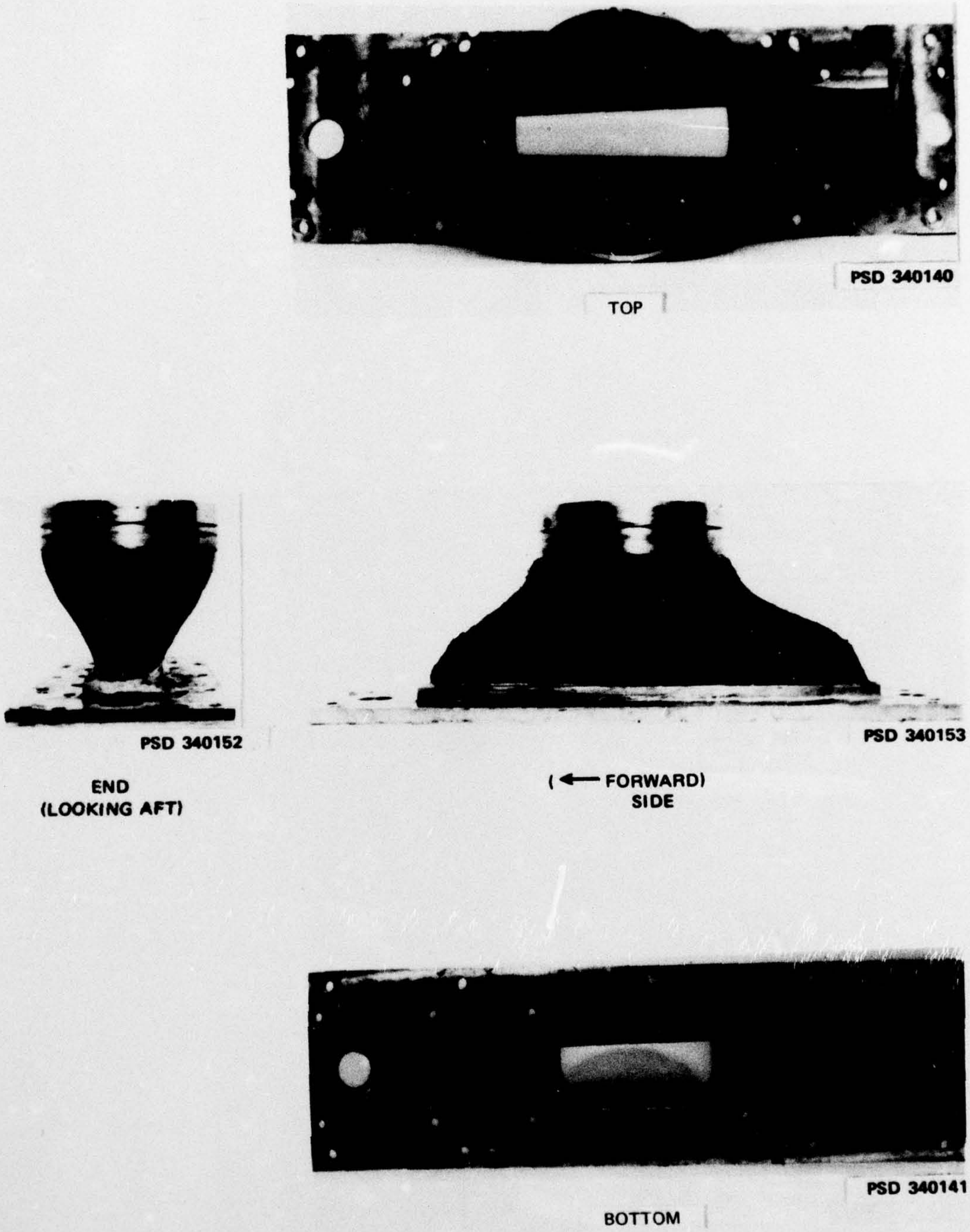

Figure 26 – Four Views of Transition Section Used with Supercavitating Model

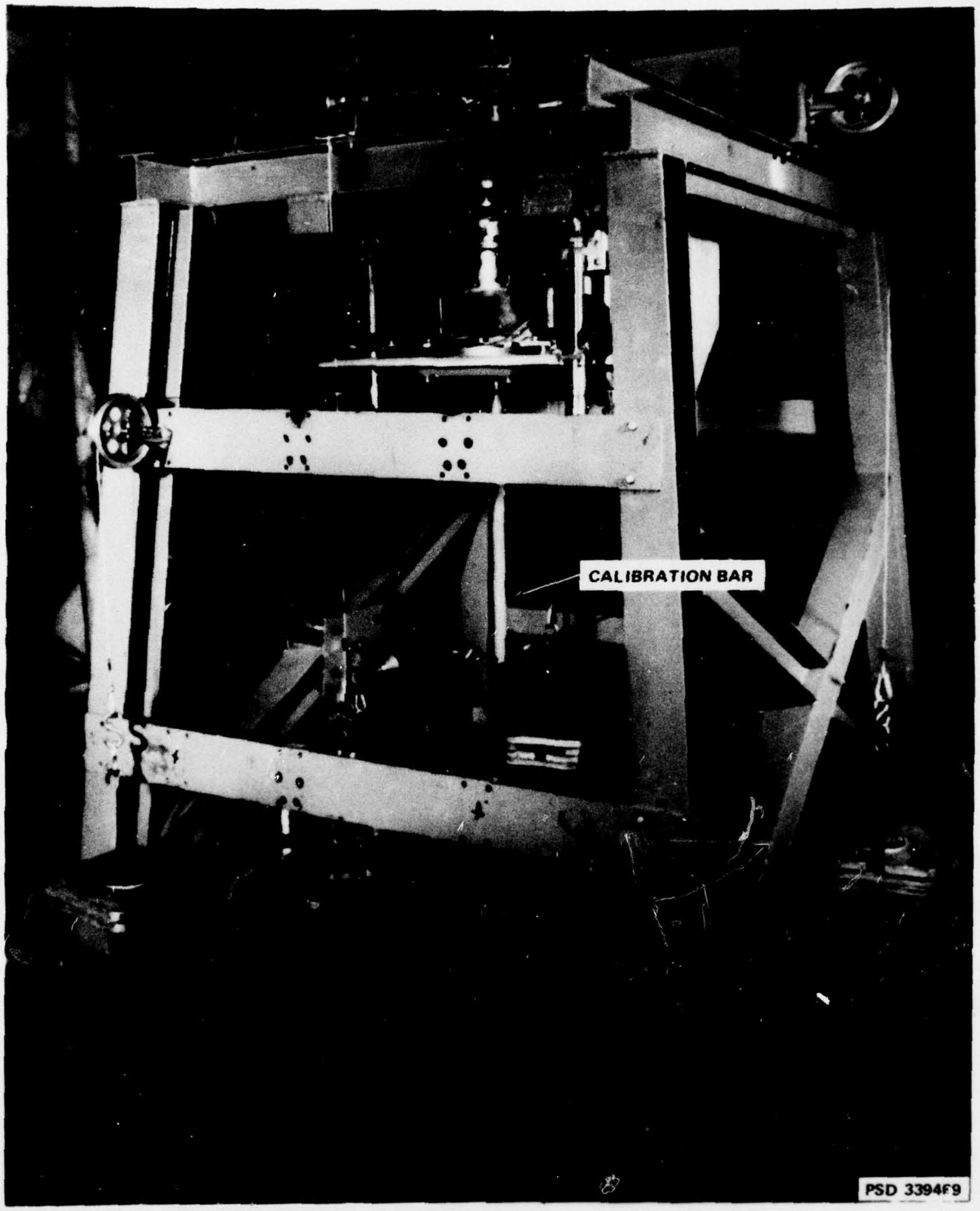

Figure 27 – Six-Component Dynamometer Mounted in Calibration Stand

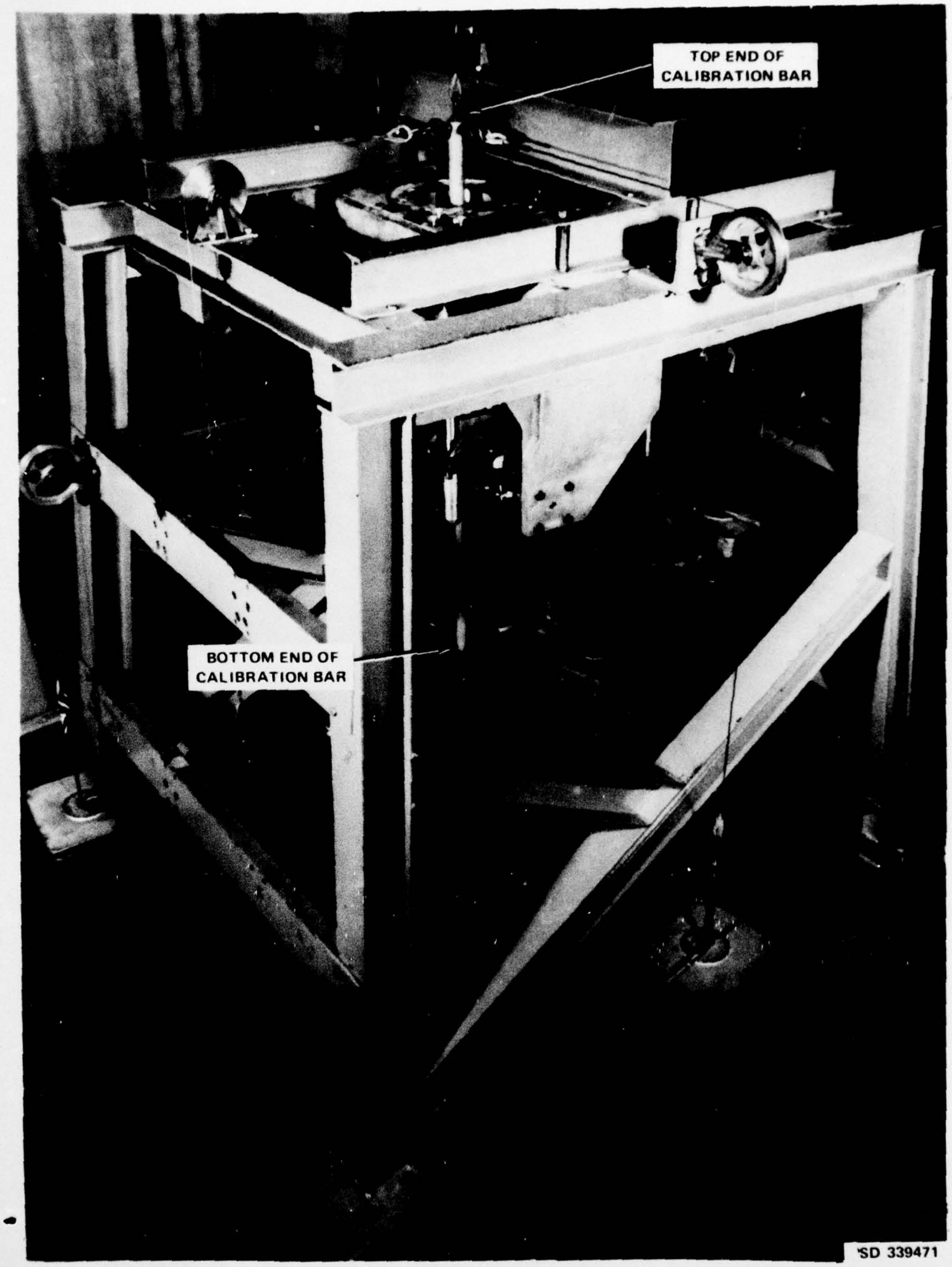

Figure 28 – Top View of Calibration Stand Showing Top of Dynamometer Calibration Bar

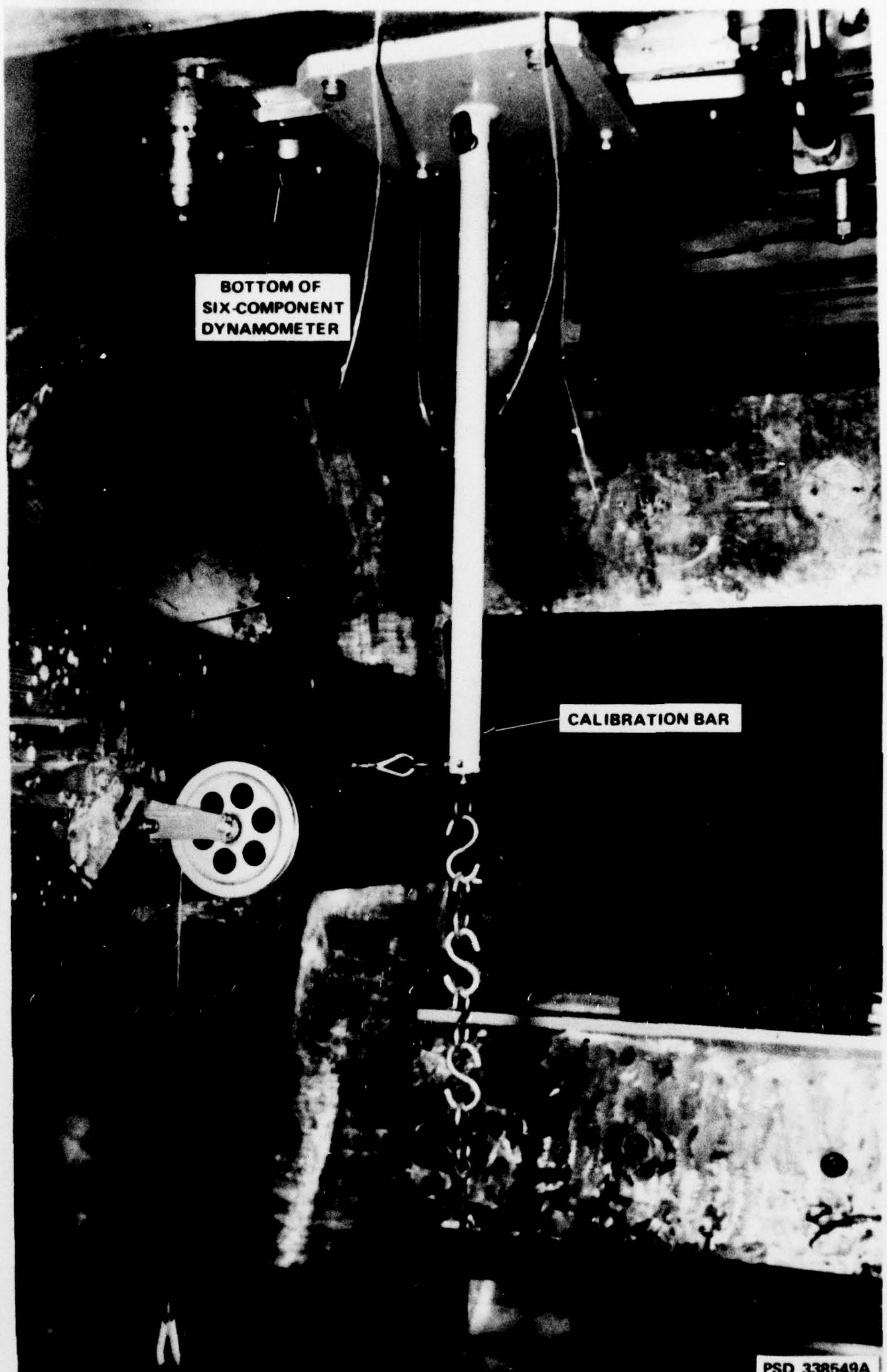

Figure 29 – Dynamometer Undergoing Final Calibration Checks Inside Tunnel Test Section

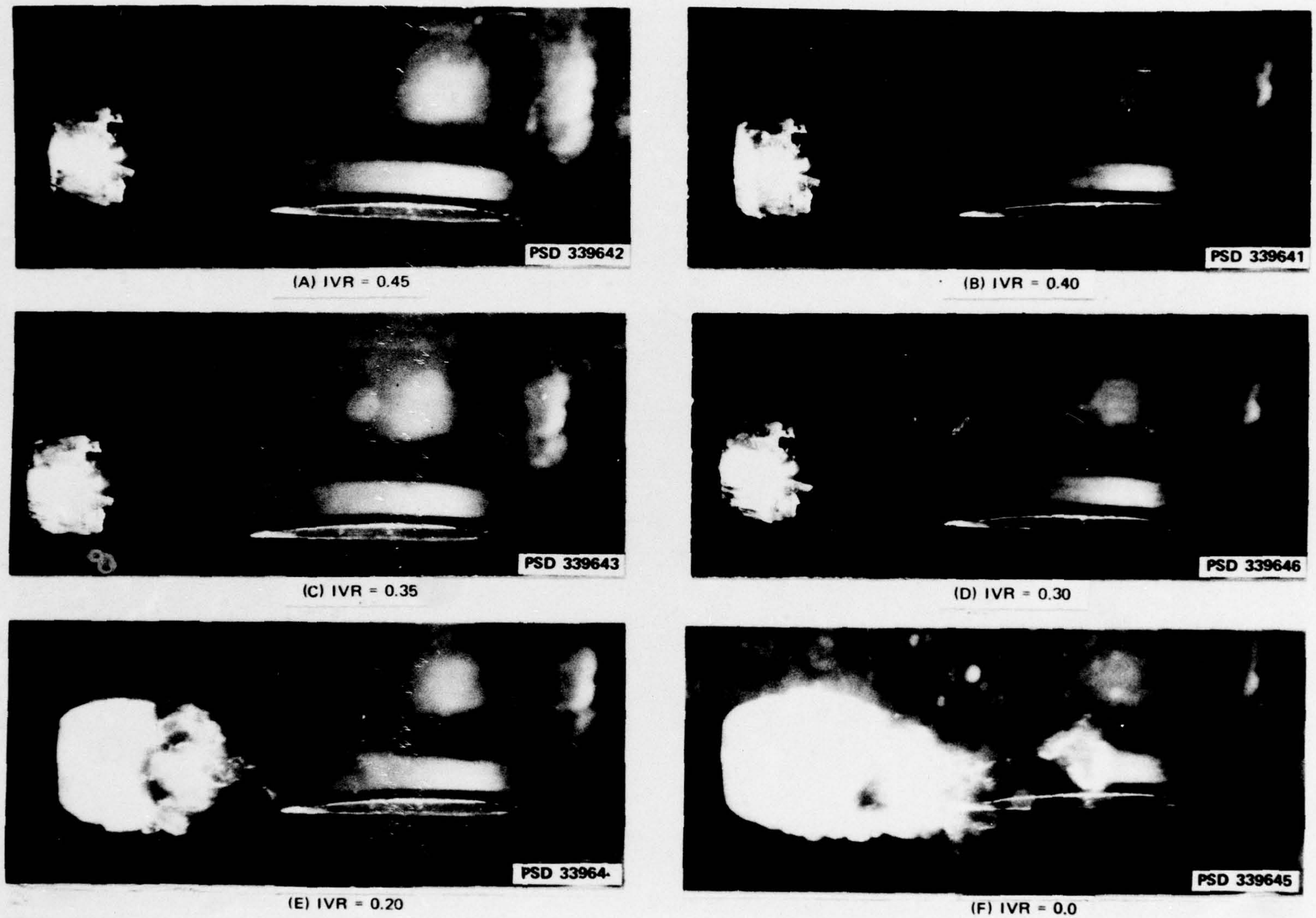

Figure 30 – Photographs Showing Development of External Lip Cavitation as the Inlet Velocity Ratio is Decreased at a Constant Free Stream Velocity of 31 ft/sec ($\sigma = 0.25$)

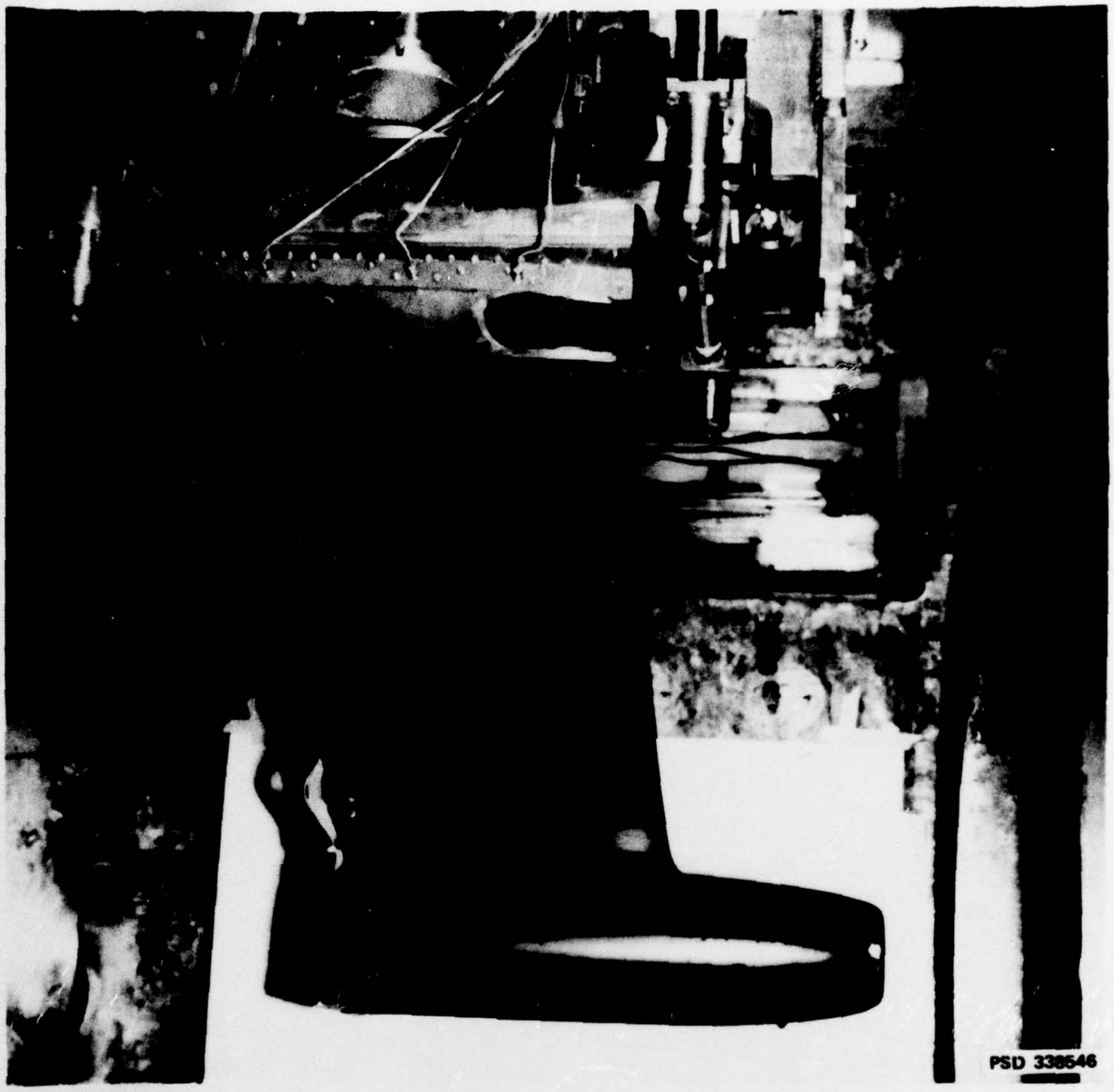

Figure 31 – Supercavitating Model Mounted Beneath 6-Component Dynamometer in DTNSRDC 36-Inch Variable Pressure Water Tunnel

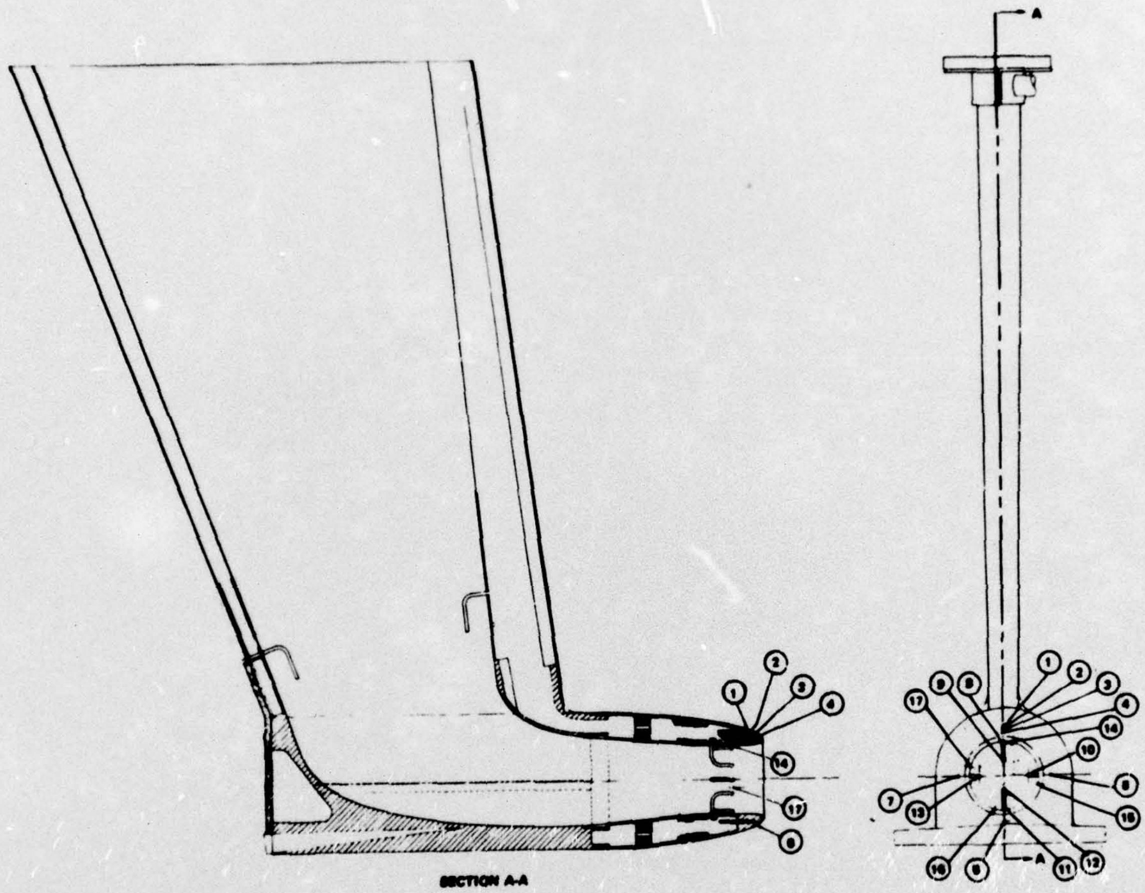

Figure 32 – Drawing of Supercavitating Model

Figure 33 – Internal View of Supercavitating Model Showing Splitter Vanes in Elbow and Strut

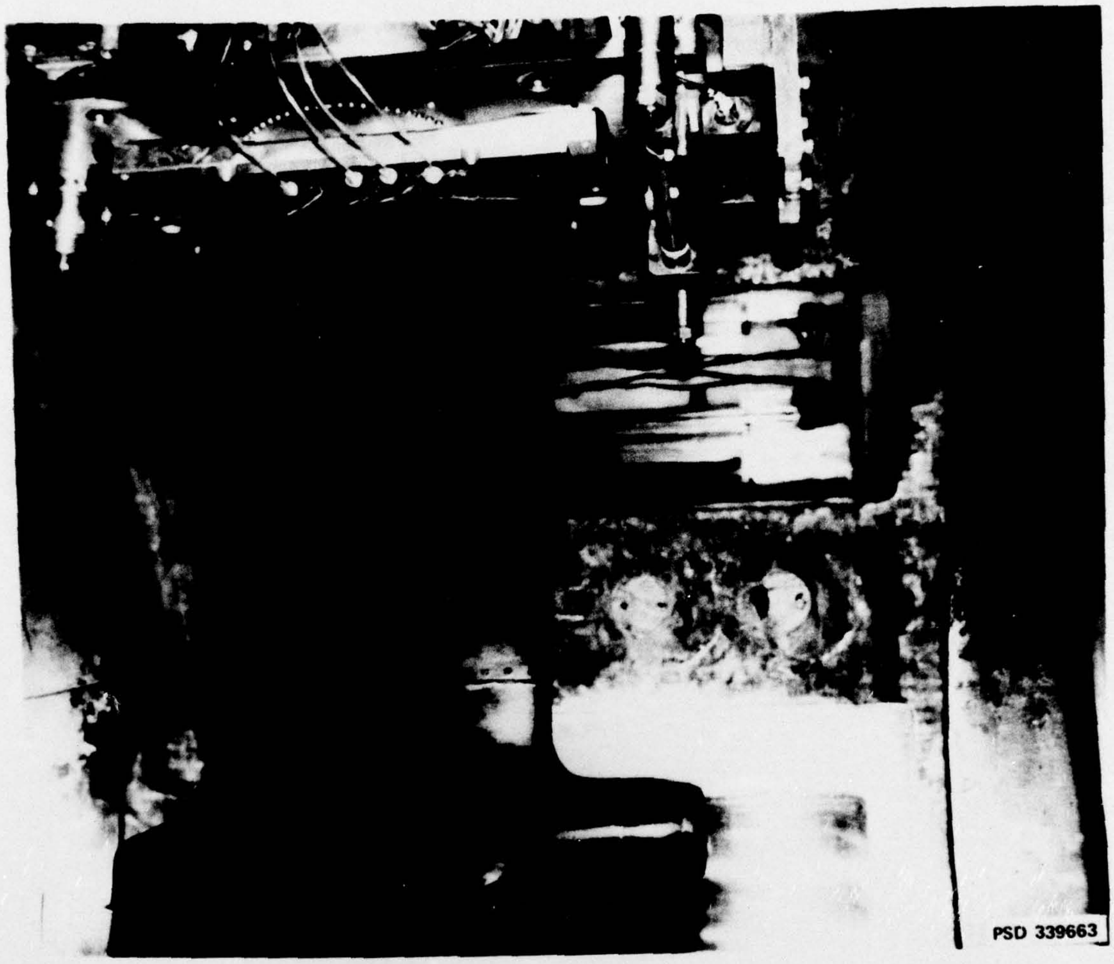

Figure 34 – Subcavitating Model Mounted Beneath 6-Component Dynamometer in DTNSRDC 36-Inch Variable Pressure Water Tunnel

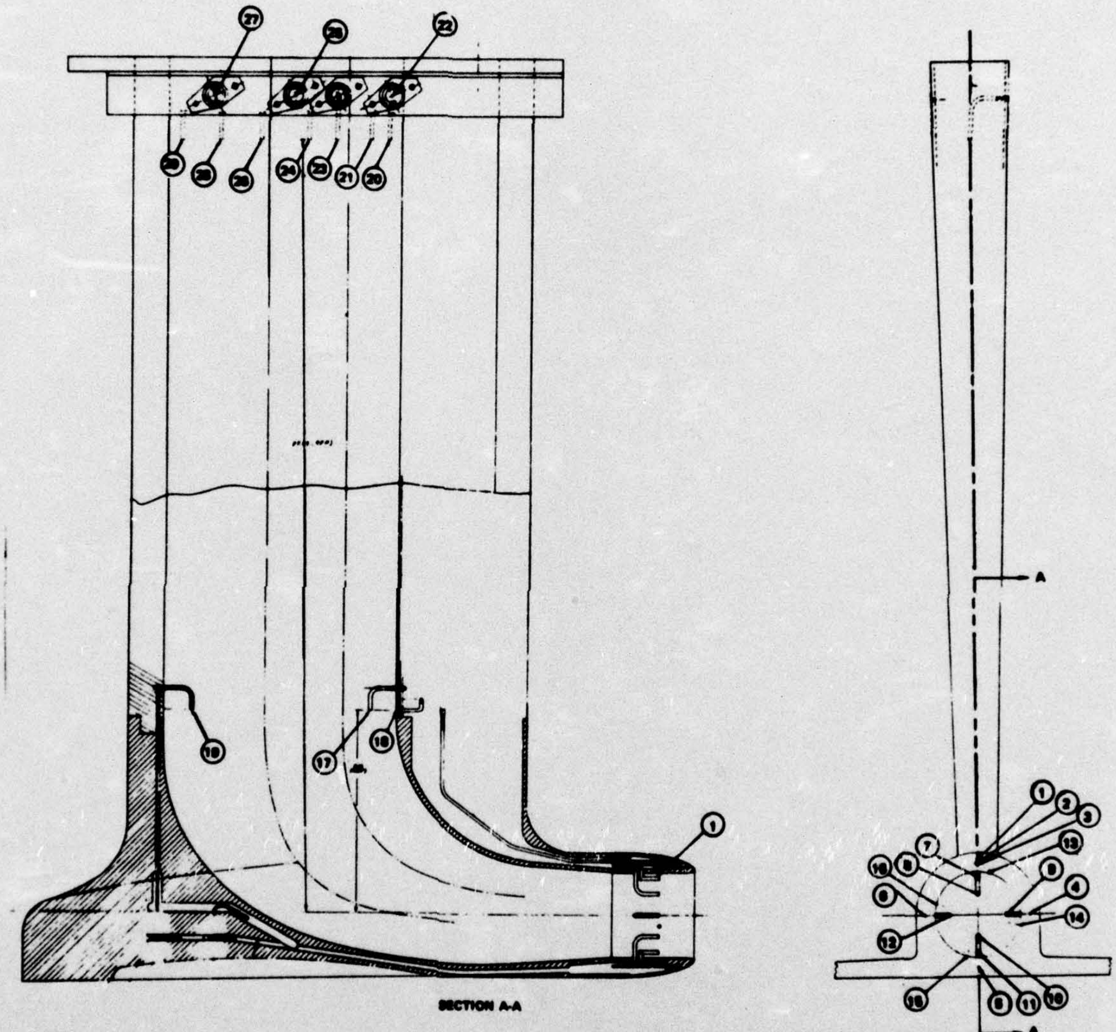

Figure 35 – Drawing of Subcavitating Model

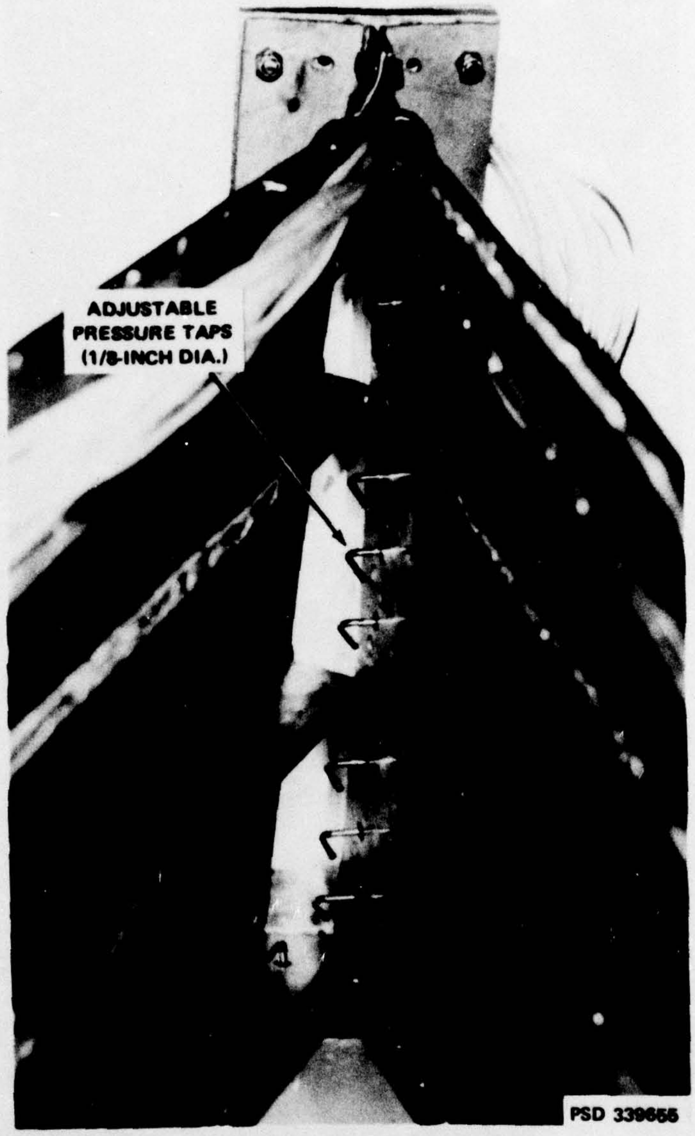

Figure 36 – Total Pressure Taps at Top of Supercavitating Strut

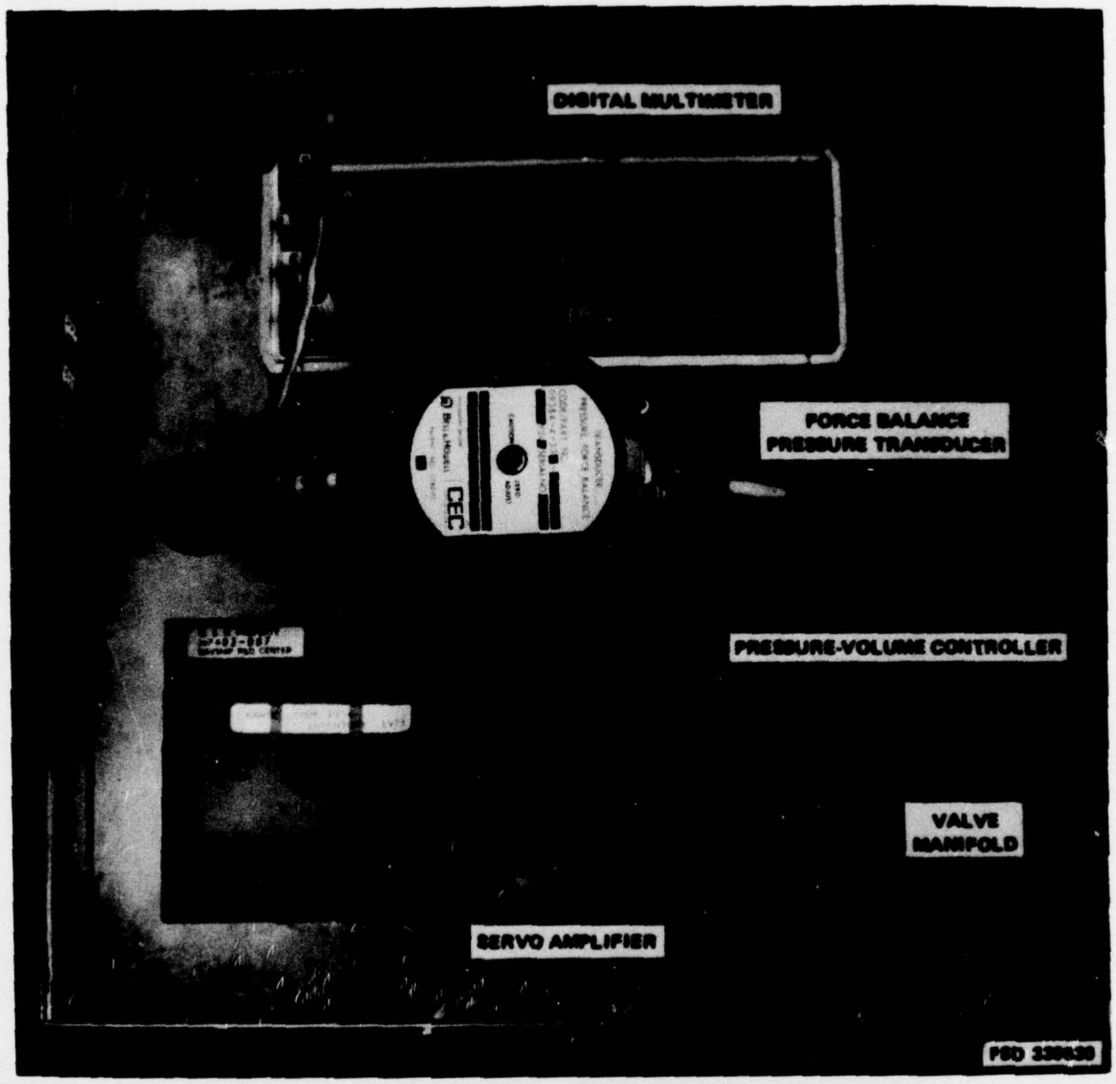

Figure 37 – CEC Electromanometer System Used for Calibrating Pressure Transducers

DTNSRDC ISSUES THREE TYPES OF REPORTS

(1) DTNSRDC REPORTS, A FORMAL SERIES PUBLISHING INFORMATION OF PERMANENT TECHNICAL VALUE, DESIGNATED BY A SERIAL REPORT NUMBER

(2) DEPARTMENTAL REPORTS, A SEMIFORMAL SERIES, RECORDING INFORMATION OF A PRELIMINARY OR TEMPORARY NATURE, OR OF LIMITED INTEREST OR SIGNIFICANCE, CARRYING A DEPARTMENTAL ALPHANUMERIC IDENTIFICATION

(3) TECHNICAL MEMORANDA, AN INFORMAL SERIES, USUALLY INTERNAL WORKING PAPERS OR DIRECT REPORTS TO SPONSORS, NUMBERED AS TM SERIES REPORTS, NOT FOR GENERAL DISTRIBUTION.